Chapter 21

Surface Defects on Continuously Cast Strands

Toshihiko Emi, Visiting Professor, Carnegie Mellon University

21.1 Introduction

Defects occurring on the surface of continuously cast strands (slabs, blooms and billets) require, in many cases, off-line surface conditioning before the strands are subjected to subsequent processing. Serious defects might not be removed by conditioning and will cause process upsets in downstream processing; hence, strands with such defects should be downgraded or scrapped. In addition, conditioning processes cause the following problems:

- Decreased productivity and interrupted production schedules.
- Yield and heat losses.
- Intermission of hot charge rolling (HCR) or hot direct rolling (HDR).
- Investment in scarfing or grinding machines and building space.
- Additional labor and utility costs.
- Environmental problems.

Many of the surface defects arising in modern continuous casting result from insufficient control of the casting operation and inadequate casting machine maintenance. This is particularly the case for casting operations during transient periods, e.g., at the start of casting, ladle changes, submerged entry nozzle (SEN) changes and at the end of casting. In these periods, fluctuations in the meniscus level of the melt, turbulence in the melt flow from the SEN, and a decrease in the temperature of the melt and flux take place in the mold. All of these events result in the formation of an irregular initial solidification shell that allows many types of surface defects to form. Measures to prevent these events have been in place for some time but are still incomplete.

Also, reoxidation of molten steel during transfer from the ladle through the tundish to the mold, and the entrainment of ladle slag, tundish slag and mold flux into the melt, become more pronounced during transient periods, causing inclusion clusters and slag patches. Regarding machine maintenance, wear of the mold plating and the mold itself, misalignment of the passline, an uneven gap, defects on supporting rolls and clogged spray-nozzle tips for secondary cooling can all produce various surface cracks. Thus, transient operation and machine maintenance must be under good control prior to optimizing steady-state casting conditions to produce strands free from surface defects.

During steady-state casting, the occurrence of surface defects is largely influenced by:

- steel grade,
- machine design, and
- casting operation.

In the early development of continuous casting, these three factors were entangled due to the underdeveloped state of engineering and technology. Accordingly, it was difficult to clarify the real cause and work out effective countermeasures. After more than 40 years of experience, however, our understanding—as well as the hardware and software for continuous casting—has advanced to near maturity, enabling us to identify the possible cause and elaborate upon countermeasures.

On the other hand, end-user requirements regarding surface quality of steel products have become more stringent, making tolerable casting defects smaller as years pass. This trend is further enhanced by the increasing implementation in conventional continuous casters of HCR and HDR, where scaling-off of minor and shallow surface defects does not occur. In an extreme case, surface cracks of 1 mm depth and 10 mm length on the strands have caused problems in downstream processing. The tolerance becomes even less for thin-slab casters, as the reduction ratio from the strand to the final product is smaller, the surface/volume ratio of the strands is greater, and off-line conditioning is virtually impossible. An extreme case is that of direct strip casting, for which no amount of surface conditioning is acceptable.

In addition, competition in international steel markets has increased considerably, driving steel mills to increase the productivity of continuous casting (CC) machines in order to match the output of the basic oxygen furnace (BOF) and hot rolling mill (HRM) with a reduced number of strands.[1] Thus, the casting speed of conventional CC machines will keep increasing. This principle also applies to thin-slab casters, as the productivity of electric arc furnaces (EAFs) will further increase. With an increase in casting speed, surface defects usually increase becuase the meniscus of steel melt in the mold tends to become more turbulent.

In light of quality and productivity constraints, therefore, trying to minimize the size and number of surface defects has been and will continue to be like trying to hit a moving target. In fact, the causes and countermeasures for surface defects have changed to some extent due to the changes in machine structure and operation. In the early stages of CC technology, large longitudinal and severe transverse cracks, often accompanied by breakouts, impaired operation, thereby considerably reducing productivity. These cracks were mostly eliminated with the optimization of the design and structure of hardware (e.g., flow control devices, SENs, mold structure, hydraulic oscillator, strand support, structure and interval of support rolls, mist spray cooling, bending/unbending arrangement, strand reduction, and devices for checking alignment of rolls and sprays) and software (e.g., mold flux, mold level control, electromagnetic flow control, secondary cooling pattern, pool end reduction).

However, high-speed casting (defined here to be in excess of 2 m/min for conventional slab casters) causes a rise in the occurrence of short longitudinal cracks associated with depression for peritectic grades. Sequential casting of multiple heats of Al-killed steel still causes an accretion of alumina inclusions on the tundish nozzle and the SEN. The accretion enhances the formation of alternating asymmetric biased flow in the mold. The biased flow results in turbulence of the metal flow in the submeniscus region in the mold, and also in deeper penetration of the main metal flow into the crater of the strand. The turbulent submeniscus flow triggers, via vortexing and emulsification, the entrainment of mold flux into the metal at the mold flux/metal boundary. The penetrating main flow carries slag inclusions, alumina clusters and mold flux emulsion into the crater. These are partly engulfed in the growing shell of the strand during flotation.

The engulfment becomes greater as the turbulence gets stronger, and penetration gets deeper with increasing casting speed. Pinholes at the strand subsurface, arising from fine bubbles of Ar injected into the SEN to reduce the accretion, are often associated with adhered alumina inclusions and cause slivers and blisters on IF steel strip. Elimination of the pinholes has not been complete as yet at high casting speeds and for Ti-containing grades. Slabs for drawn and ironed (DI) cans, plastic-laminated DI cans, and exposed panels for automobiles all demand that alumina clusters entrapped at the subsurface be minimal in number, concentration and size. Deep oscillation marks on austenitic stainless steel slabs are often associated with segregation of P and Ni at their bottom. Such marks are responsible for the formation of transverse cracks, short longitudinal cracks and a surface pattern on the cold rolled strip, and they prevent slabs from being rolled without conditioning.

This chapter reviews the current knowledge regarding surface defects, and it presents practicable means for producing strands free from surface defects by optimizing equipment and caster operation. To aid the reader in researching a particular defect, classification of the defects is given first, followed by the characteristic features, influential factors, causes and preventive measures.

21.2 Classifications and Appearance of Surface Defects

Typical surface defects are schematically shown in Fig. 21.1. The defects include the following with a number of variants:

- longitudinal facial or corner cracks,
- transverse facial or corner cracks,
- star cracks and hot shortness,
- longitudinal and transverse depressions,
- deep oscillation marks with solute segregation,
- bleeding,
- inclusion clusters,
- slag patches or entrapped slags/scums, and
- gas holes, including blowholes and pinholes.

Good reviews on this subject have been made available by Brimacombe and Sorimachi,[2] Schwerdtfeger,[3] the Iron and Steel Institute of Japan (ISIJ),[4] McPherson and McLean,[5] and Wolf.[6]

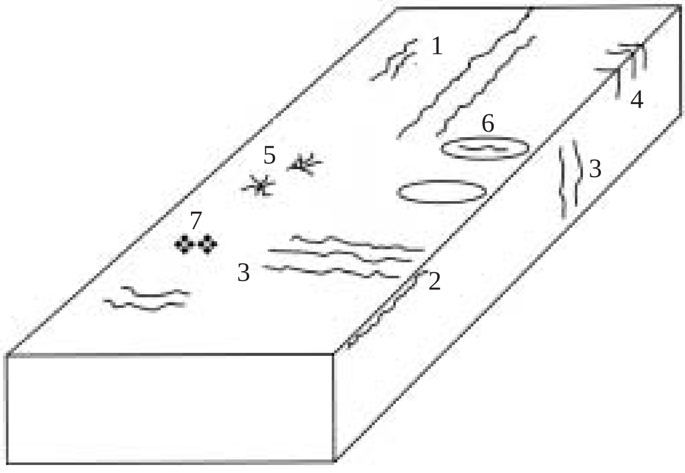

Fig. 21.1 Surface defects on a CC strand: (1) longitudinal facial cracks, (2) longitudinal corner cracks, (3) transverse facial cracks, (4) transverse corner cracks, (5) star cracks, (6) transverse depressions and (7) inclusion clusters.

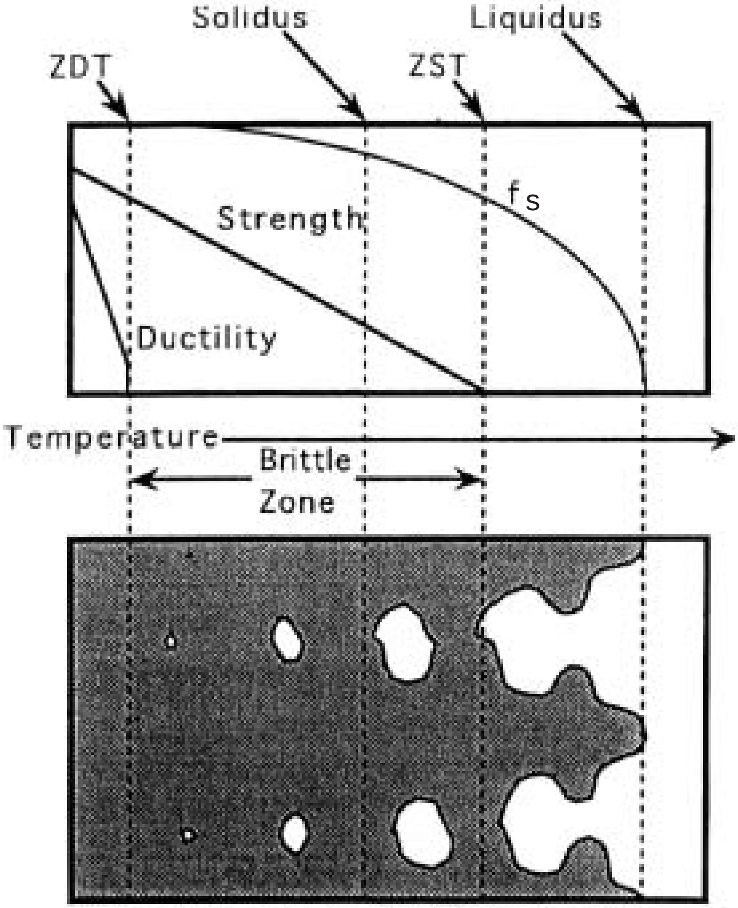

Fig. 21.2 Zero strength temperature (ZST), zero ductility temperature (ZDT) and f_s in the mushy zone. *From Ref. 11.*

21.3 Surface Cracks

21.3.1 Longitudinal Cracks

When molten steel is cooled in a CC mold, a thin shell forms and grows. Emi[7] defined the temperature below which steel begins to exhibit strength or ductility as zero strength temperature (ZST) or zero ductility temperature (ZDT). An Instron-type high-temperature tensile strength tester was employed by Schmidtmann and Pleugel[8] to explore the tensile strength of steels near their solidus temperatures. Shin et al.[9] found with a similar but more advanced tester that the solid fraction (f_s) at ZST is about 0.6–0.8 for the "in-situ" solidifying Fe-C-1% Mn alloys, as shown in Fig. 21.2. This is the fraction in which dendrite arms interact to resist tension. The ZDT for the same alloys corresponded to a higher solid fraction of near 1.0. However, a different view was raised by Mizukami, Yamanaka and Watanabe[10] on C-Cr steel, that f_s for ZDT is 0.8, nearly the same as that for ZST. The relation between ZST, ZDT and f_s by Umeda[11] is schematically shown in Fig. 21.3.[11]

An example of ZST, ZDT and TRSG (temperature range of strength generation) by Shin et al.[9] is also shown in Fig. 21.4. The tensile strength near ZST decreases linearly with temperature. Many data indicate that the tensile strength of steels that solidify in the δ- or γ-phase at temperatures somewhat below ZST is less than 5 MPa—very low due to the remaining liquid between the dendrites. Also, the ductility of the shell just below ZDT is very low, a few percent in elongation. Both ZST and ZDT show strain rate dependence.

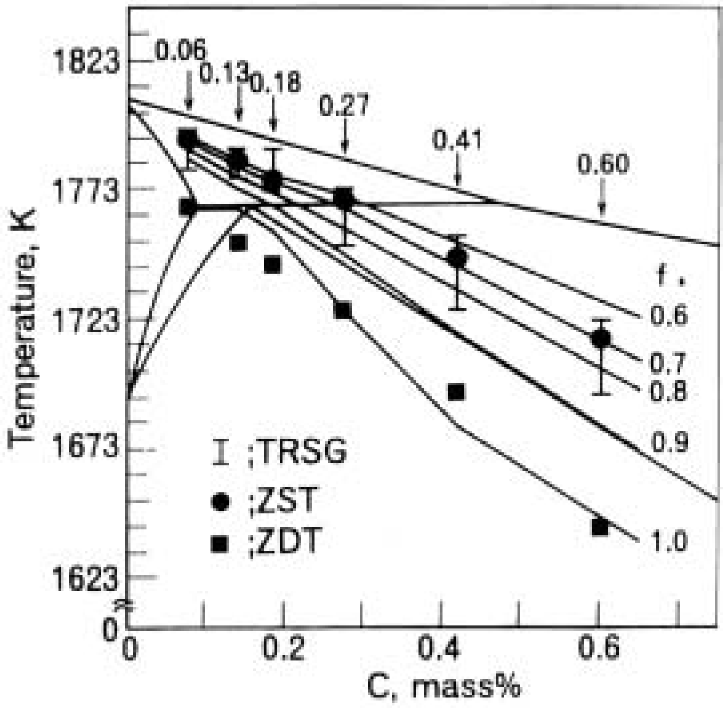

Fig. 21.3 Zero strength temperature (ZST), zero ductility temperature (ZDT) and the temperature range of strength generation (TRSG) for Fe-C-1% Mn alloy. *From Ref. 9.*

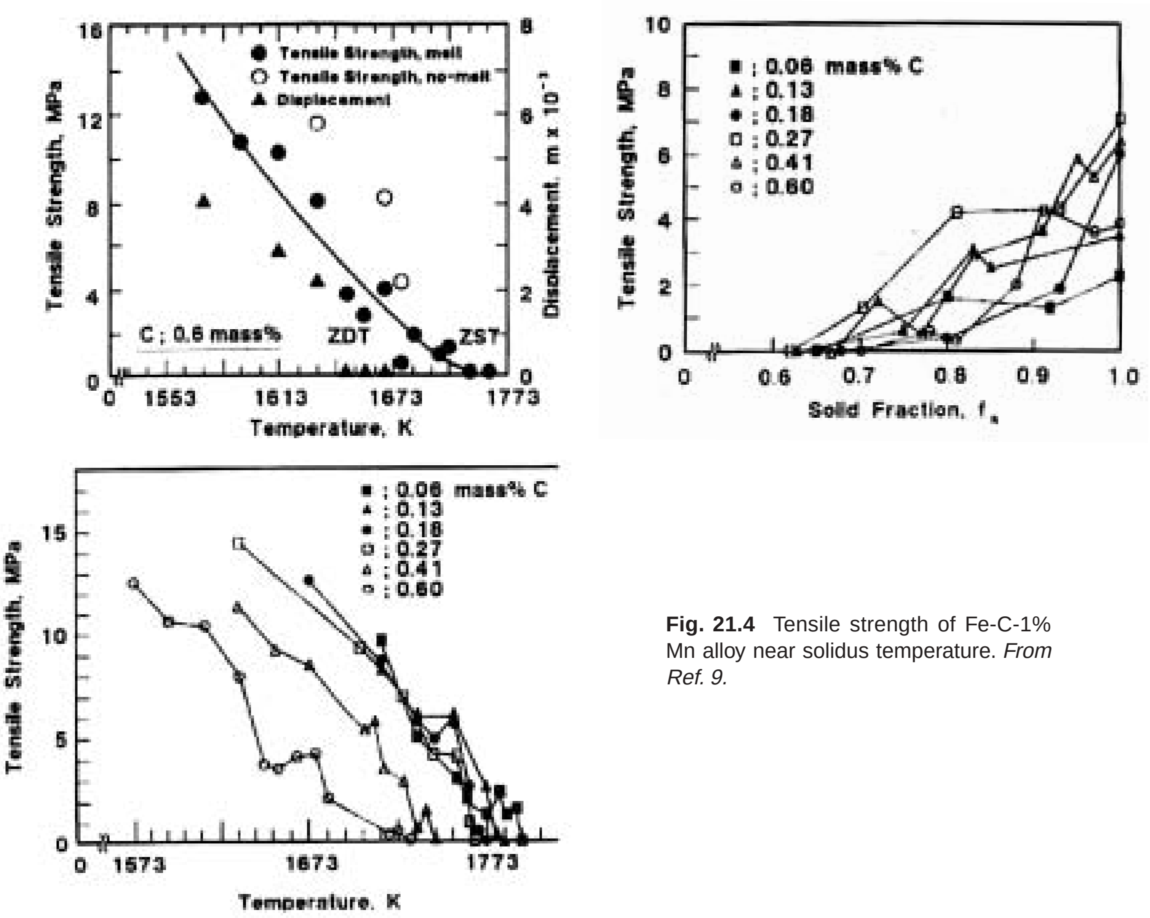

Fig. 21.4 Tensile strength of Fe-C-1% Mn alloy near solidus temperature. *From Ref. 9.*

Generally speaking, the Instron-type testers require careful control of dendrite growth direction during tensile tests, whereas submerged split chill tensile (SSCT) testers worked out by Ackermann, Kurz and Heinemann[12] need precise control of uniform shell growth around the mold. Difficulties involved in the control result in the scatter and inaccuracy of the observed data.

The initial solidification of the steel shell in the CC mold takes place just below the meniscus of the melt. At this stage, the shell is still at temperatures close to ZST and ZDT; hence, it has very low tensile strength and near-zero ductility. Frictional, fluid dynamic and tensile stresses arising from strand withdrawal and mold oscillation are applied to this weak and brittle shell, as discussed by Schwerdtfeger and Sha.[13] Also, volume contraction upon solidification and thermal stresses upon cooling impose additional stresses on the shell. When the sum of these stresses or strains exceeds the tensile strength or ductility of the shell, cracks occur. The occurrence of the cracks is enhanced by uneven growth along the mold perimeter of the initial shell caused by meniscus fluctuation and submeniscus flow turbulence. Many factors contribute to crack formation to a different degree, causing a variety of cracks.

21.3.1.1 Longitudinal Facial Cracks

21.3.1.1.1 Characteristics

In the mid-1970s, while CC technology was still in the early stages of development, the occurrence of large cracks extending a few meters long and 10–30 mm deep was not uncommon. An example of such long and deep facial cracks is shown by Brimacombe, Weinberg and Hawbolt[14] in Fig. 21.5. This particular crack formed in the withdrawal direction on the mid-face of a 1500-mm-wide

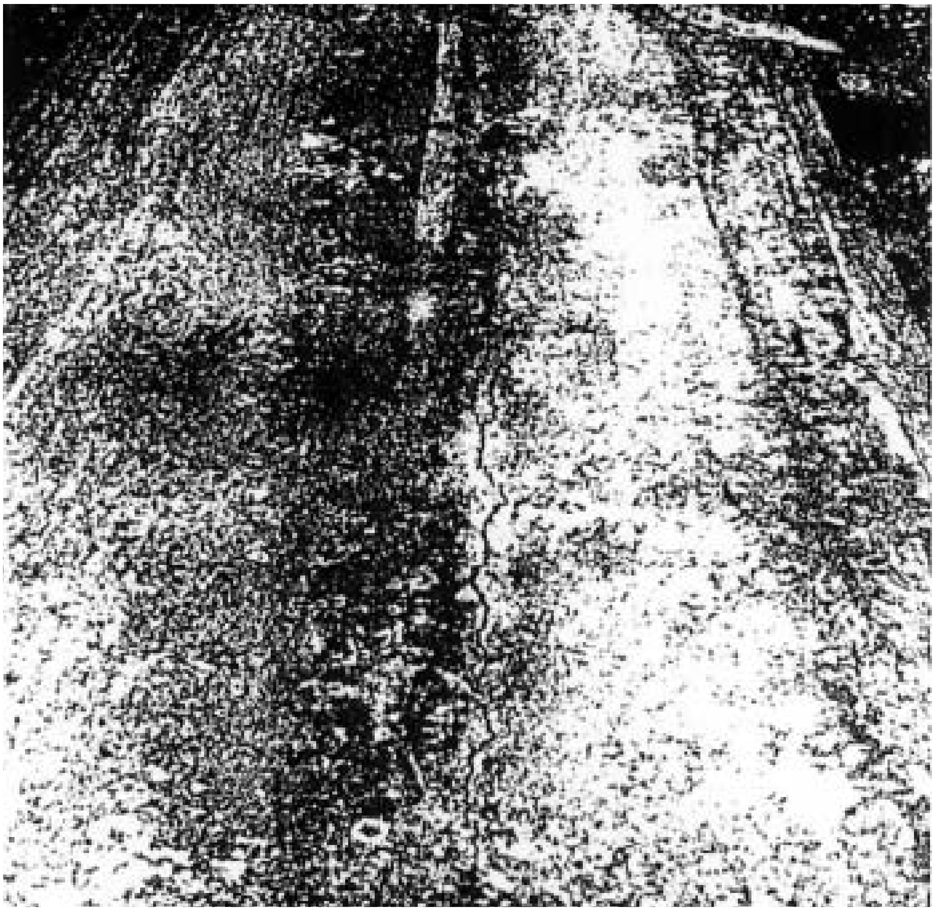

Fig. 21.5 Large longitudinal facial cracks on a 1500-mm CC slab. *From Ref. 14.*

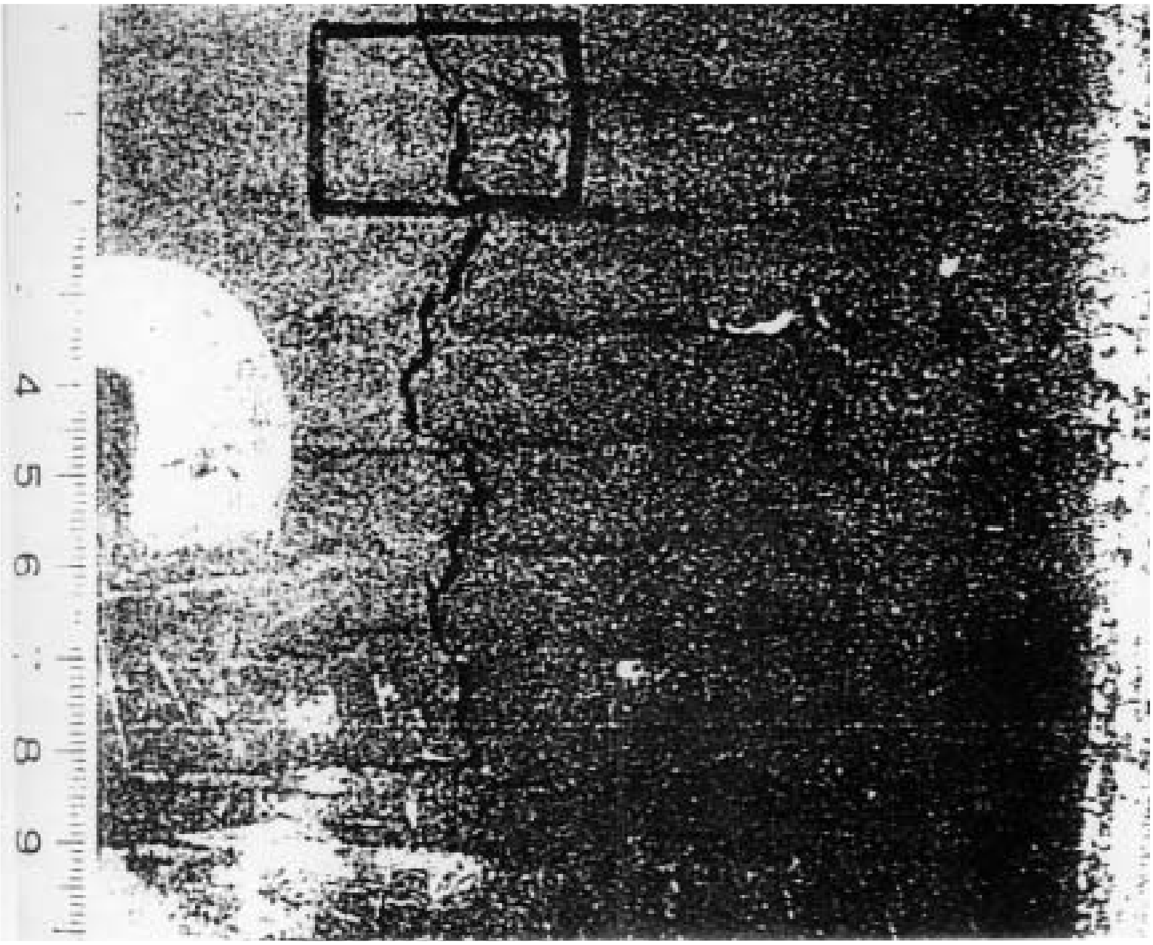

Fig. 21.6 Large longitudinal facial cracks (Type-1 LFC) on a carbon steel slab (courtesy of NKK).

CC slab. Today, however, because of technology's maturation, such cracks are seen much less frequently unless a serious failure in operation and/or maintenance occurs. Such cracks, should they occur, are observed mostly during transient periods of casting operation.

Today, typical longitudinal facial cracks may be classified into two types:

- Type-1 longitudinal facial cracks (Type-1 LFC hereafter) are, as shown in Fig. 21.6, above 100 mm long and less than a few millimeters deep and can be removed by off-line conditioning. The cracks occasionally accompany depression. Primary dendrite arms are observed along the cracks.

- Type-2 cracks (Type-2 LFC hereafter) are much shorter (less than 20–30 mm) and shallower (1 mm or less) facial cracks formed in the withdrawal direction. They are not limited to the mid-face but can be scattered or clustered at mid- to quarter-width of the wide face. A sectional view of the crack cut perpendicular to the length in the thickness direction is shown in Fig. 21.7. Type-2 LFC occurs often on peritectic steels, particularly in the 0.10–0.16% C and even more so in the 0.12–0.15% C range for carbon steels. These carbon ranges are site-specific, depending on the local condition of the mold, machine and its operation. Conditioning is mandatory.

The occurrence of these cracks became evident in the late 1970s to early 1980s, when high-speed casting was practiced for better productivity, even on crack-sensitive peritectic grades. Critical casting speeds for peritectic grades in conventional and thin-slab casters today are around 2 m/min

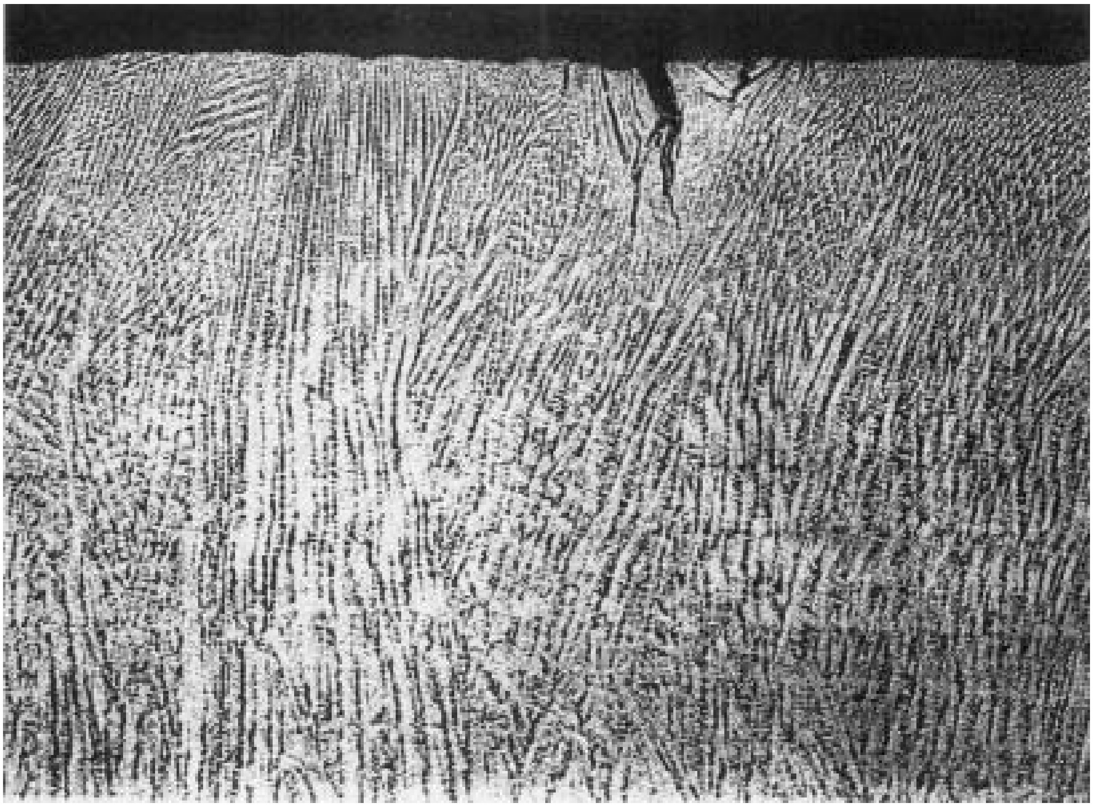

Fig. 21.7 Small longitudinal facial crack (Type-2 LFC) on a carbon steel slab (courtesy of NKK).

and 4 m/min, respectively, even after all available measures are taken, thereby imposing a productivity bottleneck.

Kohno et al. carried out a detailed metallographic investigation on different types of longitudinal facial cracks generated by molds, with artificially made defects (grooves) of different sizes.[15] The investigation revealed that:

- Local segregation of C, Mn, P and S precedes the cracks in both the length and depth directions.
- The segregation occurs along the primary dendrite arms, and shallow segregation is exposed on the slab surface. Longitudinal facial cracks develop in the length and thickness directions of the strand along such segregation.
- On the other hand, deep segregation passes through γ-grain boundaries or across γ-grains. The cracks often propagate along γ-grain boundaries into slabs.
- Secondary dendrite arm spacing indicates that the solidification rate was slower at the cracks. The slab surface shows that it deformed at temperatures below Ac_3, and the cracks opened up after the deformation.

21.3.1.1.2 Influential Factors, Causes and Countermeasures

Thermal and mechanical factors that have been known to increase the occurrence of the cracks are related to CC machines and their operation as follows:

1. Shallow mold taper.
2. Mold with large width/thickness ratio or large width.
3. Increasing width of the mold flux streak, or increasing width of the defect at the meniscus level on the mold, as shown by Kohno et al. in Fig. 21.8.[16]

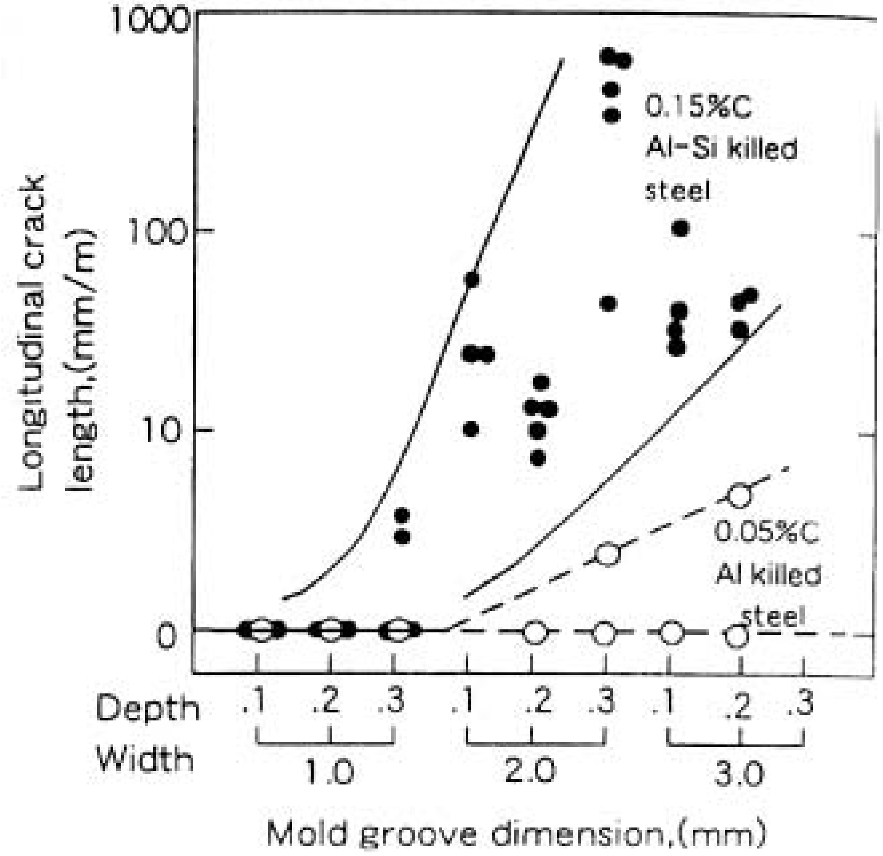

Fig. 21.8 Effect of mold groove depth on the occurrence of longitudinal facial cracks on a CC slab. *From Ref. 16.*

4. Deviation from unity of the ratio of cooling water flow rate per unit of surface area for the wide face to that of the narrow face.
5. Abrupt change in the meniscus level in the mold.
6. Excessively cool meniscus temperature during transient periods of casting.
7. Turbulent and/or asymmetric biased flow of the melt out of the SEN into the mold.
8. Irregular mold oscillation.
9. Intensive spray cooling below the mold (particularly with cool water).

Otherwise, most influential to the occurrence of the cracks are:

10. Peritectic steels, and
11. Mold flux properties.

Among them, 1–6, 8 and 9 have been more or less resolved; hence, the influence of 7, 10 and 11 has become more important in parallel to the progress of high-throughput/high-speed casting.

For peritectic 0.1–0.2% C steels, many investigations have been made since the pioneering work, including the above-mentioned metallographical study by Kohno et al.;[15] production scale crack formation tests with artificial mold defects by Saeki et al.;[16] and a mathematical model calculation by Matsumiya et al.[17] According to Saeki et al.,[16] the crack occurs where heat extraction is 10% less than that of the normal part.

Nakato et al.[18] made extensive two-dimensional measurements of mold temperature. They found, as shown in Fig. 21.9, that the crack increases with the widthwise irregular distribution of mold

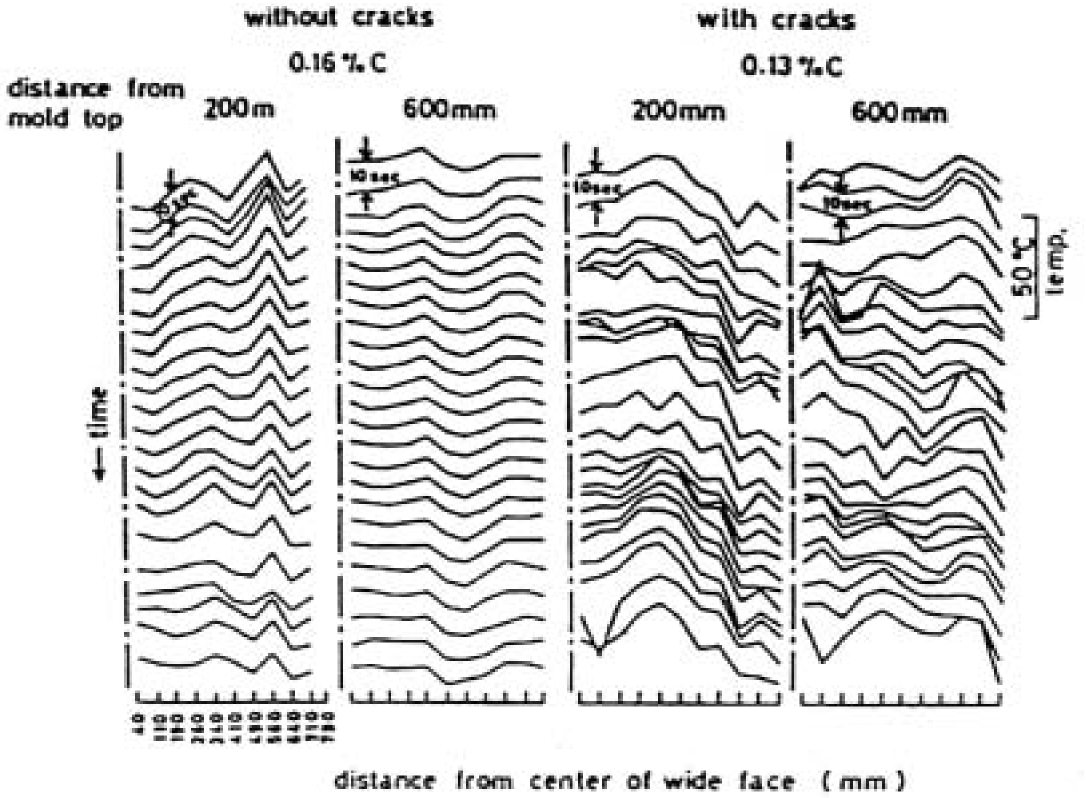

Fig. 21.9 Irregular widthwise mold temperature distribution from the meniscus to 600 mm below for a peritectic steel slab with longitudinal cracks (right). *From Ref. 18.*

temperature and an increased rate of local temperature fluctuation in the mold. Also, the irregular distribution and increased rate of fluctuation initiate at the meniscus in the mold and extend to 600 mm below the meniscus without being appreciably reduced. Locally excessive inflow of mold flux occurs between the mold wall and the top end of the shell near the meniscus, and the delay in the shell growth continues, amplifying to the bottom of the mold.[18]

The excessive local streak of mold flux is caused by (a) the irregular formation of the initial solidification shell along the mold perimeter that is caused by submeniscus flow turbulence and meniscus level fluctuation and (b) excessively fluid mold fluxes, especially those with slower melting rates.

From those investigations, the sequence of the occurrence of longitudinal facial cracks has been shown to be as follows:

1. Peritectic steels exhibit, as summarized by Schwerdtfeger,[19] twice as large a volume contraction as ordinary carbon steels upon the peritectic transformation.
2. When the shell is formed in the mold, the peritectic transformation occurs some distance inside the shell surface and near the solid/melt boundary. This causes the large contraction inside the shell that makes the shell surface deform concave against the mold wall.
3. When there persist areas where the shell is hot and weak due either to the excessive infiltration of mold flux or to the defect on the mold wall, those areas are lifted from the mold wall, resulting in micro air gaps and further delays of solidification.
4. The concave areas are in better contact with the mold wall, becoming stronger as the temperature is lower, and are more or less constrained so as not to shrink; hence, the shrinkage strain concentrates on the lifted hot areas.

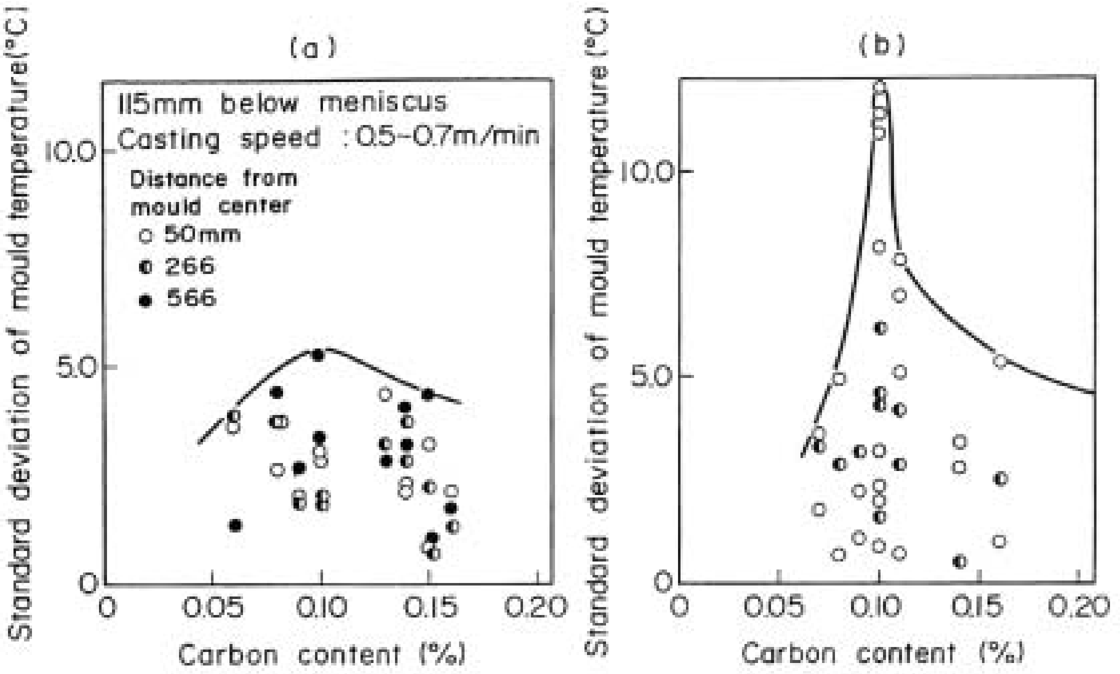

Fig. 21.10 Mold temperature fluctuation with a conventional mold (a) and a mild cooling grooved mold (b). *From Ref. 21.*

5. Consequently, dendrites there are torn apart, and the crevices are filled by solute-enriched interdendritic melt.
6. When the surface of the lifted areas undergoes intensive cooling below the mold, thermal stress overcomes the strength of the lifted areas and causes a crack.
7. In an extreme case, where mold taper is too shallow, the surface of the lifted area will also be split open and cause a crack.
8. High S content and a low [Mn]/[S] ratio in the steels increase the cracks.
9. In conventional casting, occurrence of the cracks (today, mostly Type-2 LFC) increases with casting speeds faster than about 2 m/min.

Sugitani, Nakamura and Watanabe[20] found that a reduced rate of heat extraction (two-thirds the normal rate) during initial solidification in the mold served to form the uniform initial shell for peritectic grades. Nakai et al.[21] tried to fabricate a micro air gap by machining fine vertical grooves on the inner faces of the mold in order to increase the interfacial heat transfer resistance for mild cooling of peritectic steel slabs. They succeeded in decreasing the heat flux from the shell to the mold by 30% and, as shown in Fig. 21.10a, decreasing temperature fluctuation in the mold plate by 50%. This reflects the formation of a uniform shell. In fact, the unevenness of the shell thickness and the occurrence of Type-2 LFC decreased by 50%, as shown in Fig. 21.11. However, the mild cooling mold with fine grooves was not industrialized due to the difficulty of maintaining the groove against wear.

Uniform infiltration of mold flux film was considered by Nakato et al.[18] as one of the most effective and practicable means to achieve the mild and uniform cooling of the initial shell in the mold. Kyoden, Doihara and Nomura[22] materialized this with a somewhat basic mold flux [(%CaO) / (%SiO_2) = 1.2–1.4] that crystallizes around 1200°C, successfully reducing the cracks at a relatively high speed of casting. Ohmiya and Schwerdtfeger[23] showed by experiments with a hot simulator that the heat transfer resistance at the flux film/mold boundary shares a large fraction of the total heat transfer resistance between the molten metal and the cooling water in the mold.

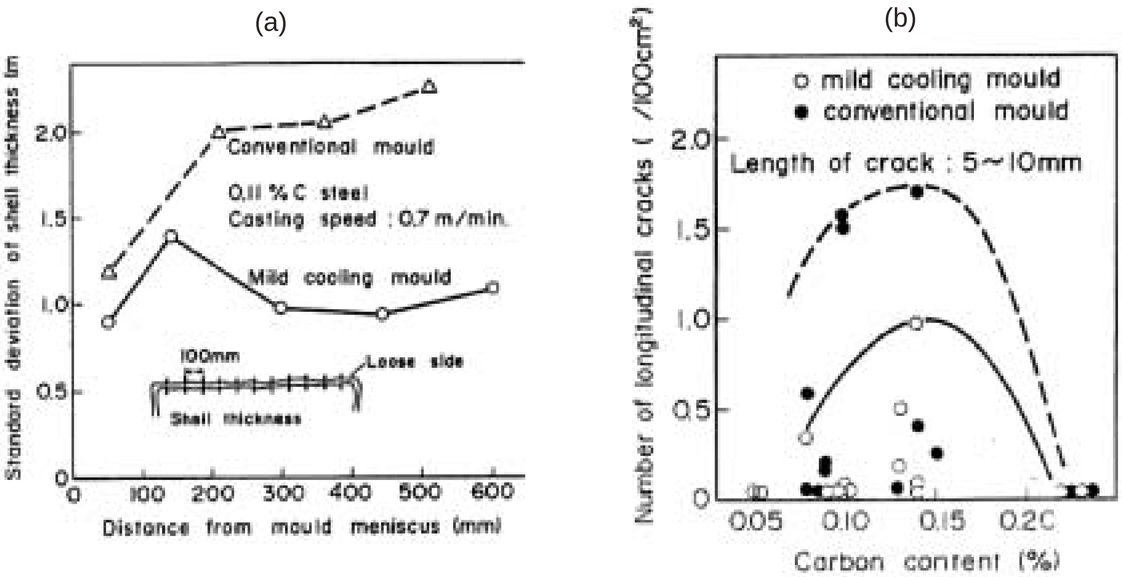

Fig. 21.11 Improved uniform shell growth (a) and longitudinal facial cracks (b) with a mild cooling grooved mold. *From Ref. 21.*

Fig. 21.12 Heat transfer resistance of flux film and flux/mold interface. *From Ref. 25.*

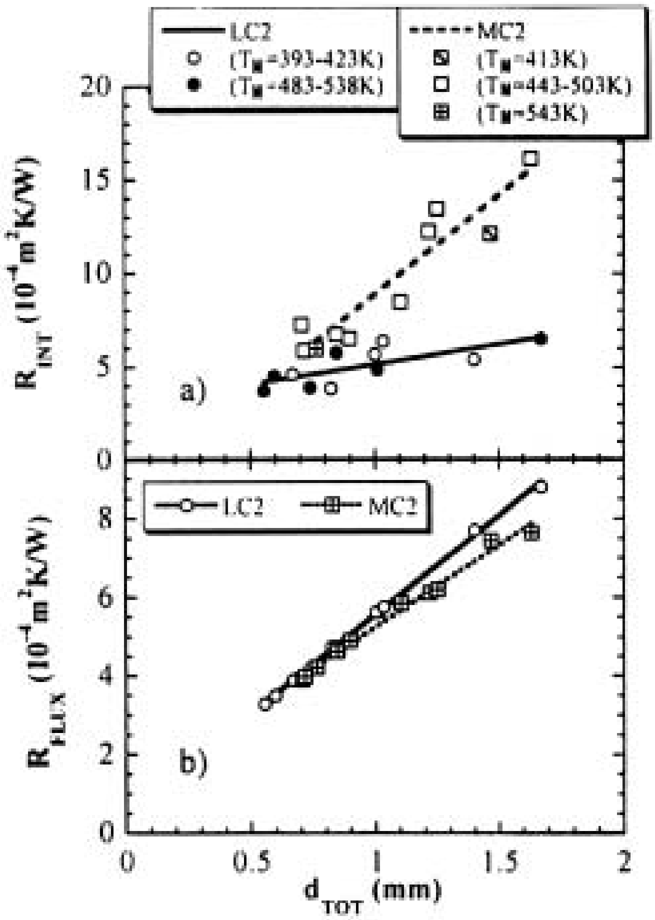

Yamauchi et al.[24] made it clear—with a method similar to that of Ohmiya and Schwerdtfeger[23]—that the basic and crystallized film reduces the total heat flux by increasing the micro air gap at the flux/mold boundary.

In fact, the basic and crystallized film reduces both radiation heat transfer through the film (by the reflection at the crystal boundaries) and conduction heat transfer at the mold/film boundary (by increased surface roughness, i.e., a micro air gap, caused by the crystallization), as shown quantitatively by Cho et al.[25] The micro air gap generated by the coarse surface of the basic crystallized flux at the flux/mold boundary shared nearly 50% of the total resistance to the heat transfer, as shown in Fig. 21.12, where LC represents low-carbon steel mold flux and MC represents medium-carbon peritectic grades mold flux. d_{tot} is the total thickness of the flux film. In the case where the gap between the SEN and the mold wall is too narrow, the supply of mold flux melt is impeded, generating this type of crack.

A detailed thermal elastic-plastic analysis by Kinoshita, Emi and Kasai[26] has shown that:

1. Although the surface of the shell is under compression all the way down to the bottom of the mold, tension is in operation beneath the skin.
2. When the tensile strength acts on the solidification front, where the shell is yet brittle by the existence of solute-enriched interdendritic melt, cracks form between columnar dendrites, pulling the liquid in between.
3. The cracks place the skin of the shell under tension, but the temperature of the skin is somewhat cooled to a ductile range; hence, the skin can deform without opening cracks on the shell surface.
4. However, if an air gap is formed, a hot spot occurs there, increasing the skin temperature again to the brittle range, and cracks open.
5. Below the mold, cracks can open, too, as the skin temperature comes into another brittle temperature range.
6. Proper narrow-face taper prevents the development of the hoop stress in the skin.

These observations reveal that the sequence of the formation of the longitudinal facial cracks is the following:

1. The growth of uniform shell is adversely influenced by (a) turbulent metal flow and (b) meniscus level fluctuation in the mold, as these factors promote local change in the starting height of shell formation in the mold, irregularity of the infiltration of mold flux in the shell/mold gap, and the formation of hot spots on the shell by the impinging melt stream.
2. The irregularity of the mold flux infiltration is increased by a too viscous or too fluid mold flux. An excessively low temperature of metal flow and a nonuniform application of mold flux also increase the irregularity. An insufficient supply of the flux melt can take place for the former flux at the SEN-inhibited mid-face of the shell. For the latter flux, a localized excessive supply of the fluid flux melt can occur. The turbulent flow and meniscus level fluctuation, often found in transient operations, enhance the above adverse effects.
3. Where the flux infiltration is excessive, heat transfer from the shell to the mold is reduced to form a hot point on the initial shell. The hot point develops toward the casting direction as hot streaks.
4. Where the infiltration is scarce, the shell gets cooler and thicker. Temperature gradients across the hot and cold parts and toward the thickness direction of the shell generate local thermal stress. The stress increases with intensive cooling in the mold

that is caused by a thin Cu mold, by cold mold-cooling water, and by mold fluxes forming a thin, glassy film at the shell/mold boundary near the meniscus.

5. Mold fluxes forming a glassy film at the mold/shell boundary promote excessive heat transfer from the shell, since heat transfer resistance at the boundary decreases and radiation heat transfer increases. The rapid cooling results in quick solidification and contraction that forms a nonuniform initial shell. Hot spots arise at convex areas of the shell, as evidenced by mold temperature monitoring, thereby developing local stress.

6. Two additional stresses are imposed on the shell. One arises from the volume change on the solidification of the initial shell, acting along the mold perimeter. The peritectic transformation occurring in peritectic carbon and stainless steels doubles the volume contraction. The other is frictional stress, acting between the shell and mold, that is caused by mold oscillation and strand withdrawal.

7. Tensile strength of the initial shell somewhat below the meniscus near the solidus temperature is very low, less than 10 MPa, and is not sensitive to the carbon content of steel but is sensitive to impurities that lower the melting point of the interdendritic melt. The strength and ductility of the peritectic steels in the temperature domain for the peritectic transformation are considerably decreased by increased [S]. The strength at the hot streaks is even lower, perhaps 1–5 MPa, due to higher temperatures.

8. When the sum of the stresses overcomes the shell strength at the hot streaks, the shell is pulled apart and forms interdendritic cracks along the hot streaks, provided that the cracks are not healed by the interdendritic melt. The cracks are reported to occur where the shell thickness is thinner by more than 10% near the meniscus.[16]

9. As the shell is withdrawn, solidification proceeds to make the shell thicker. The contraction of the shell increases, particularly at the wide face of the slabs, to pull the shell away from the narrow face. If the narrow-face taper is too shallow (approx. ≤ 1%), an air gap forms between the shell and narrow face, making static pressure of the melt in the crater act as a hoop stress on the shell. Choice of the taper should be made with full awareness of the compromise between corner crack formation and mold wear.

10. When the thermal and hoop stresses are increased in the mold to make the sum of all stresses overcome the tensile strength of the shell at the hot streaks, the shell fractures along the streaks as well. The fractures in such a case are intergranular and without healing, and they run through the boundaries of austenite grains that are coarsened by exposure to higher temperatures beneath the hot streaks.

11. The cracks usually propagate longer and deeper into the shell below the mold in the secondary cooling zone because of an additionally generated thermal stress from an intensive and nonuniform spray-water cooling. This type of crack increases when the spray cooling is so intene as to bring the shell surface into the brittle temperature range II (embrittlement by MnS film precipitation at γ-grain boundaries) that is schematically shown in Fig. 21.13 by Suzuki, Nishimura and Yamaguchi.[27] Brittle temperature range I stands for the near-solidus temperature range, as discussed earlier.

12. Poor maintenance of passline alignment, rolls and roll gaps that contributes to additional shell stress increases the cracks.

13. In billet casting, rhomboidity gives rise to the formation of cracks. Rhomboidity arises from uneven cooling of the faces of the CC mold.

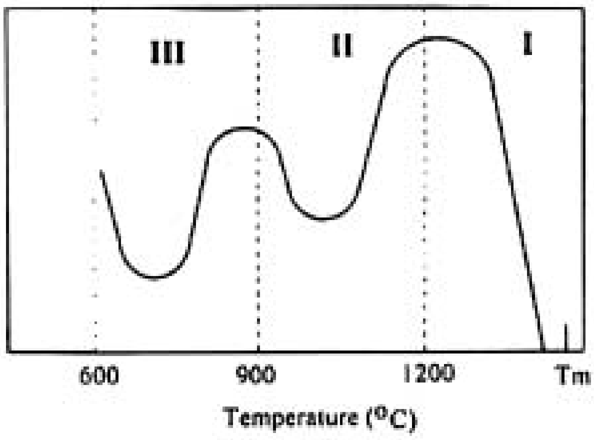

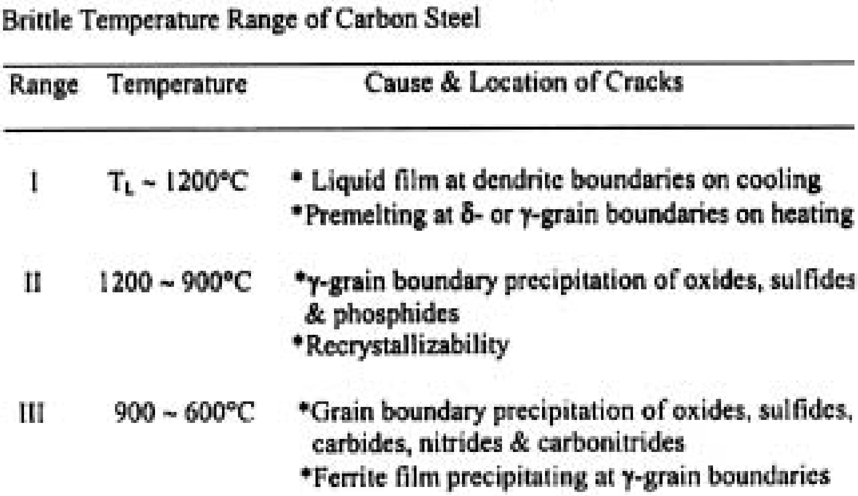
Brittle Temperature Range of Carbon Steel

Range	Temperature	Cause & Location of Cracks
I	T_L ~ 1200°C	* Liquid film at dendrite boundaries on cooling *Premelting at δ- or γ-grain boundaries on heating
II	1200 ~ 900°C	*γ-grain boundary precipitation of oxides, sulfides & phosphides *Recrystallizability
III	900 ~ 600°C	*Grain boundary precipitation of oxides, sulfides, carbides, nitrides & carbonitrides *Ferrite film precipitating at γ-grain boundaries

Fig. 21.13 Three high-temperature brittle ranges of carbon steel. *From Ref. 27.*

Countermeasures to prevent the cracks, therefore, are the following:

1. Minimize the turbulence of metal flow, particularly submeniscus flow, by optimizing metal transfer operations and tundish design during transient periods and by using an electromagnetic flow controller for high-throughput casting and round billet/bloom casting.

2. Minimize meniscus fluctuation by utilizing integrated control of metal transfer from the ladle to the tundish to the mold and by reducing nozzle accretion with cleaner melts and less reoxidation during casting.

3. Minimize excessive temperature drops during transient operations by optimizing ladle and tundish preheating, ladle stirring, metal transfer operations, and with tundish heating.

4. Reduce heat transfer in the mold by the use of a slightly basic mold flux having a higher crystallizing temperature that provides the flux film with a rough surface at the mold/film boundary. The surface roughness (micro air gap) and crystallized film reduce, respectively, the conduction and radiation heat transfer from the shell to the

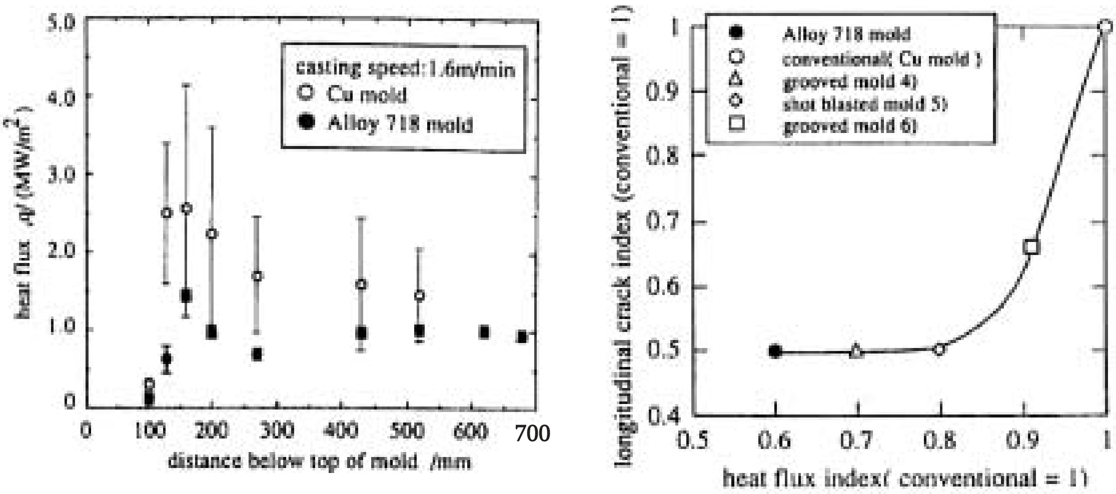

Fig. 21.14 Decrease in heat transfer and longitudinal cracks by mild cooling in a CC mold. *From Ref. 28.*

mold. Consequently, more uniform heat transfer and, hence, uniform growth of the shell results, thereby decreasing excessive development of localized heating and resultant shell stresses.

5. Use a mold made of a heat-resistant alloy that has low thermal conductivity. So far, low thermal conduction has been synonymous with inferior heat resistance that causes sticker breakouts and intolerable wear. Yamauchi et al.[28] applied Alloy 718 (53% Ni, 19% Cr, 3% Mo, 19% Fe, 5% [Nb + Ta], 0.5% Al and 0.9%Ti) to a pilot plant CC mold (110 mm T x 400 mm W x 700 mm L), and obtained promising results, as shown in Fig. 21.14.
6. Implementation of an air-mist spray system for the secondary cooling is effective for avoiding nonuniform and excessive cooling below the mold. Kohno et al.[29] showed that the occurrence of the cracks decreased to 1/18 for larger cracks (Type-1 LFC) and 1/10 for smaller cracks (Type-2 LFC-2) with the mist cooling.

21.3.1.2 Longitudinal Corner Cracks

21.3.1.2.1 Characteristics

An example of longitudinal corner cracks is shown in Fig. 21.15. This type of crack occurs in the vicinity of the corner of billets and blooms in the

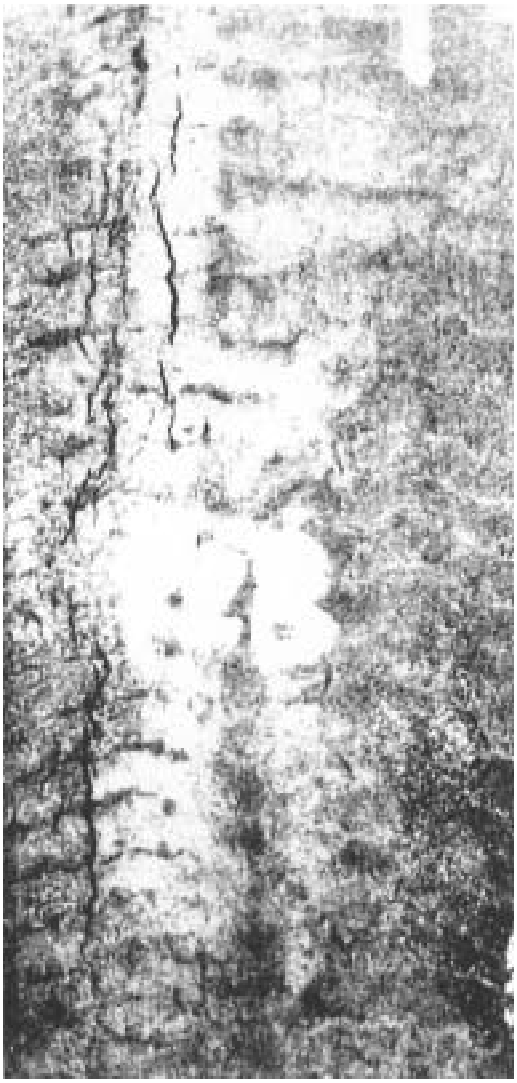

Fig. 21.15 Longitudinal corner crack (courtesy of NKK).

withdrawal direction, often along the middle of the quadruple circle of the strand at the corners of the mold or along the junction between the corner and face. Slabs also experience this type of crack in high-speed casting of peritectic grades. Features of the cracks are the same as those for the longitudinal facial cracks. Conditioning is unavoidable. Heavy cracks can cause breakouts.

21.3.1.2.2 Influential Factors, Causes and Countermeasures

Major factors that generate cracks include the following: turbulent melt flow, meniscus fluctuation, erratic impingement of metal flow in the mold, a mold profile causing bulging and/or nonuniform cooling that brings forth a local delay in shell growth, excessively high temperature of the melt in the mold, and thermal stress arising from intensive cooling of strand corners in the secondary cooling zone.

The mechanism for the occurrence of longitudinal corner cracks is largely the same as that of longitudinal facial cracks. Thermal elastic-plastic analysis by Kinoshita, Kitaoka and Emi,[30] validated by commercial casting, explains that the corner cracks occur in the following sequence, as shown only partly in Fig. 21.16, where the deformation of the contour of the outer surface of the shell is in shown in µm on the bottom left axes:

1. Some distance below the meniscus, a shell is formed all along the perimeter of the mold that shrinks due to the cooling on the wide face, thus pulling the narrow-face shell away from the mold wall to form an air gap when the mold taper is shallower and not consistent with the shrinkage.

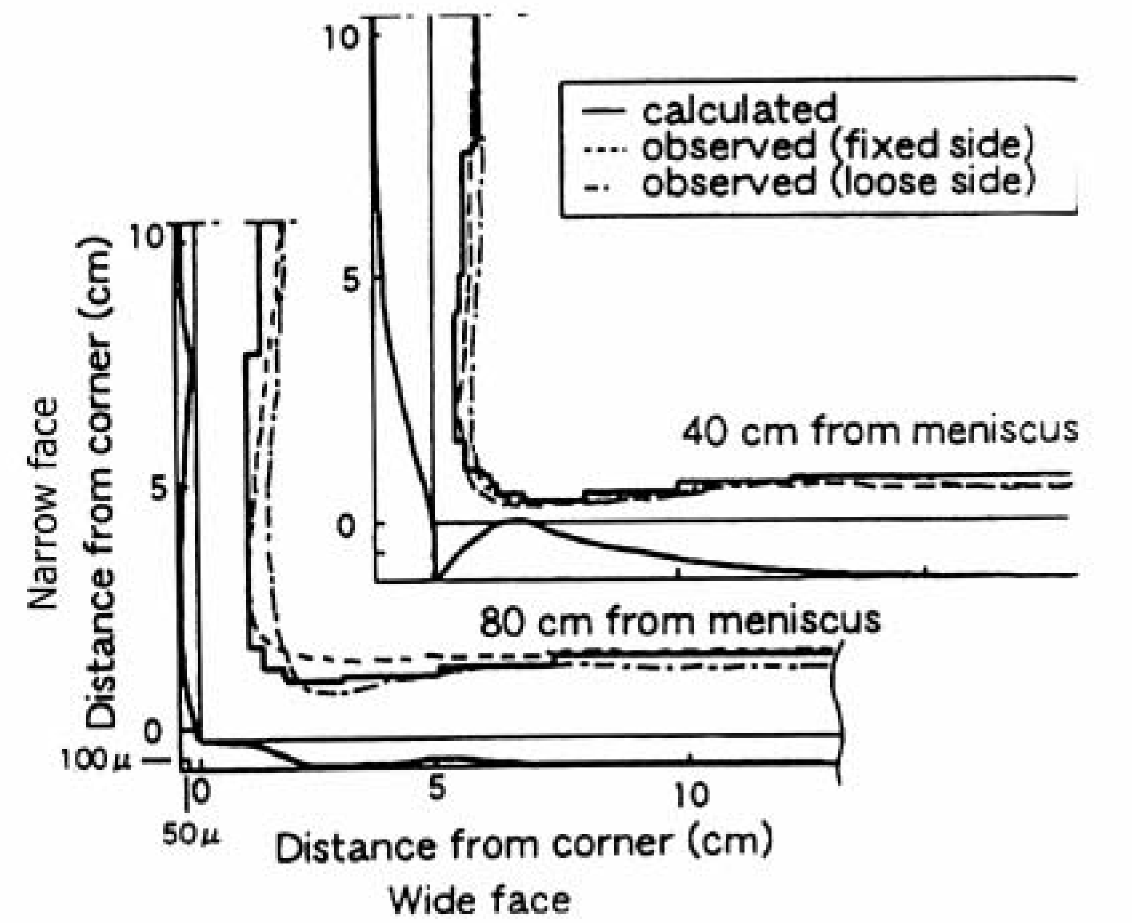

Fig. 21.16 Calculated contour of a slab solidifying in a CC mold. *From Ref. 30.*

2. The narrow-face shell is reheated by the air gap, and the strength is decreased, whereas the corner of the shell is grown in a thick rectangular channel shape due to two-dimensional heat extraction at the corner.
3. Static pressure imposed by the molten steel makes the weak mid-face of the shell bulge toward the mold wall, but not much near the corner area, since the corner shell has become a stiff rectangular channel. Thus, an air gap is created near the stiff corner of the narrow-face shell.
4. The bulging, however, makes the corner shell rotate somewhat toward the adjacent face, thereby detaching the near corner part of the shell of that face away from the mold wall. This results in air gap formation on the adjacent shell at the near corner area in the withdrawal direction.
5. Thus, hot and brittle streaks occur at the air gap near the corner on either or both sides of the two faces.
6. For billets and blooms, increased rhomboidity causes the cracks on the corners that are expanded beyond the rectangular angle. The rhomboidity is enhanced by: (a) uneven cooling between the four faces of the mold, (b) excessively strong cooling in the mold, (c) the same for secondary cooling by the water spray covering the strand corners, (d) misalignment of support rolls and the mold, and (e) weak containment by the support rolls of the strand.

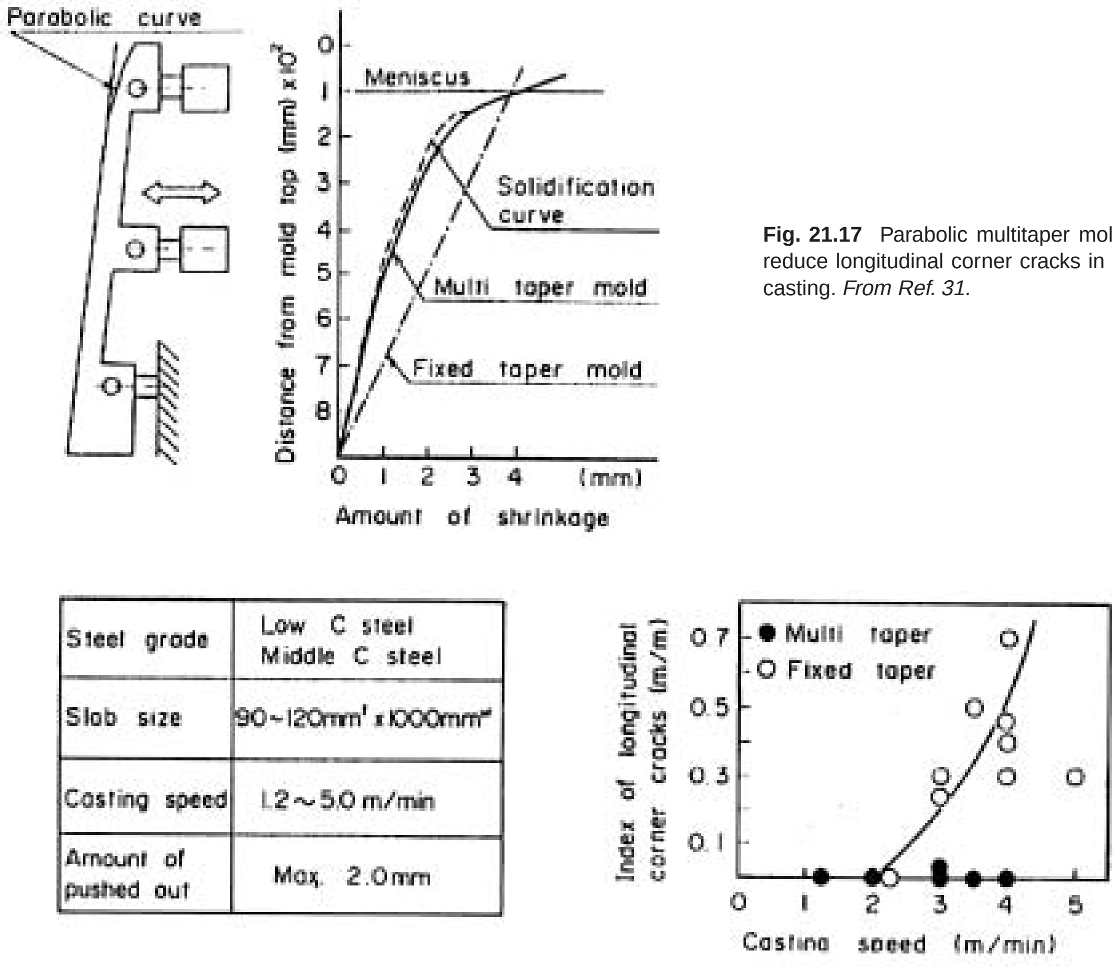

Steel grade	Low C steel Middle C steel
Slab size	90~120mm^t x 1000mm^w
Casting speed	1.2~5.0 m/min
Amount of pushed out	Max. 2.0mm

Fig. 21.17 Parabolic multitaper mold to reduce longitudinal corner cracks in slab casting. *From Ref. 31.*

7. The stresses arising from the solidification, thermal gradient, shrinkage and deformation (against the rhomboidity) pull the streak apart, forming the longitudinal corner cracks.

Effective countermeasures that contribute to decreasing the cracks are, as in the case of longitudinal facial cracks, to minimize the internal stress rate caused by volume contraction and the external stresses of thermal and bulging origin, and to maximize the shell strength by decreasing the contents of impurity elements. The following measures have been reported to be effective:

1. Implementation of electromagnetic flow control to minimize the turbulent flow in the mold, and integrated optimization of the equipment and its operation to reduce meniscus level fluctuation.
2. Conversion from “oil casting + block mold” to “powder casting + assembled plate mold.”
3. Reduction of the corner radius.
4. Use of parabolic mold taper to compensate for the shrinkage in the mold, as shown in Fig. 21.17 by Murakami et al.[31]
5. Decrease of the specific spray water ratio in the secondary cooling zone.
6. Further desulfurization of the steel melt by flux injection.

21.3.1.3 Longitudinal Flange/Fillet/Web Cracks

21.3.1.3.1 Characteristics

These cracks appear at the flange and web of the strand cast beam blanks, as shown in Fig. 21.18 by Saito, Kodam and Komoda.[32] They look like longitudinal facial cracks but are less frequently accompanied by slag streaks.

21.3.1.3.2 Influential Factors, Causes and Countermeasures

The occurrence of the cracks becomes more marked with:

1. [S] and [Mn],
2. Too low viscosity of mold flux melt,

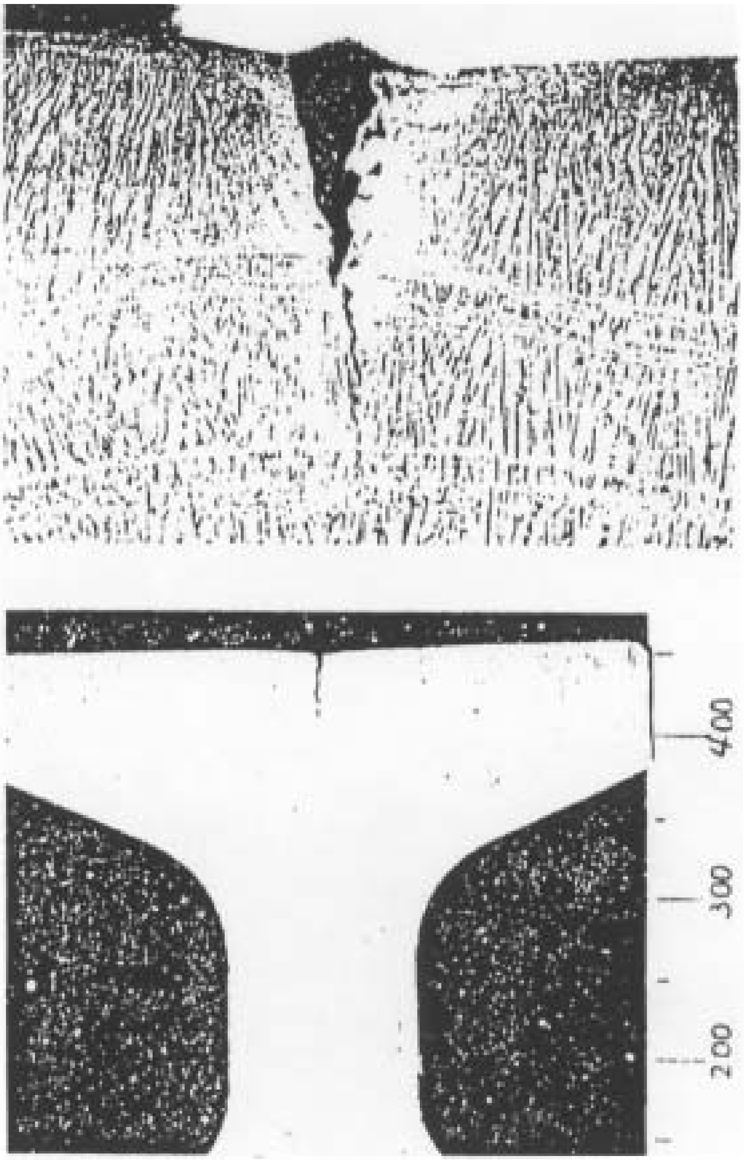

Fig. 21.18 Flange crack on a continuously cast beam blank. *From Ref.32.*

3. Horizontal vibration of mold oscillation that causes displacement of the strand from the designed trajectory,
4. Excessive mold cooling with high flow rates and low water temperatures,
5. Nonuniform cooling of the mold across the flanges and fillets, and
6. Excessive secondary cooling below the mold.

Reasons for the occurrence of these cracks are similar to the longitudinal facial cracks on slabs, blooms and billets. In beam blank casting, however, the strands are more confined by the dogbone type mold; hence, more attention is required to sustain rather slow but uniform cooling of the shell during initial solidification, i.e., securing a uniform flow of mold flux melt into the mold/strand gap, and uniform and mild cooling of the shell in the mold. Also, precise maintenance of the passline is important.

For these objectives, the following measures have been reported effective:

1. Decreasing [S] to be less than 0.015% for [Mn] of 0.5–1.4%, although this limitation can be less strict by having the following factors optimized.
2. Using a relatively more viscous flux melt than that for bloom casting with a reasonable melting rate to avoid localized infiltration.
3. Decreasing the horizontal displacement of the mold during oscillation to be less than 0.3 mm (preferably 0.1 mm), along the order of the liquid mold flux film thickness.
4. Decreasing the mold cooling water flow rate, using warm water for cooling, particularly in winter in a cold area, and optimizing a slit pattern for the mold cooling water.
5. Implementing mold taper not only on the flange side, but also on the fillet side (0.9%).
6. Decreasing the application of secondary spray water below the mold.

Kim et al.[33] developed a two-dimensional transient coupled thermoelastoplastic finite element model and obtained results similar to number 5 mentioned above.

21.3.2 Transverse Cracks

Transverse cracks are commonly experienced major cracks usually found on slabs, blooms and billets. The mechanism of their formation and measures to prevent them have been made clear. However, the increased popularity of high-rate production of microalloyed steels and hot direct rolling has made

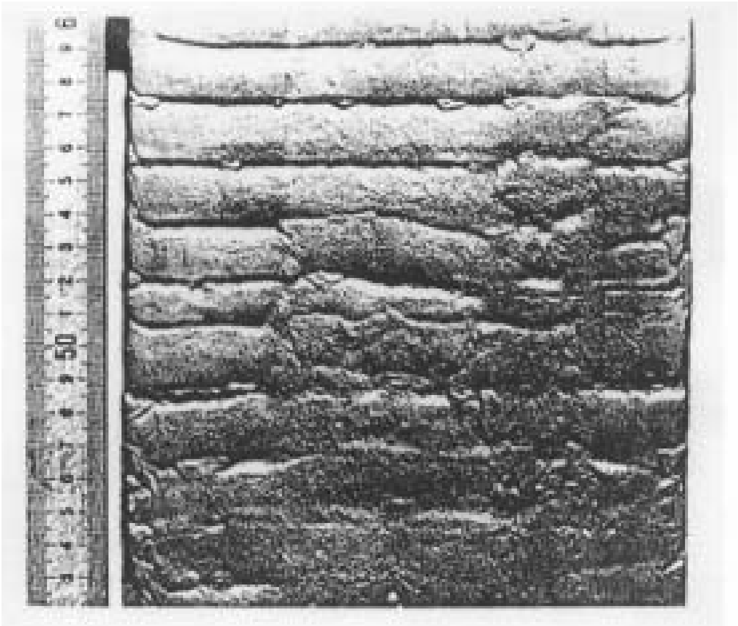

Fig. 21.19a Deep oscillation marks that caused transverse facial cracks. *From Ref. 34.*

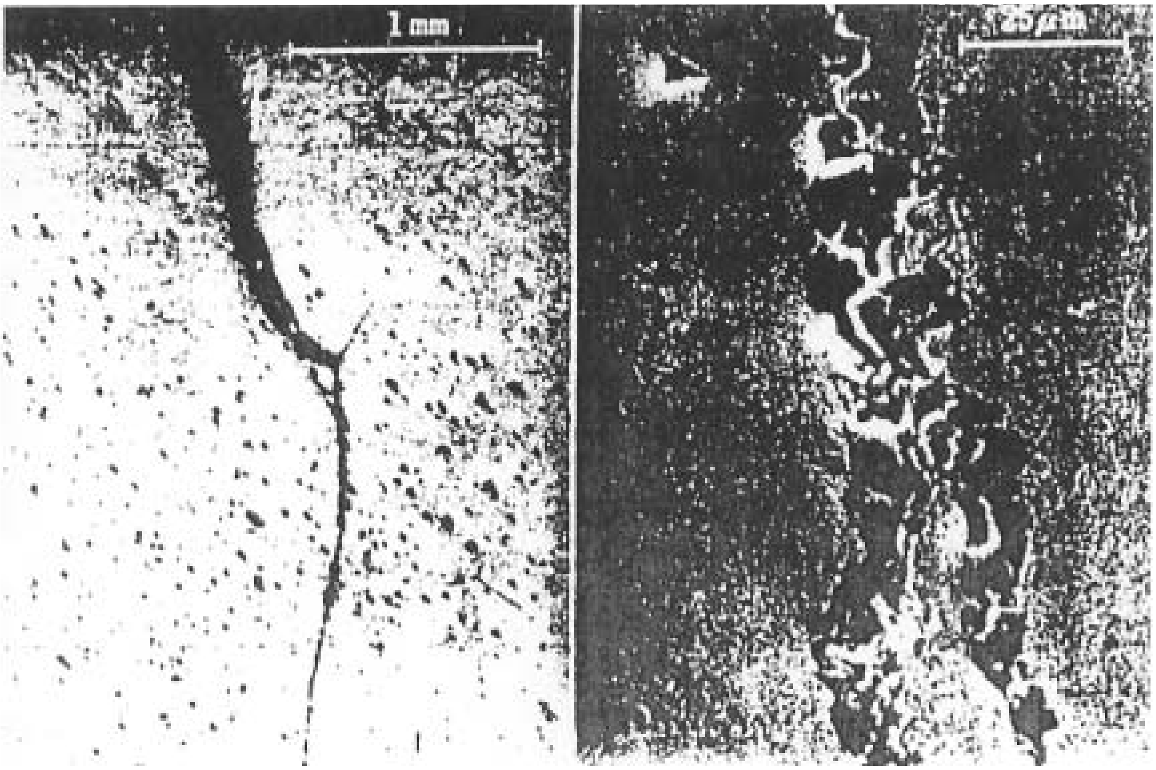

Fig. 21.19b Cross-sections of transverse facial cracks. *From Ref. 34.*

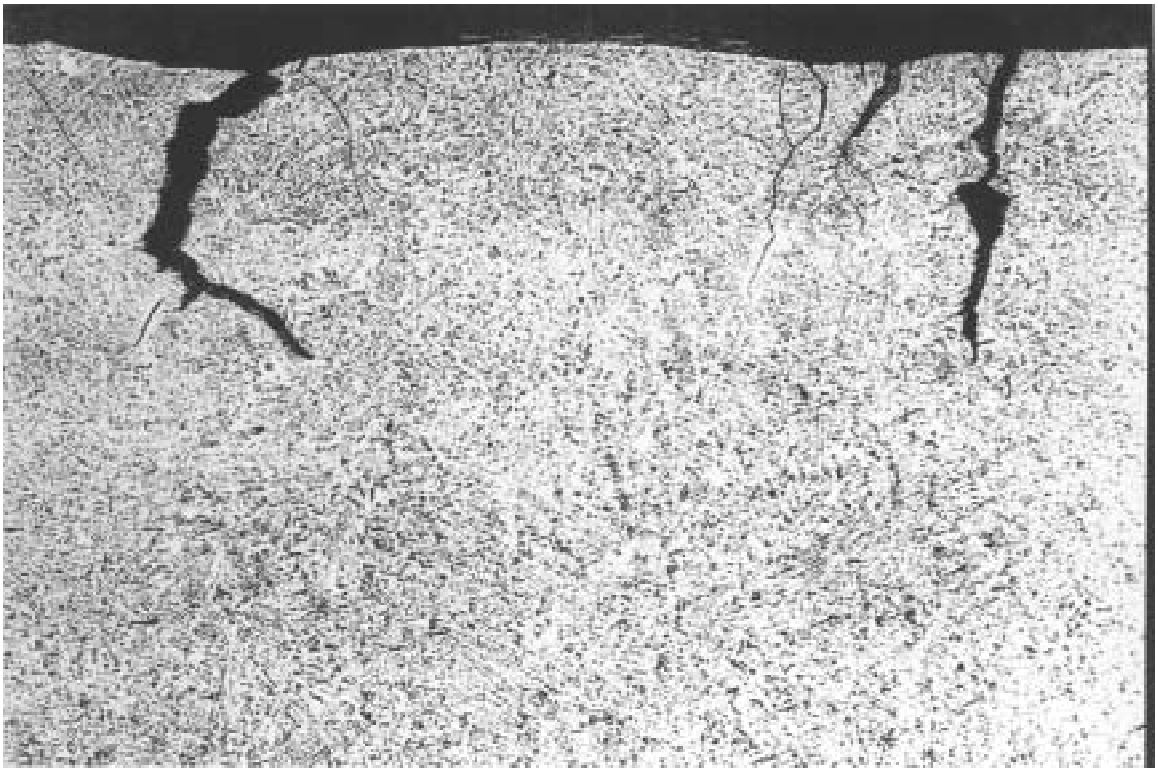

Fig. 21.19c Macroetched cross-sections of transverse facial cracks at oscillation marks.

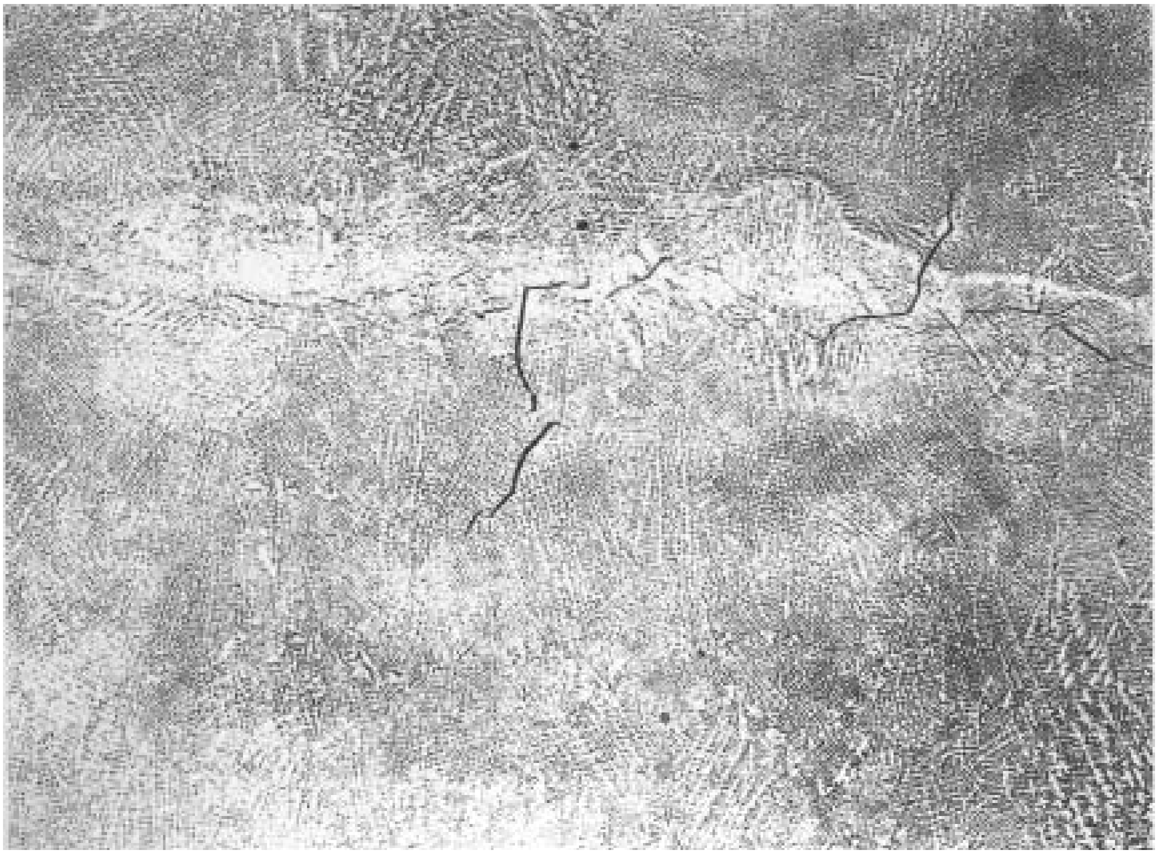

Fig. 21.19d Cracks at the bottom of an oscillation mark revealed by machining (white area is solute segregation).

implementation of the measures not always satisfactory. Complete prevention of transverse cracks remains a moving target.

21.3.2.1 Transverse Facial Cracks

21.3.2.1.1 Characteristics

The cracks originate at the bottom of deep oscillation marks, as shown by Harada et al. in Figs. 21.19a, b,[34] c and d. In the thickness direction, they develop to a shallow depth, form a kink and further propagate along austenite grain boundaries to a depth of 2–5 mm. They run transverse to the withdrawal direction either on the faces or on the corners of strands to a length of 10–100 mm along the oscillation marks. Subscale is usually formed along the cracks from the surface to the kink. However, no subscale is found from the kink to the tip of the cracks. Detailed and careful investigations occasionally identified the precipitates of Nb(CN) and/or AlN near the cracks. Transverse depressions usually accompany the transverse cracks. SC-grade high-carbon steels under unfavorable conditions show intergranular cracks of this kind with internal oxidation and decarburization, and they require conditioning.

21.3.2.1.2 Influential Factors, Causes and Countermeasures

The observation shown in Fig. 21.19b and the theoretical calculation of the thickness of the subscale indicate that the cracks formed in the mold and propagated in the top part of the secondary cooling zone to the kink.[35] The cracks further develop from the kink to the top in discernible sizes during unbending.

The occurrence of the cracks is influenced by the strength/ductility of the shell surface and the stress/strain imposed on the shell. The former depends on steel chemistry and the temperature of

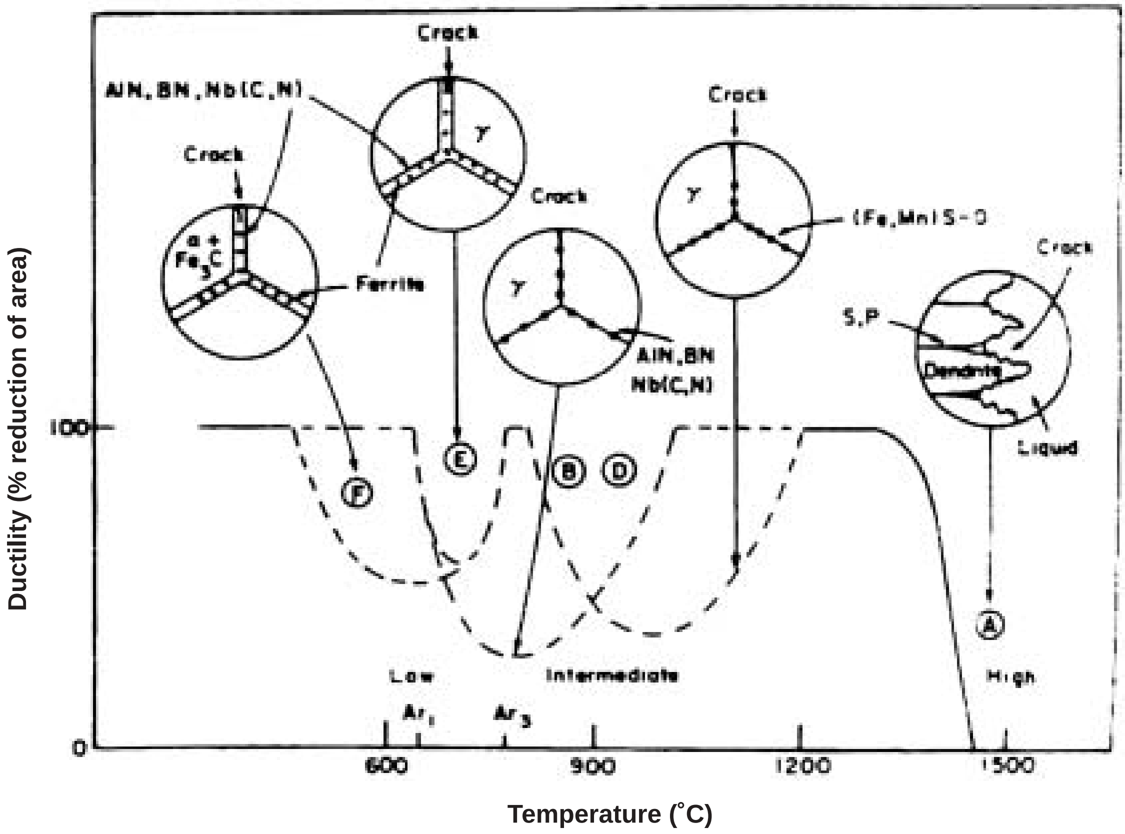

Fig. 21.20 Modified conceptual high-temperature brittle range of steel. *From Ref. 37.*

the shell, whereas the latter depends on thermal and mechanical origins. The cracks become appreciable when the following conditions are met:

1. Unbending of the strands occurs in the brittle temperature range of 750–850°C (can be 700–900°C). The brittleness in this temperature range has been confirmed to be due to (a) hardening by the precipitation of fine AlN, Nb(C, N), VN and/or V_4C_3 and/or (b) precipitation of a ferrite film along the austenite grain boundaries during $\gamma \rightarrow \alpha$ transformation, as previously shown in detail by Suzuki et al.[36] and later modified by Thomas et al. in Fig. 21.20.[37]
2. Peritectic steels and steels containing [C], [N], [Al] and [Nb] (occasionally [V]) in excess of superficial solubility product (3–5 x 10^{-4} for [Al][N], depending on the grade of steels). The peritectic steels give rise in the strain due to the contraction upon peritectic transformation and become brittle due to coarse γ-grain formation. In steels containing the above solute elements, on the other hand, the fine precipitates (a few tens of nm) form in the secondary cooling zone at the grain boundaries of the shell surface. These precipitates make the strand surface brittle at 700–900°C ,where unbending was usually practiced. For [Nb], Miyashita et al.[38] showed Fig. 21.21 as an empirical criterion for the carbonitride formation. Not only the precipitation of Nb(C, N), but also the inhibition of dynamic recrystallization of γ-grains are considered responsible for the embrittlement by Nb. Mintz reviewed the influence of N, V, Ti and residuals (Cu, Sn, S and P) on the hot ductility of steels.[39]
3. Intensive water-spray cooling, resulting in nonuniform and excessive cooling of strand surface. The surface undergoes overcooling below A_3 in the water pool above the support roll/strand contacts in the top zone of the strand, and subsequent

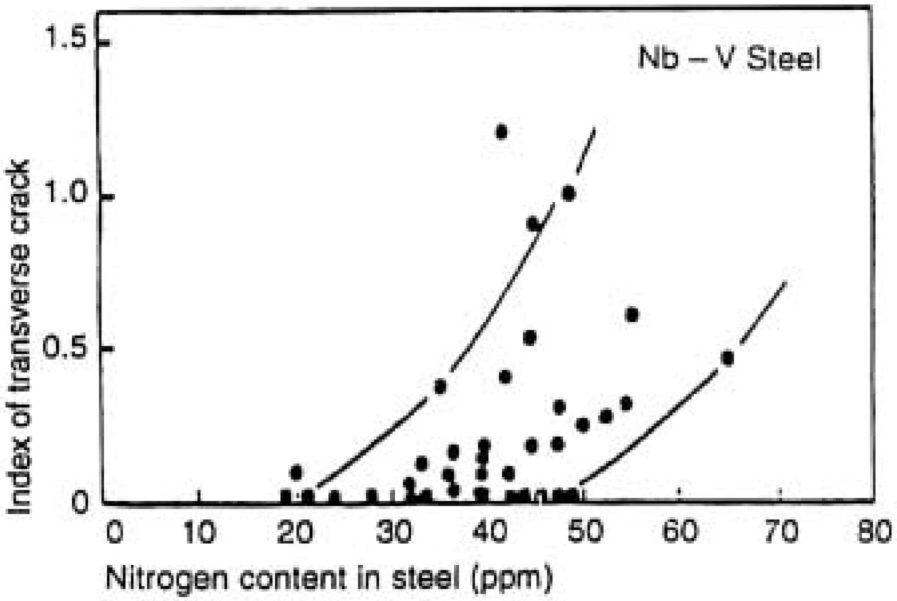

Fig. 21.21 Transverse crack as influenced by precipitation of NB caronitrides. *From Ref. 38.*

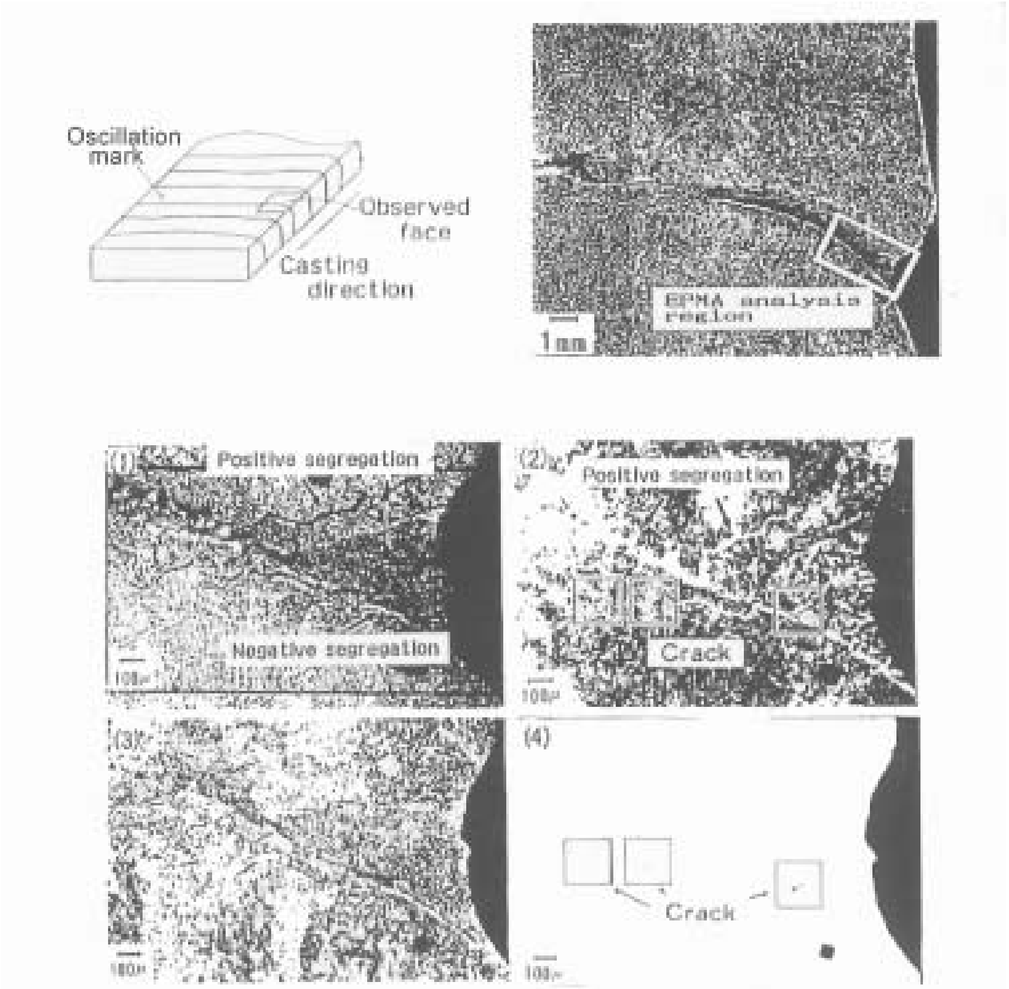

Fig. 21.22 Transverse cracks at oscillation marks.

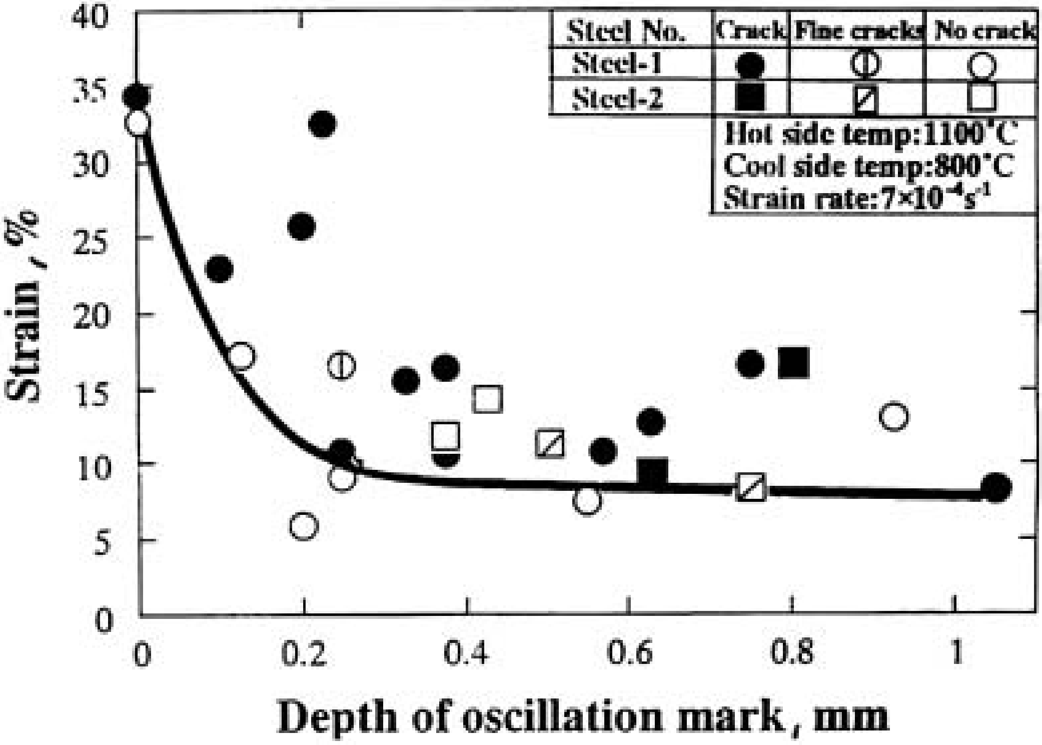

Fig. 21.23 Effect of oscillation mark depth on ductility. *From Ref. 41.*

reheating above A_3 after passing the support rolls. The fine precipitates of AlN do not form until 800°C (770–850°C) on cooling, but they do precipitate at 700–1000°C on heating. Accordingly, the above thermal cycles, repeated cooling and reheating across the critical temperature between the rolls in the secondary cooling zone, promote the precipitation, making the grain boundaries even more brittle.

4. Steels containing Ni. They are susceptible to the transverse cracks when intensive secondary cooling is adopted for unbending. Studies reveal that this is due to the combination of the facts that (a) the brittle temperature range extends to the low-temperature side with Ni and (b) tightly adhered scale, a characteristic of Ni-containing steels, increases the breakdown temperature of film boiling in the secondary cooling. In other words, transition boiling occurs at a higher temperature, impeding uniform cooling.[40]

5. Deep oscillation marks, as shown in Fig. 21.22. They effectively increase the occurrence of the transverse cracks by decreasing the critical strain above which the cracks can form on the strand surface. Suzuki et al.[41] have shown that the oscillation marks act as a notch to considerably decrease the high-temperature ductility of the cast strand. As shown in Fig. 21.23, tolerable critical strain for peritectic high-tensile C-Mn-Al steel containing Nb, Al and N sharply decreases to 1/4 as the mark depth increases from 0 to 0.2 mm (without Nb) or ≤ 0.1 mm (with Nb), and then remains almost constant for a mark depth of up to 1.0 mm. The mark becomes deeper and its curvature smaller with increasing negative strip time (lower oscillation frequency) and lower mold flux viscosity, as shown in Fig. 21.24a and b, resulting in a greater notch effect.

Fig. 21.24a Relationship between oscillation frequency and the depth of oscillation marks for different stroke lengths.

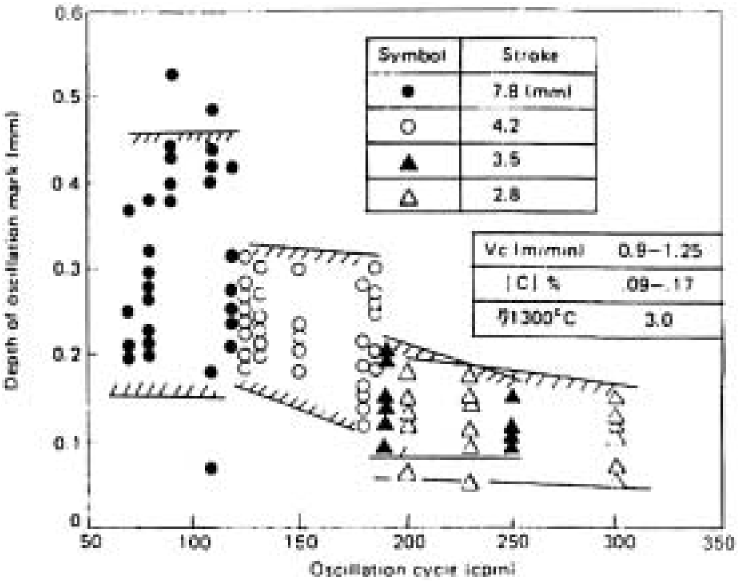

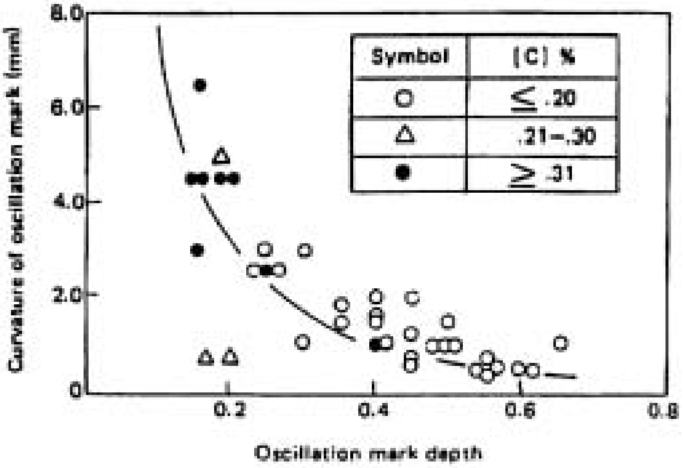

Fig. 21.24b Relationship between oscillation mark depth and the curvature of the oscillation mark.

6. Regarding the different forms of the oscillation marks, Emi et al.[42] investigated in detail the dendrite structure of the marks and revealed two kinds of nail- (or hook-) like marks. They stated, "One form is that an excessive heat extraction developed a thick, nail-like shell which did not bend back toward the mold during withdrawal of the shell despite increasing static pressure of the steel melt. Then, the melt was forced to flow over the tip of the nail, sweeping the flux melt away from the gap between the shell and mold wall, forming a double-skin-like cold shut [see Fig. 21.25a]. This was not the case when a thinner shell formed under mild cooling conditions [see Fig. 21.25b]. The thin shell (nail/hook) was bent back toward the mold wall due to the ferrostatic pressure. The pitch of the marks is found identical to that between the nails (hooks)."

7. In addition to the "Overflow" type and "Bent-back" type, a hybrid type was found by Tomono, Kurz and Heineman[43] that has the tip of the nail/hook somewhat remelted by the overflowing melt. This may be called the "Remelt-Overflow" type. The three types are schematically shown in Fig. 21.26. The Overflow type and Remelt-Overflow type show solute segregation on the upper surface of the nail/hook as the result of melt overflow, which carries over solute enriched melt

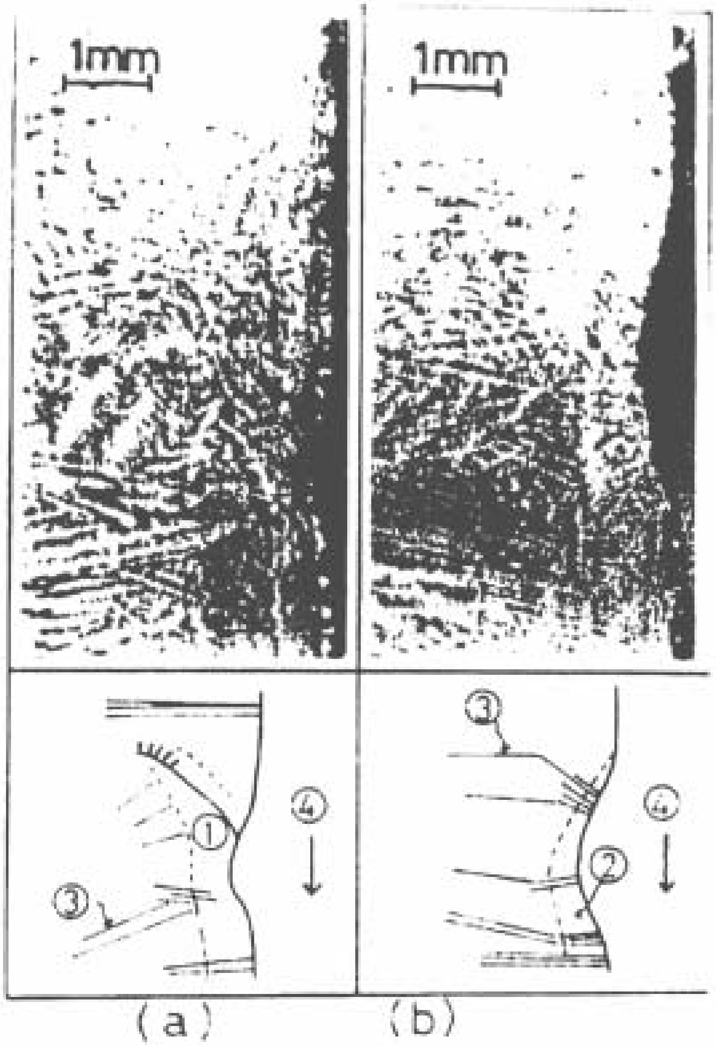

Fig. 21.25 Overflow and Bent-back type oscillation marks. *From Ref. 42.*

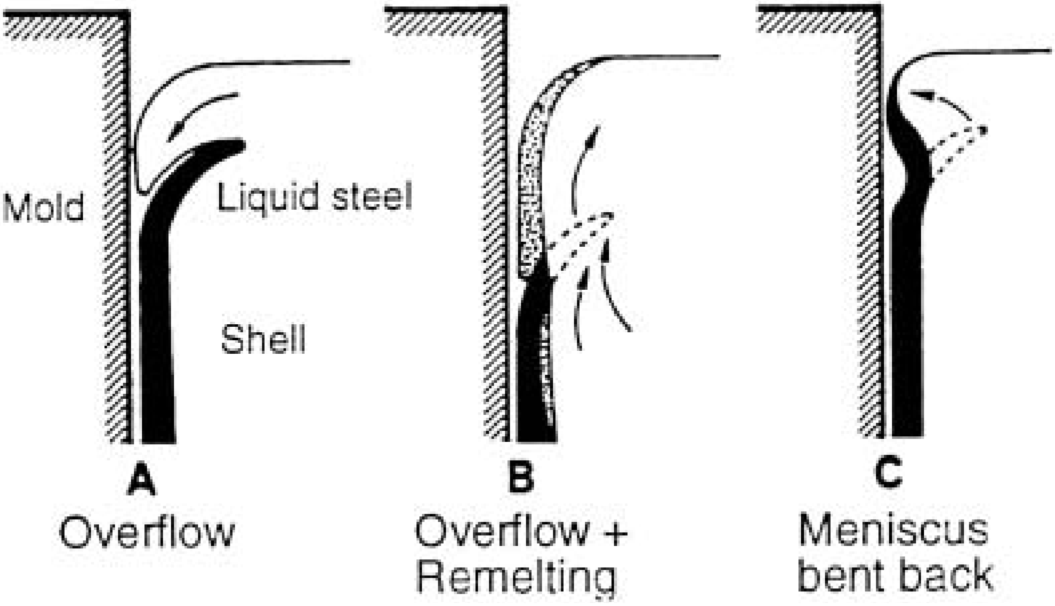

Fig. 21.26 Three modes of oscillation mark formation.

Fig. 21.27a Decreased thermal cycle in secondary cooling with air-mist spray.

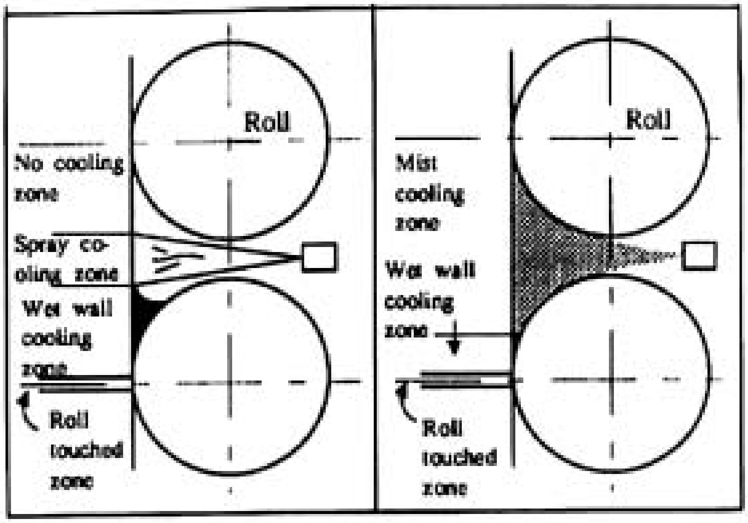

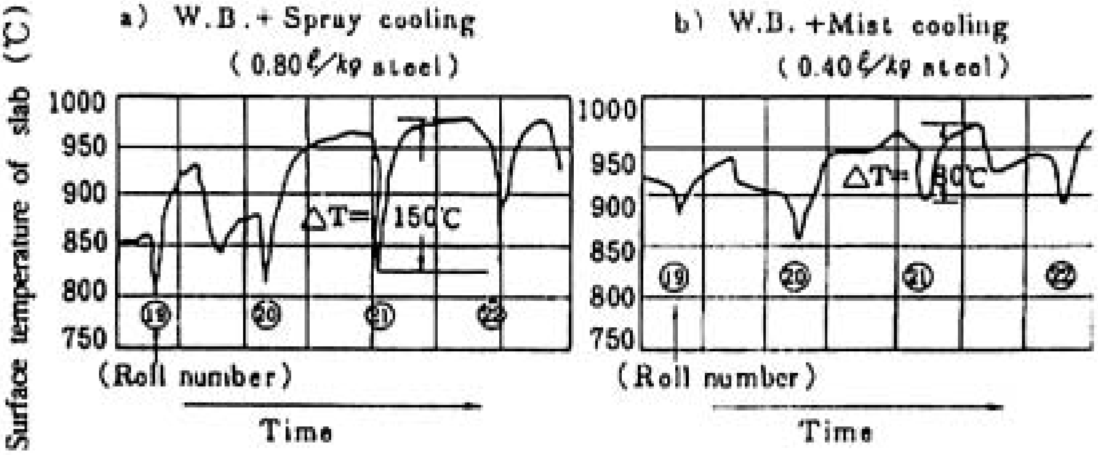

from the solid/melt interface. Also, the upper surface and overflow melt are not necessarily welded. Instead, there can exist a cold shut when the meniscus temperature is low and/or when cooling from the mold is intensive. If a tensile stress is applied to this part toward the withdrawal direction, transverse cracks may occur.

8. The bottom of the oscillation marks often accompanies solute segregation, as discussed in detail in the oscillation mark segregation section. Austenite grain size at the bottom gets coarser as a consequence of slower cooling there. Thus, the mark bottom is susceptible to brittle fracture due to a stress concentration at the austenite grain boundaries.

9. There is another class of this type of crack originating in the mold. The crack formation is enhanced by nonuniform formation of the initial shell that is caused by an uneven inflow of mold flux melt into the mold/shell gap when the submeniscus flow is turbulent, meniscus level fluctuates, meniscus temperature is low and/or the viscosity of the flux melt is too high. When the flow of flux melt into the mold/shell boundary decreases at high casting speeds, the friction at the boundary increases locally with viscous flux melts. That frictional force causes the transverse cracks at the bottom of the oscillation marks while still in the mold.

10. Tensile strain arising from unbending above the brittle temperature zone enhances the propagation of the cracks. Thus, the upper surface of the strand shows more

cracks in curved CC machines. Thicker slabs also form more cracks. Additional strains caused by insufficient lubrication in the mold; misalignment; seized, bent and/or worn support rolls; and bulging of the strand all contribute, to a different degree, to the occurrence and propagation of cracks in more than just the upper surface.

These observations indicate that the sequence of crack formation is as follows:

1. Deep oscillation marks form as a consequence of turbulence in the submeniscus flow, meniscus level fluctuation, low meniscus temperature, low-frequency mold oscillation, long negative strip time and excessively low/high mold flux viscosity.
2. The bottom of the marks tends to have solute segregation and cools slower, resulting in coarse austenite grains with solute-segregated weak boundaries.
3. Friction with the mold, improper taper of the mold, misalignment between the mold and strand, and/or thermal stress at the exit of the mold from water sprays cause the formation of cracks along the austenite grain boundaries at the bottom of the oscillation marks, where stress concentrates.
4. Frictional forces acting between the liquid or solid mold flux film and the shell increase in high-speed casting, e.g., thin-slab casting. A balance between the force and shell strength is an important issue to prevent breakouts and transverse cracks.
5. Seized, bent and worn rolls, and off-alignment of segments can propagate the cracks.
6. Cyclic cooling by water sprays in secondary cooling enhances the embrittlement of the shell due to an enhanced formation of the fine carbonitride/nitride precipitates.

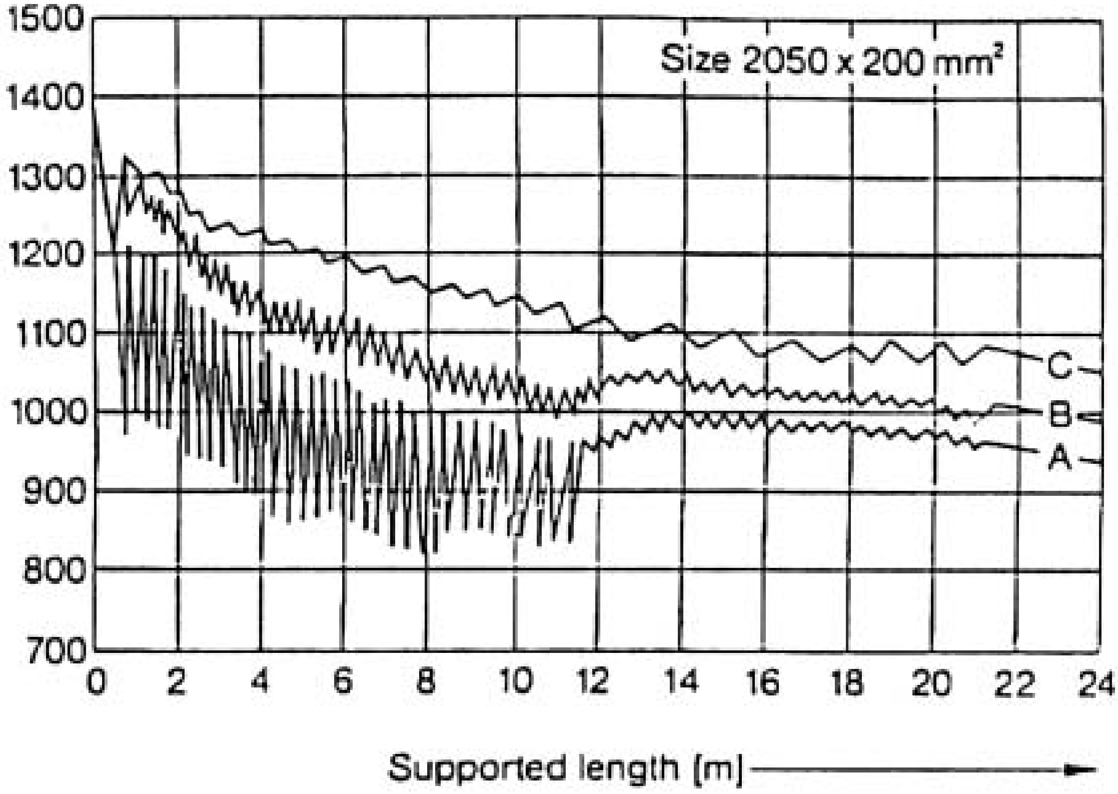

Fig. 21.27b Calculated thermal cycle in the secondary cooling zone of a CC machine. A = Spray cooling 0.7 l/kg; B = Air-mist cooling 0.2 l/kg; C = Dry casting.

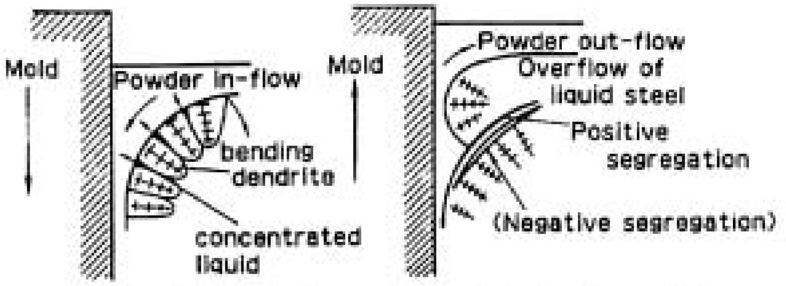

(a) During negative strip period (b) During positive strip period

Fig. 10. Formation mechanism of segregation at the meniscus.

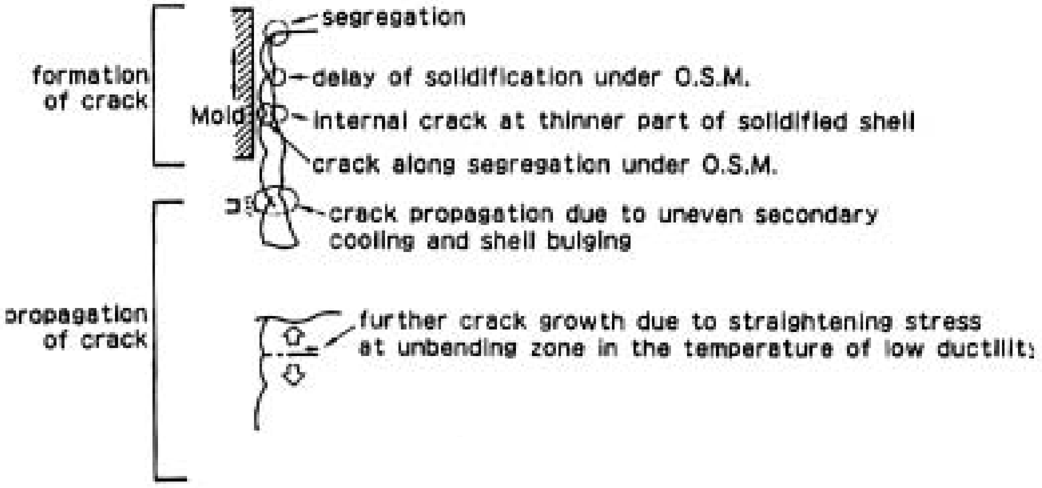
segregation
formation of crack
delay of solidification under O.S.M.
Mold
internal crack at thinner part of solidified shell
crack along segregation under O.S.M.
crack propagation due to uneven secondary cooling and shell bulging
propagation of crack
further crack growth due to straightening stress at unbending zone in the temperature of low ductilit

Fig. 21.28 Mechanism of transverse crack formation at oscillation marks.

Thermal cycling is much influenced by the mode of cooling, as shown in Fig. 21.27a and b.

7. When the strand is straightened at the unbending point where the strand surface temperature is in the brittle range, a tensile strain is imposed on the embrittled upper surface of the strand and the cracks propagate if the strain surpasses the critical value.

The above sequence is also schematically shown by Mizoguchi et al. in Fig. 21.28.

Measures to prevent crack formation are, therefore, to:

1. Reduce [Nb], [Al] and [N] within the specification, not to exceed the solubility product.
2. Control the submeniscus flow turbulence and stabilize the meniscus level in the mold.
3. Optimize mold flux viscosity and mold oscillation to result in an oscillation mark depth < 0.2 mm.
4. Provide good machine maintenance regarding alignment, rolls and mist sprays.

Unbending, therefore, has been practiced in a temperature range either higher or lower than the brittle range. When unbending is carried out at higher temperatures, the spacing of support rolls should be kept at a minimum. Otherwise, ferrostatic pressure makes the hot and weak shell bulge

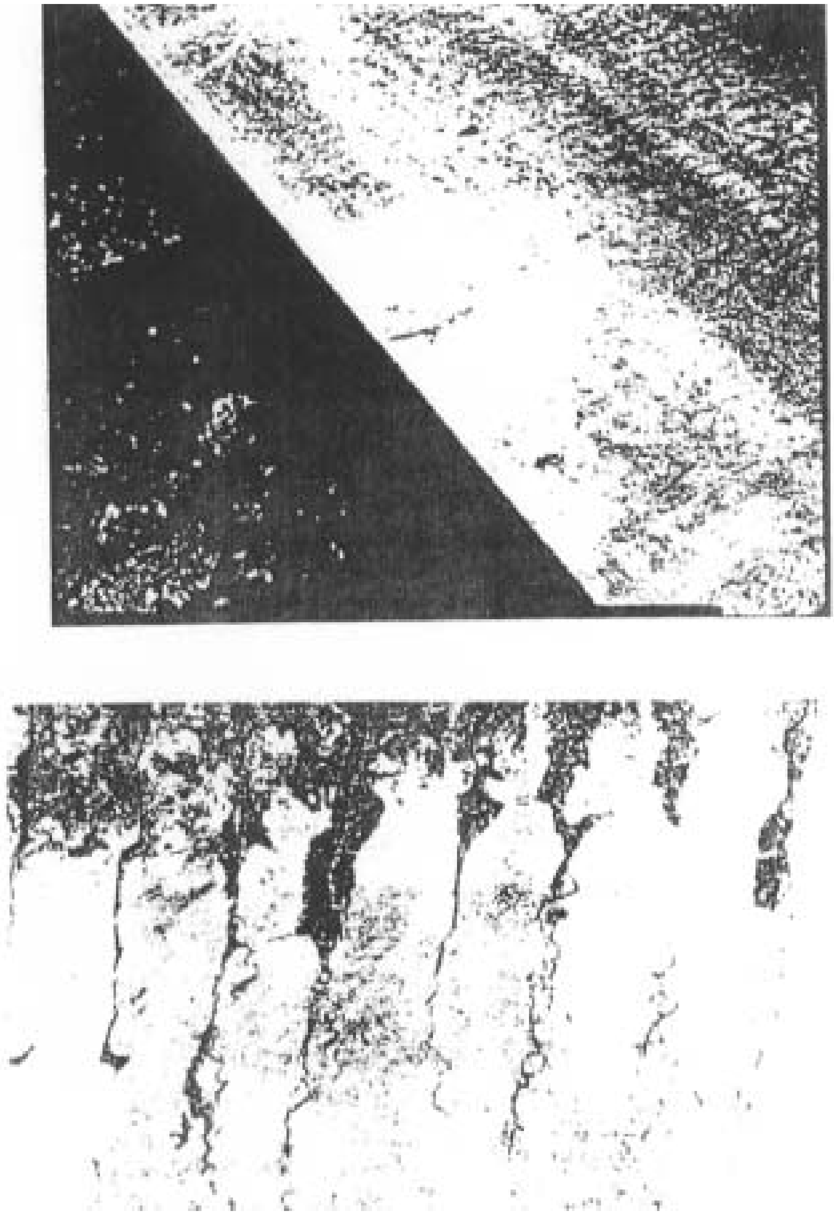

Fig. 21.29 Surface and cross-section views of tansverse facial cracks.

between the rolls, causing internal cracks. CC technology is, however, developing toward higher casting speeds and HDR that favor higher-temperature unbending. In fact, Maehara et al.[44] found that HSLA steels (0.15% C-0.4% Si-1.3% Mn-Nb-V-Al) considerably embrittle from prestraining during continuous casting to make the brittle temperature range much enlarged to 750–1050°C. This is due to dynamic precipitation in γ-grains and on the grain boundaries of fine NbC that harden the grain and cause strain to concentrate to precipitate-depleted soft grain boundary proximity. Consequently, the proximity is split from the boundary precipitates to form voids that agglomerate to cause fracture.[44]

Accordingly, higher-temperature unbending with smaller spacing of support rolls has become a mandatory standard for modern casters for HDR since the mid-1980s. This move has been enhanced by the implementation of mist spray cooling that provides the strands with much better uniform cooling than water sprays to allow the shell to withstand bulging without overcooling the shell corners. Thus, it is advisable to keep the strand surface temperature above 900°C all the way

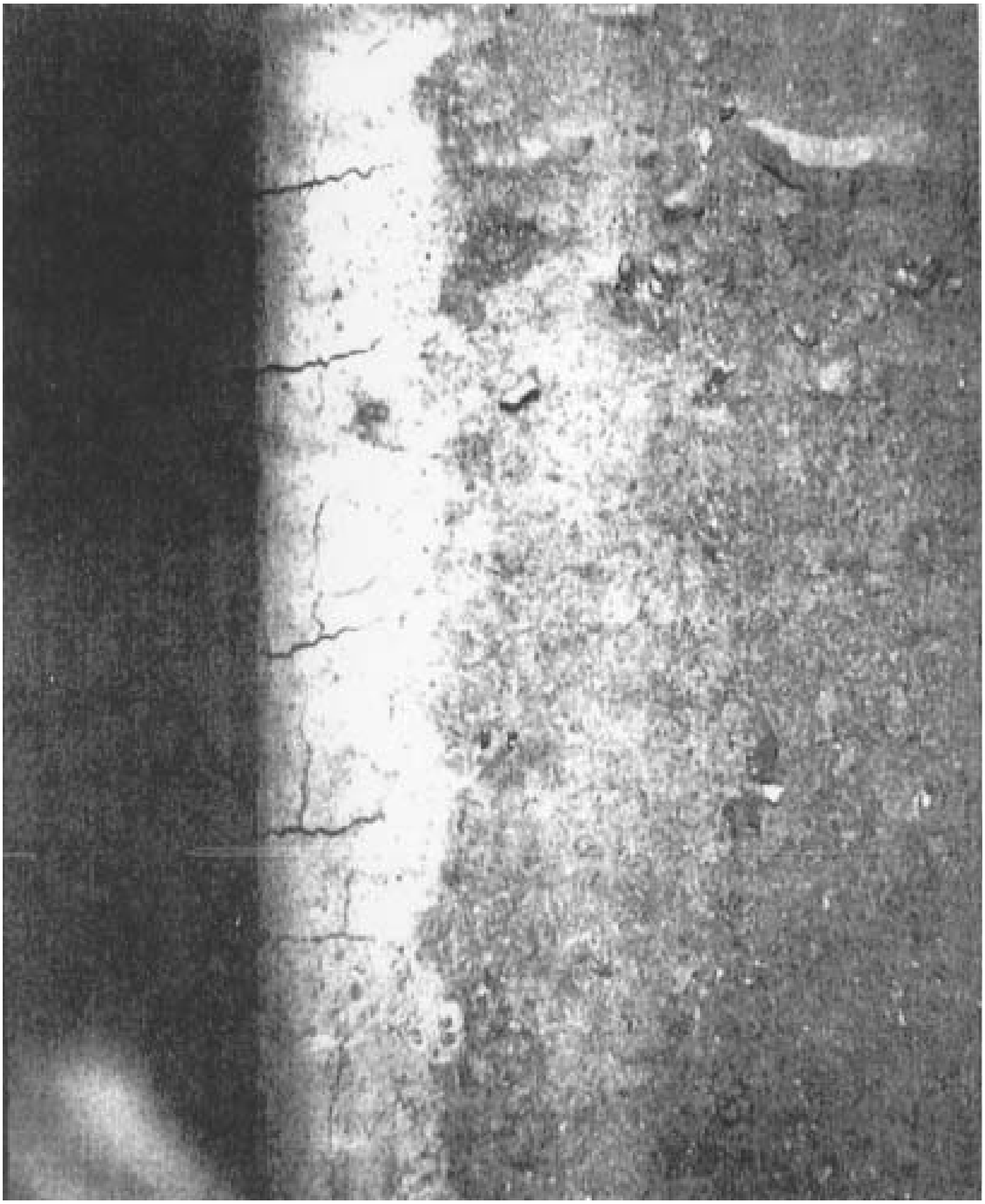

Fig. 21.30 Transverse corner cracks.

from the mold bottom through the secondary cooling zone to the unbending point, with milder and more uniform mist spray cooling at reduced unit water consumptions.

If cooling below 900°C becomes unavoidable, secondary cooling must be made uniformly strong to cool the strand surface below the brittle 770–850°C range and not allow reheating of the strand until it reaches the unbending point. The drawbacks of this operation are an obvious heat loss for HCR. In addition, it can cause internal cracks at the unbending point, since some of the subsurface area always comes into the brittle temperature range. Thus, this method is not recommended.

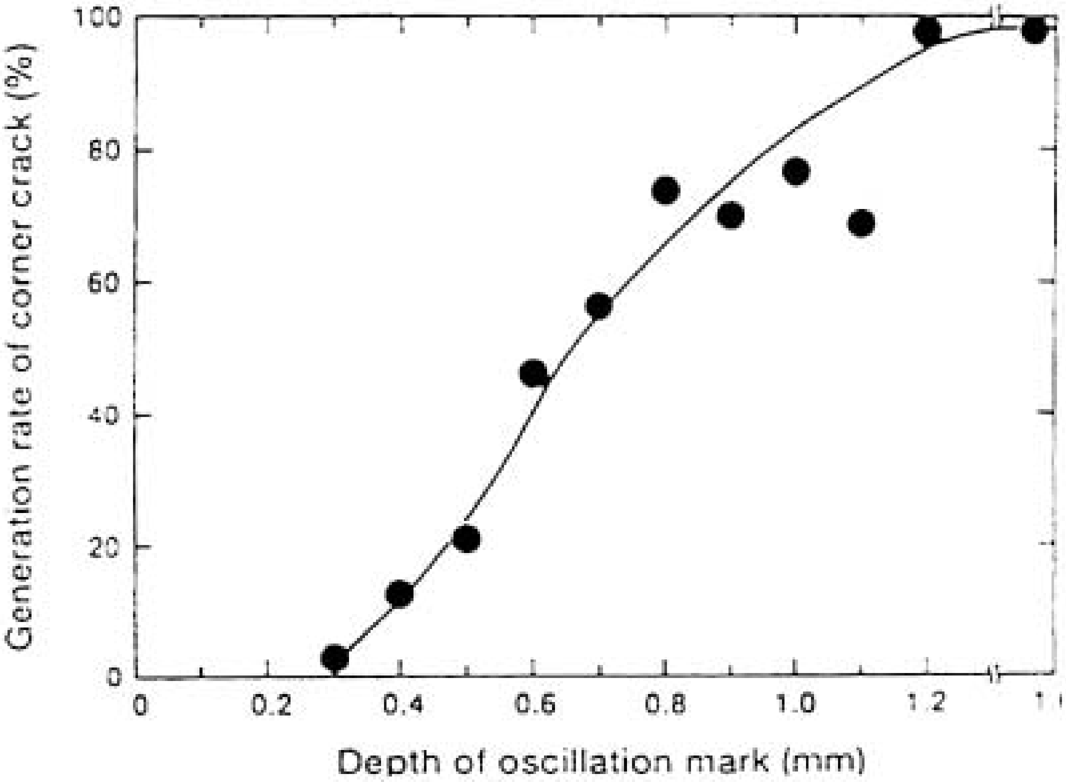

Fig. 21.31 Transverse corner crack generation versus depth of the oscillation mark.

21.3.2.2 Transverse Corner Cracks/Bleeding

21.3.2.1.1 Characteristics

The cracks arise just as transverse facial cracks do: along deep oscillation marks and prior austenite grain boundaries, but at the corners of the strand, as shown in Figs. 21.29[45] and 21.30. As many of these cracks result in edge cracks in hot rolling, conditioning is mandatory. In an extreme case, various forms of metal leakage and bleeding can take place, mostly from the bottom of the oscillation marks and cracks, growing more at the corner than at the face of the strands. Excessive bleeding results in breakouts.

21.3.2.1.2 Influential Factors, Causes and Countermeasures

In slab casting, corners are subject to more overcooling than are faces; hence, they are more easily in the brittle temperature range, forming cracks from the tensile stress of unbending. Deep oscillation marks promote the occurrence of the cracks, as shown in Fig. 21.31. In billet and bloom casting, the cracks increase with increased Cu and Sn that are introduced from scrap and that impair high-temperature ductility. Thus, the additional measures to those mentioned in Section 21.3.2.1.1 are (1) preventing excessive cooling of corners by decreasing spray cooling below the mold and in the secondary cooling zone, and (2) selecting scraps for decreasing Cu and Sn content.

21.3.3 Star Cracks

These cracks are difficult to find in the as-cast state when the strands are covered with scale. Thus, they are found after scarfing, as shown in Figs. 21.32 and 21.33. The cracks develop along austenite grain boundaries radially or network-like and appear as starlight streaks, with a depth of a few to 10 mm. The cracks can induce transverse facial cracks. Locally heavy conditioning can remove

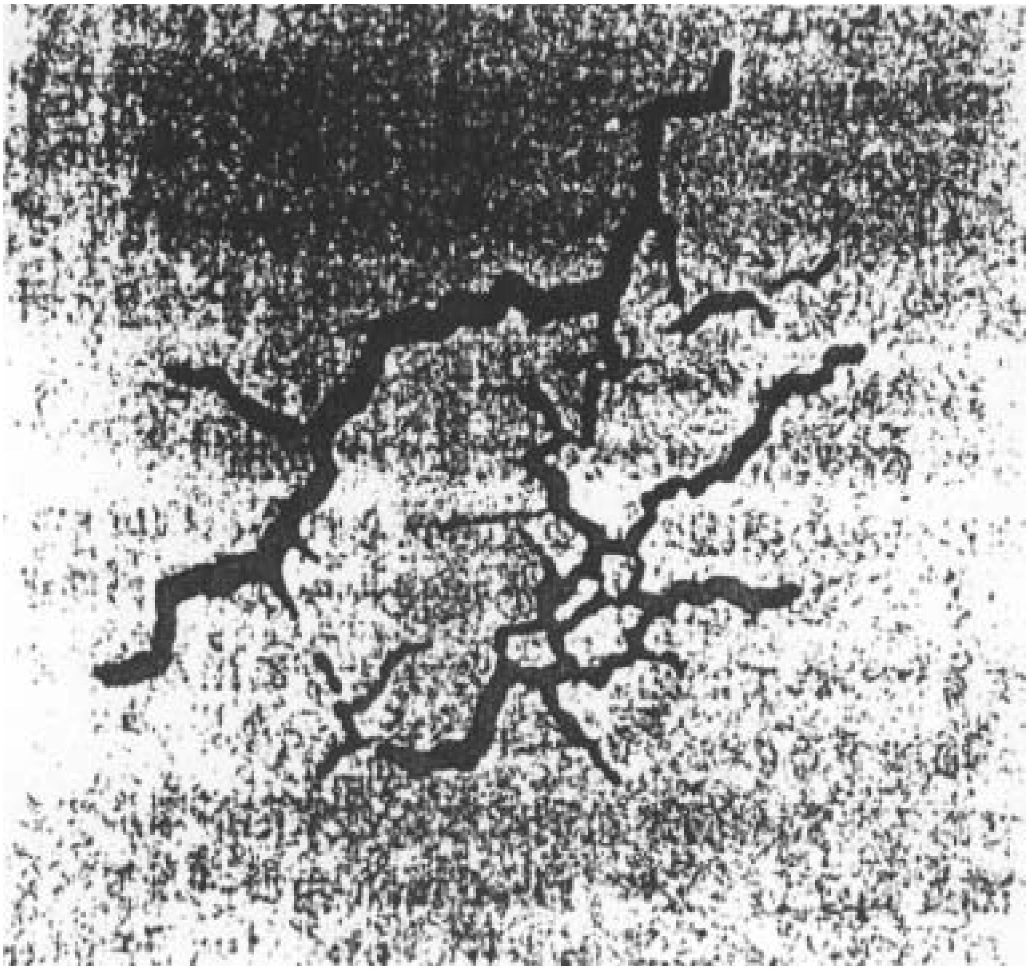

Fig. 21.32 Surface view of a star crack.

them if carefully executed, but it can cause some defects after subsequent rolling, such as streaks and double skin on the product if the conditioning is not done properly.

21.3.3.1 Characteristics

In many cases, Cu is detected at the scale/steel interface and fractured grain boundaries. High-tensile-strength steels containing Al, Nb and V are more susceptible to this crack.

21.3.3.2 Influential Factors, Causes and Countermeasures

Star cracks, often accompanied by Cu, increase when the lubrication at the mold/shell boundary by oil or mold flux melt is insufficient. They also arise when mold wear occurs due to misalignment of the passline or from excessive taper. The cracks form in the following sequence:

1. The strand shell at high temperatures in the mold comes into contact with the Cu mold under a frictional force.
2. The Cu becomes attached to the hot shell and stays there. As Cu is less oxidized than Fe and the diffusivity of Cu is small at the shell surface temperatures, a Cu-enriched area occurs beneath the surface scale layer, a part of which forms liquid around 1100°C.

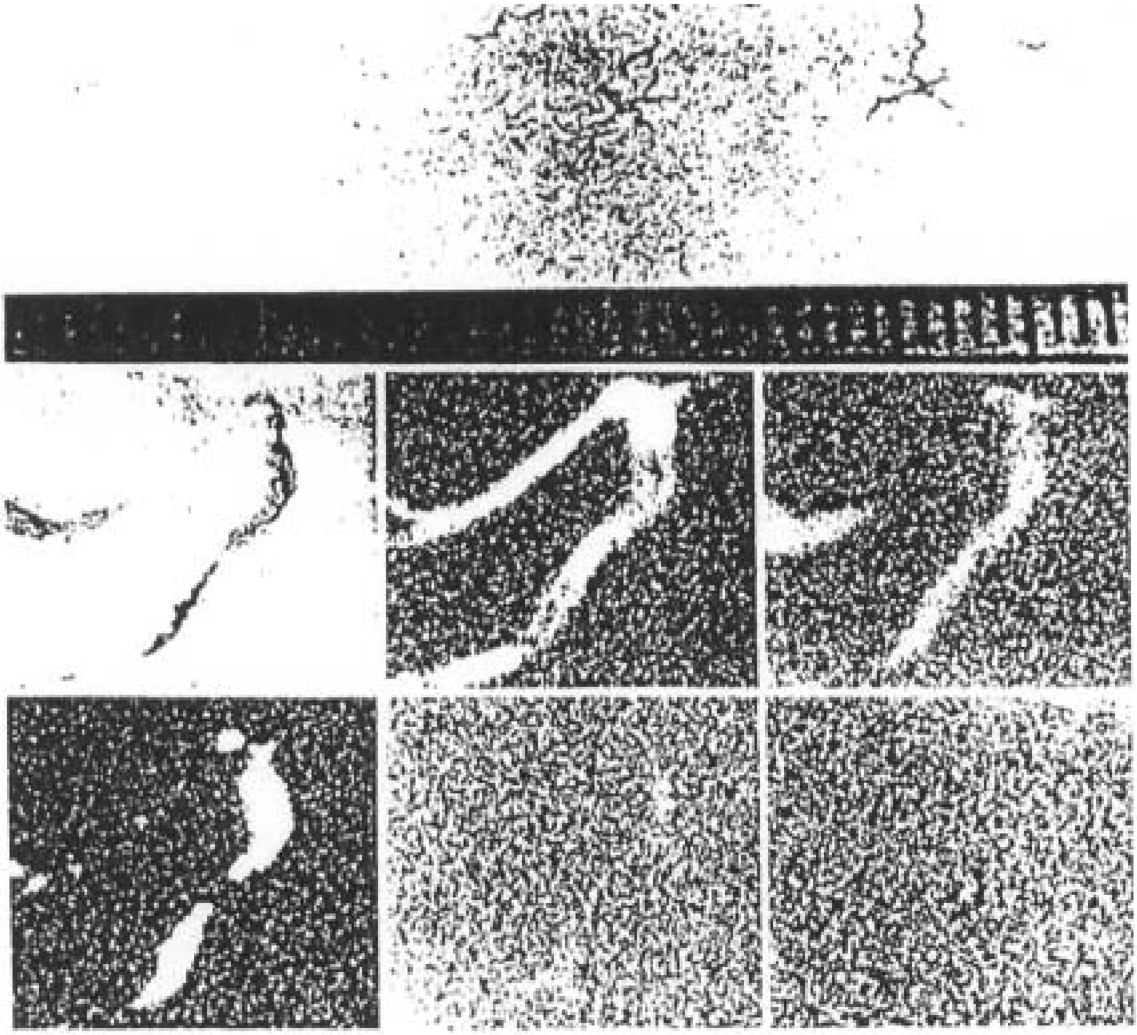

Fig. 21.33 Cu distribution in a star crack. Top: slab surface. Bottom: EPMA figures: top center Cu; top right O; bottom, left to right, Ca, Na, F.

3. The liquid penetrates along and embrittles the austenite grain boundaries where cracks occur, even under small thermal and/or mechanical stresses applied to the strand below the mold. The penetration rate of liquid Cu into grain boundaries has been described in terms of the balance between the diffusion of vacancies from austenite to the liquid Cu tip at the boundary and the inflow of liquid Cu into the grain boundary.[45] The rate can be faster when the inflow is enhanced by applied stress.
4. Intensive cooling in and below the mold helps to generate thermal stress, causing more cracks. There is a view that large variations of heat flux can cause similar cracks even without Cu (steel grade not specified). Those would be a variety of subsurface cracks.[46]

Thus, countermeasures for the star crack formation involve preventing direct contact between the Cu mold and strand shell, decreasing heat flux and its fluctuation in mold, and reducing excessive thermal stress development using one of the following: (a) a mold flux melt with relatively low viscosity, (b) Ni- or Ni-alloy-plated molds, and (c) mild spray cooling below the mold. In particular, mold plating has proved to be effective at stopping the occurrence of star cracks. A thin coating of

Cr has been implemented, but it wears quickly and loses the beneficial effect in long-lasting sequential casting. Accordingly, a thick plating of Ni, which is robust against wear, has been successfully employed in many plants. A variety of hard versions like Ni-P, Fe-Ni, Ni-Co and Ni-Cr have also been reported successful. Use of a hard Cu alloy with a higher melting point is also an alternative under special conditions for cost reasons.

21.3.4 Cracks from Copper in the Steel Melt

This has been a well-known subject for hot working, and it is not limited to continuously cast strands. However, increased Cu in scrap causes hot shortness on CC strands cast in EAF meltshops that operate with high scrap ratios.

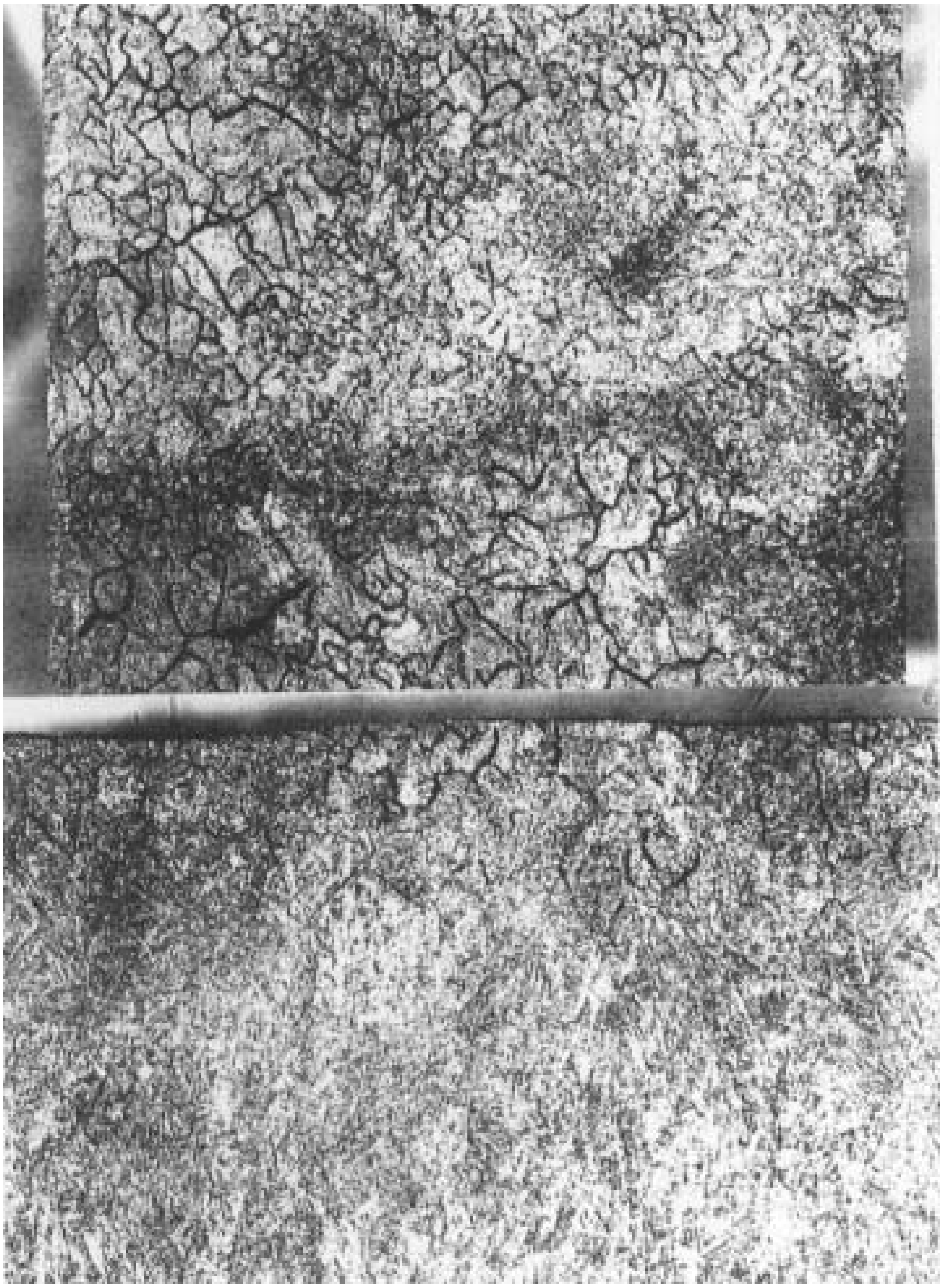

Fig. 21.34 Subsurface cracks. Top: plan view; bottom: vertical cross-section.

21.3.4.1 Characteristics

Intergranular cracks along austenite grains occur at and above 1050°C, and the threshold temperature increases with increasing [Cu] and decreasing [Si]. In practice, the cracks on CC billets are shallow (0.2–2 mm) and network-like on the surface. They are difficult to detect by visual inspection, but they develop into tears during roughing, causing unacceptable seams on the product.

21.3.4.2 Influential Factors, Causes and Countermeasures

1. The cracks do not occur at higher temperatures where liquid FeO-2FeO•SiO_2 eutectic forms in the scale to wet and entrap liquid Cu droplets.
2. During deformation, the cracks grow deeper first, then open wider. Liquid Cu penetrates along γ-grain boundaries while the cracks are developing in the early stage of deformation.[47]
3. Critical concentration, [Cu]*, was best repesented by [%Cu] + 10[%Sn] - [%Ni], which was 0.2 for peritectic carbon steel and 0.3 for high-carbon steel, reflecting a coarser γ-grain size for the former.
4. Higher casting speed and soft secondary cooling decrease surface strain, making the surface temperature higher to favor the eutectic formation, and also decrease the surface temperature fluctuation. As a consequence, hot tears and seams originating from the intergranular cracks were considerably decreased.[48]

21.3.5 Subsurface Cracks

21.3.5.1 Characteristics

Subsurface cracks occur in the subsurface of high-carbon blooms, and they are difficult to detect during hot rolling. These cracks may open up on the surface during subsequent reheating and scaling off, thereby oxidizing and causing a double skin and scab streaks on the rolled products. An example is shown in Fig. 21.34.

21.3.5.2 Influential Factors, Causes and Countermeasures

These cracks arise when thermal stress imposed on the subsurface of strands exceeds the tensile strength of the subsurface, as discussed in the section on transverse facial cracks. Transverse facial and corner cracks mentioned in the foregoing sections can occur

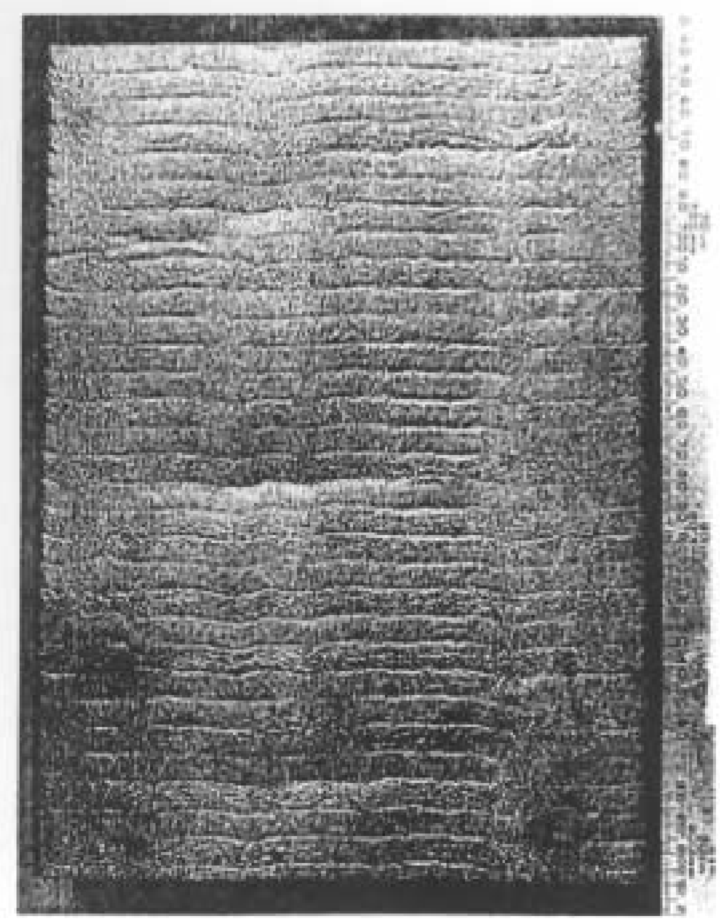

Fig. 21.35 Transverse depressions.

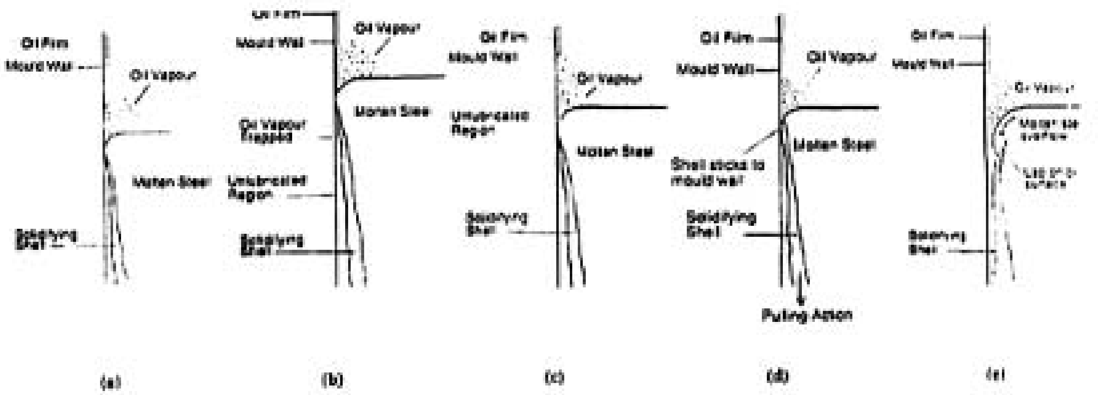

(a) Metal Level Stable

(b) Metal level rises and dries up oil on hot face, creating unlubricated regions

(c) Metal level falls through dry, unlubricated regions on the hot face and sticks to the wall

(d) Sticking enhances the local heat transfer and causes partial freezing of the meniscus

(e) Liquid steel overflows out and solidifies on the mould wall to create a lap on the billet surface

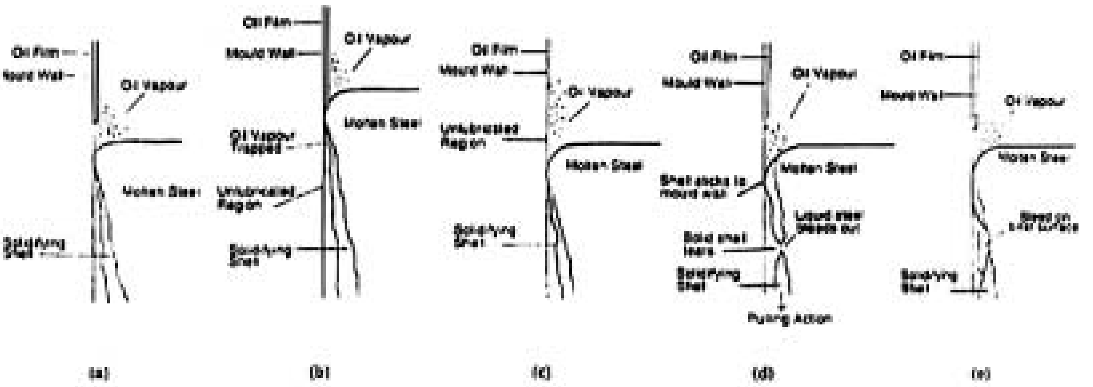

(a) Metal Level Stable

(b) Metal level rises and dries up oil on hot face, creating unlubricated regions

(c) Metal level falls through dry, unlubricated regions on the hot face and sticks to the wall while being pulled by the withdrawal rolls

(d) Pulling force exerted by the withdrawal rolls causes the thin and weak shell to tear / rupture

(e) Liquid steel bleeds out and solidifies on the mould wall to create a bleed on billet surface

Fig. 21.36a Mechanism of depression formation in oil casting.

in the subsurface area if the ductility of the area is impaired by being brought into the brittle temperature ranges.

21.4 Depressions

A depression is a local concave deformation on the faces of strands, as shown in Fig. 21.35. The deformation develops toward the withdrawal direction (longitudinal depression) or along oscillation marks (transverse depression). A cavity between the mold wall and the depression is filled with mold flux melt in powder casting or gas in oil casting, retarding growth of the shell.

Generally, such deformation is triggered by heterogeneous contraction due to peritectic transformation of the initial shell and mechanical pressure due to mold taper being too steep. Fluid mold flux melt solidifying in a glassy state may, in some cases, accelerate the development of a depression in powder casting for two reasons:

1. Increased heat transfer across the flux film caused by a decreased micro air gap and thermal resistance at the mold wall/flux film boundary. This can enhance locally nonuniform rapid cooling and cause heterogeneous contraction of the shell, and

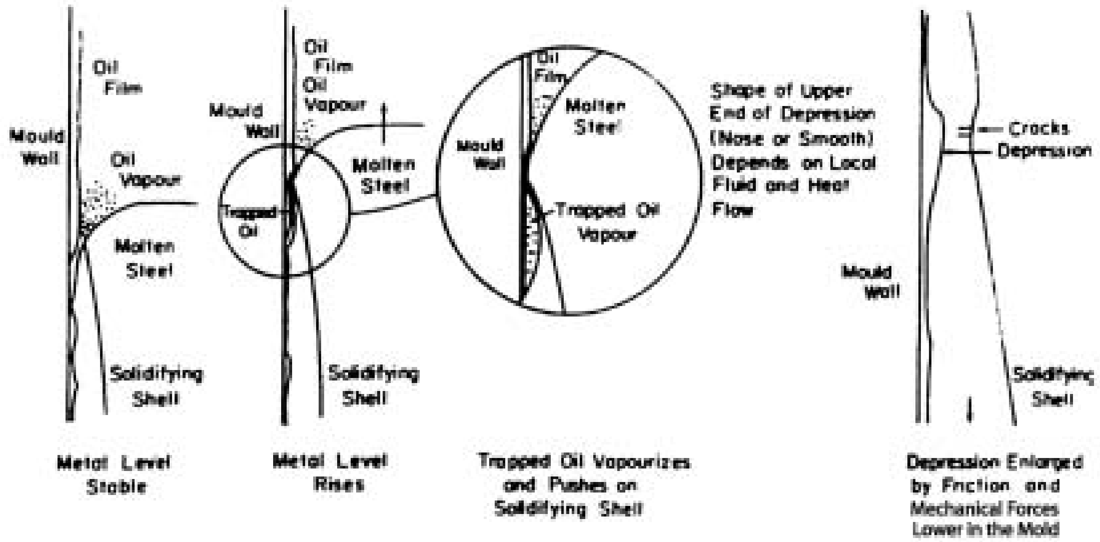

Fig. 21.36b Mechanism of depression formation in oil casting.

2. Excessive flux melt flowing into the shallow cavity formed between the mold wall and the depression.

For oil casting, a nonuniform and uncontrolled flow of oil causes an abrupt formation of gas that pushes the thin and soft shell away from the mold to form depressions, as depicted by Samarasekera et al. in Figs. 21.36a and b.[49] Such deformation promotes further delay of solidification at the depression.

In all cases, the cooling rate at the depression is delayed, solidification is delayed, the shell temperature gets higher than other parts and the subsurface grains get coarser, providing the shell with a high risk of crack formation along the grain boundaries. Relatively slow cooling of the initial solidification shell reduces the heterogeneous contraction by minimizing local heat flux fluctuation. However, longitudinal and transverse depressions have some differing features, which we will discuss in the following sections.

21.4.1 Longitudinal Depression/Slag Streak

21.4.1.1 Characteristics

This is a shallow groove observed occasionally on the mid-face or near the corner in the strand withdrawal direction on peritectic carbon and stainless steel and round castings. Sometimes it is called a slag streak, as it accompanies the mold flux. An example on a round billet is shown in Figs. 21.37 and 21.38. Heavy longitudinal depressions cause surface and subsurface cracks, and require conditioning.

21.4.1.2 Influential Factors, Causes and Countermeasures

1. Longitudinal depressions arise more on round casting of peritectic carbon steel and are not limited to the start of casting. In casting rounds, contact between the mold and shell can never be uniform in the circular direction. This nonuniformity is enhanced by the local meniscus level fluctuation and the deviation of mold taper from the shrinkage of the round strands in the withdrawal direction. The area of the initial shell in loose contact with the mold on the shell perimeter is thinner, hotter and hence weaker; is constrained by stiff neighbors; and is further pulled back from the mold wall as solidification proceeds, even against the ferrostatic pressure of the

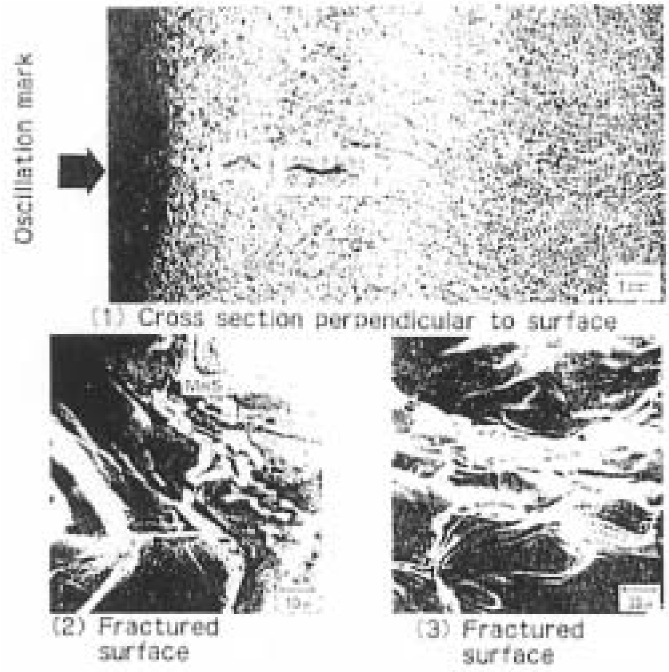

(1) Cross section perpendicular to surface

(2) Fractured surface

(3) Fractured surface

Fig. 21.37 Transverse corner cracks formed at oscillation marks in depressions.

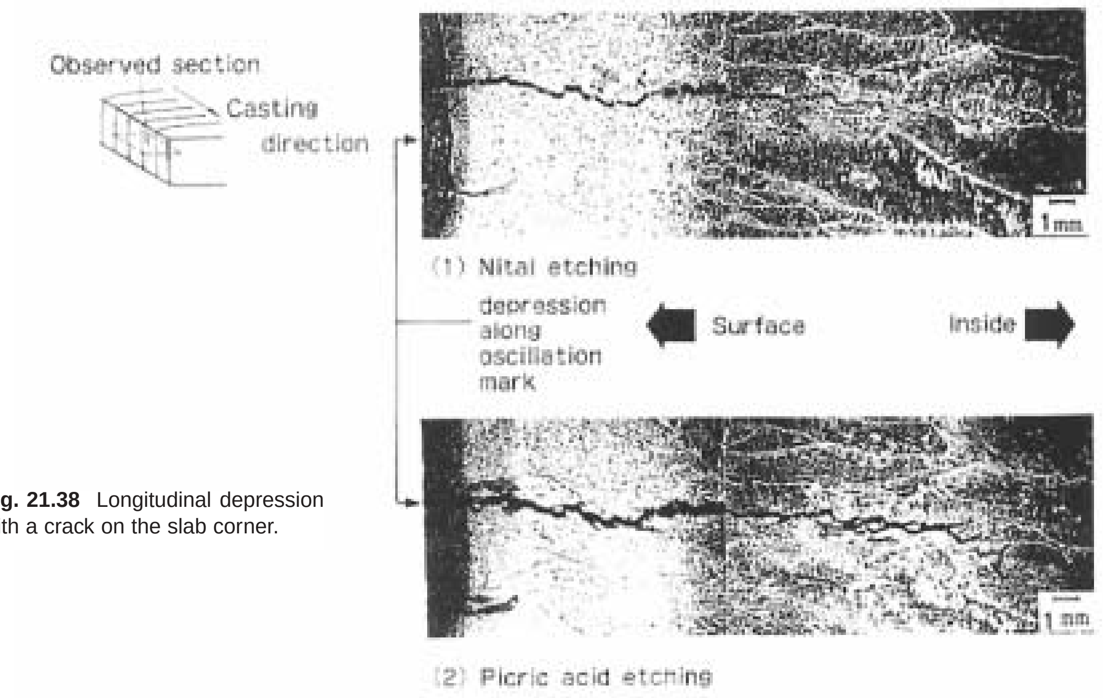

(1) Nital etching

(2) Picric acid etching

Fig. 21.38 Longitudinal depression with a crack on the slab corner.

steel melt. As this event lasts for some time while the strand is withdrawn, the depressions turn into longitudinal ones.

2. Logical countermeasures that have proved to be effective include the following: mold level fluctuation control, variable taper such as parabolic taper, and through mild cooling by choosing a mold flux with the proper melting rate and viscosity.
3. In slab casting, longitudinal depressions occur when the supply of mold flux melt to the mold/shell boundary becomes insufficient at mid-face, where the hoop stress is the highest on solidification. This depression is a precursor of longitudinal cracks,

and countermeasures for this are the same as discussed in the section on longitudinal cracks.

4. Longitudinal corner depressions arise when an improper taper is chosen. Excessive taper of the narrow face obviously forms off-corner depressions. Too shallow a narrow-face taper induces bulging, which acts to buckle the corner deformation arising from enhanced cooling at the corners. The buckling causes the off-corner portion of the shell to detach from the mold wall, inducing longitudinal off-corner depressions.

21.4.2 Transverse Depression

21.4.2.1 Characteristics

This type of depression occurs in the transverse direction, often cyclically toward the lengthwise direction of the strand. As shown in Fig. 21.35, their length is a fraction of the width of the strand for powder casting, but almost the entire width for oil casting. The width of the depression may cover a few oscillation marks, and the depth may be up to a few millimeters. Oscillation marks with excessive depth and/or solute segregation are observed as a transverse depression that requires conditioning. Peritectic grades, low-carbon high-Mn steel and austenitic stainless steel are sensitive to the occurrence of transverse depressions.

21.4.2.2 Influential Factors, Causes and Countermeasures

Transverse depressions tend to occur during the start of casting, when the temperature of the steel melt is low, the supply to the meniscus of mold flux melt is insufficient and the meniscus level fluctuates. Under the above conditions, the meniscus in the mold is cooled to promote abrupt initial solidification. A stiff initial shell forms nonuniformly along the periphery near the meniscus and irregularly toward the withdrawal direction, developing into the depression.

In the transient period of the casting operation, the melt level in the mold can fall in a short period of time. Such sudden level fluctuations cause shallow transverse depressions and short longitudinal cracks. This is due to the following sequence:[50] The level drop makes the shell bend toward the lowered meniscus. When the melt resumes its previous level, the melt flows over the shell tip to form a new shell that is closer to the mold wall. The deeper the drop, the more the bending and overflowing, generating deeper depressions that often accompany solute segregation.

The above sequence for the formation of depressions is not limited to the transient period. During steady-state casting, whenever local meniscus fluctuation is caused by turbulent submeniscus flow, there is a risk of a depression. This is particularly so when the melt temperature is low and the heat flux is high at the meniscus.

Steels that are subject to peritectic solidification are far more sensitive to depressions due to their greater volume contraction on solidification. Proper measures to avoid depressions are to use an exothermic, fast-melting starter flux and to keep the tundish full at initiation of casting while external tundish heating is supplied. For peritectic steels, oil casting hardly offers a depression-free surface, as it causes nonuniform hard cooling at the meniscus.

21.5 Solute Segregation at Oscillation Marks

Solute segregation arises at the bottom of oscillation marks on both carbon and stainless steel strands that are up to 1 mm deep. In the conventional reheating and rolling process, this depth is scaled off for carbon steel, and hence does not cause problem. As discussed earlier, however, it can be a root cause of transverse cracks if the amount of the scale-off is limited in an advanced hot direct rolling environment (HDR). For austenitic stainless steels, the segregation ([Ni] and [P])

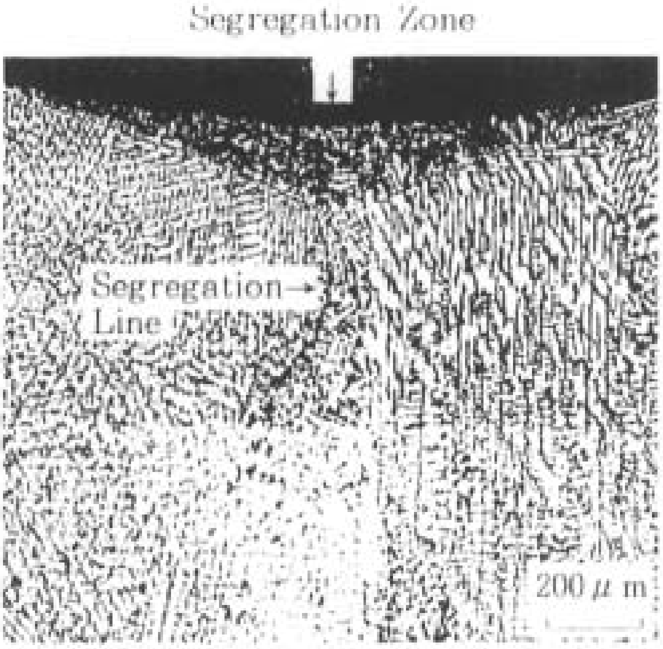

Fig. 21.39 Segregation caused by leaking through a crack at the bottom of the oscillation mark of an SUS304 slab. *From Ref. 52.*

will not be scaled off during reheating. Unless removed by conditioning, the remains cause an inhomogeneous pattern or even defects during subsequent cold rolling. This phenomenon has been one of the major reasons why continuous casting of slabs was not free from surface conditioning.

21.5.1 Characteristics

The three types of solute segregation, which can be a cause of surface cracks, were schematically shown in Fig. 21.26.

For SUS304 slabs, two types of abnormal structure at the bottom of the oscillation marks are reported in detail by Takeuchi et al.[51] One is coarse, equiaxed dendrites enriched with Ni and other solute elements filling the bottom of the oscillation marks to a thickness of 50–600 μm. The other is entrapped mold flux at the bottom of the marks.

21.5.2 Influential Factors, Causes and Countermeasures

The formation mechanism has been discussed in terms of pumping by a slag rim (Emi), engulfment by bending back (Tomono), dynamic pressure of slag flowing in the mold/shell slit (Takeuchi and Brimacombe) (all of these supplement and predict t_N dependence of slag consumption), and slag inflow in the slit during positive strip time, t_p (Tsutumi et al.). Real-life cases require further clarification by precise monitoring and analysis of reliable industrial observation.

The “Overflow” type occurs, as discussed earlier, when a coarse nail/hook is formed under excessive heat extraction or from a cool melt. In carbon steels, it accompanies the segregation of solutes (mostly Mn and P) that come over with the overflowing melt from the solidification front along the top of the nail/hook to the bottom of the oscillation mark. Otherwise, the P segregation occurs through the interdendritic cracks in the nail/hook. This mechanism has been mentioned in the transverse crack section.

Accumulation of a solute-enriched steel melt to the bottom of the oscillation mark occurs in stainless steel by (a) the overflow and (b) the formation of a crack (breach) in the nail/hook on bending,

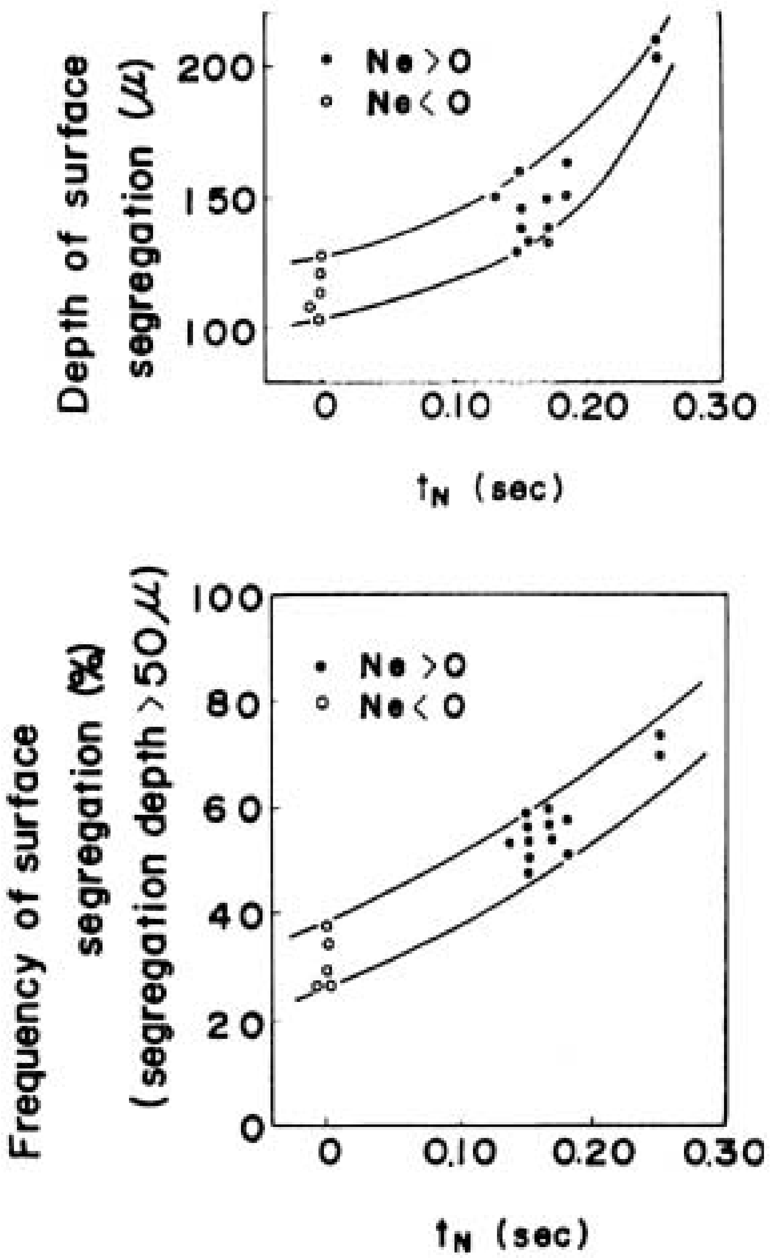

Fig. 21.40 Increase of oscillation mark segregation with negative strip time.

as clearly shown by Hojo et al.[52] in Fig. 21.39. The crack allows the solute-enriched melt to leak out (bleed) during the positive strip period.

The deeper the oscillation mark, the greater the occurrence and degree of surface segregation, as shown in Figs. 21.40, 21.41 and 21.42.[53] Decreasing negative strip time, t_N, by increasing oscillation frequency, f, and decreasing stroke, s, of the mold reduces the depth of the oscillation mark considerably, as shown in Fig. 21.42, although marks do exist even at $t_N = 0$. The dependence of t_N on f, s and the withdrawal speed is given in Fig. 21.43. High-cycle, short-stroke oscillation by a resonance mold reduced the mark depth and breakout considerably, as shown in Fig. 21.44.[53] Under such conditions, however, the consumption of mold flux and the infiltration of the mold flux film tend to decrease. Care must be taken not to cause a breakout of the strand shell by optimizing the choice of mold flux. Minimizing meniscus level fluctuation is also a requisite.

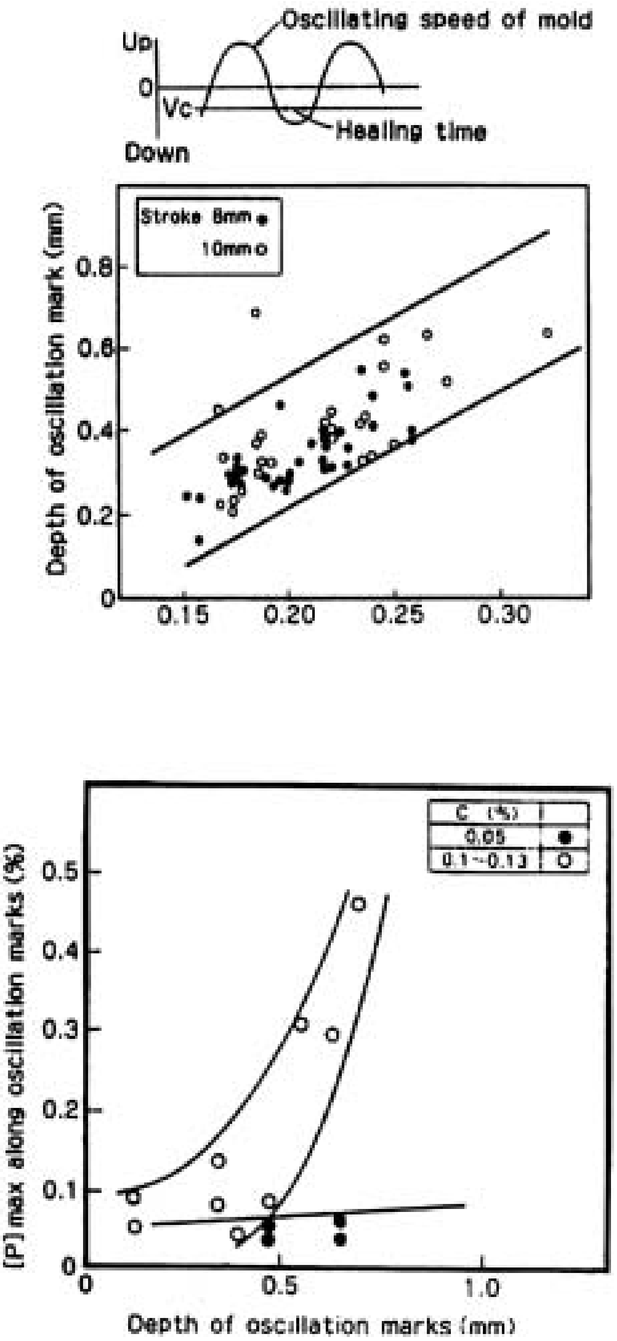

Fig. 21.41 Oscillation mark depth and segregation influenced by negative strip time.

21.6 Inclusion Clusters

Subsurface accumulation or surface-opening of large clusters, ranging in size from a detectable lower limit of a few hundred micrometers to an exceptionally large few tens of millimeters, has called for renewed attention in making IF steels for EDDQ-SEDDQ sheet and tin-mill black sheet for PET-coated DI cans. Unless manually and carefully inspected after scarfing, these are difficult to find before hot rolling. Mostly, these are found as process-upsets such as breakage during cold working of rods and wires or as slivers and blisters on the surface of annealed or cold rolled sheet.

The slivers show up in different forms. During hot rolling followed by cold rolling, alumina clusters are partly crushed and distributed along the metal flow toward the rolling direction as fragmented

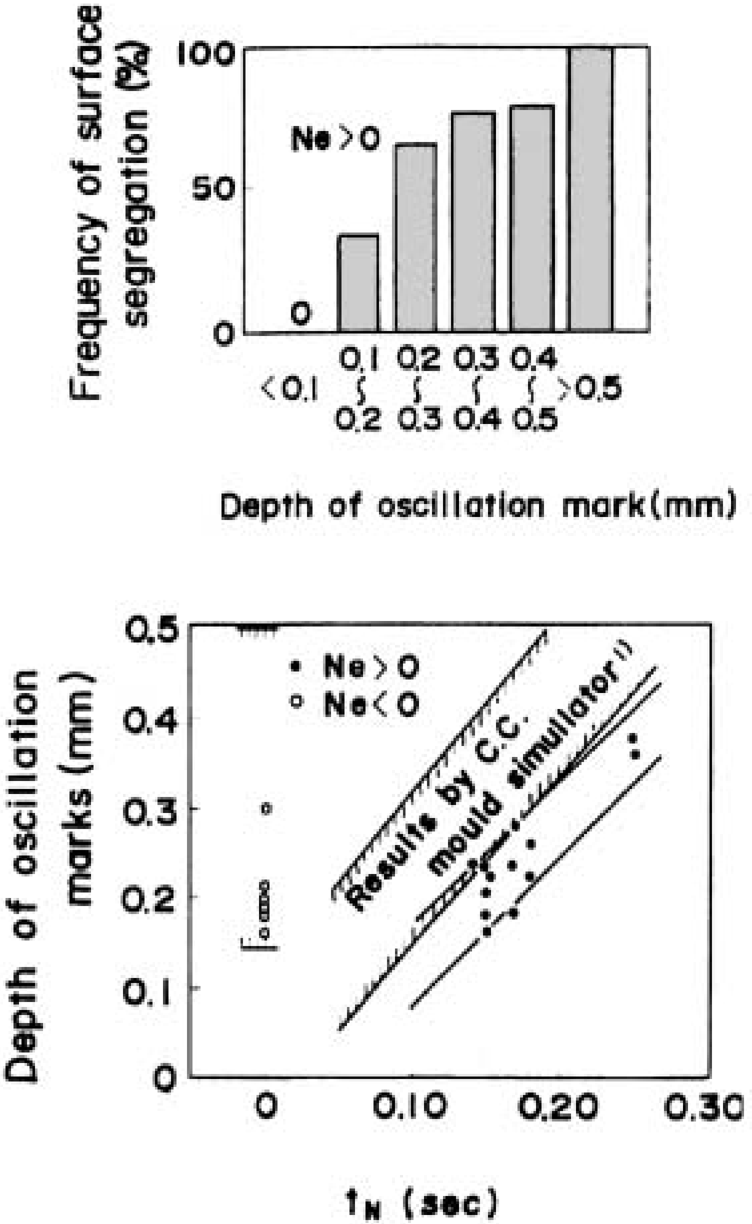

Fig. 21.42 Depth of oscillation mark and segregation with negative strip time.

strings. When the clusters are located near the surface of the shell, metal skin on the string breaks during rolling, and the clusters are exposed to form slivers. Otherwise, the metal skin swells without breaking, forming blisters during annealing after the rolling due to the expansion of gases beneath the skin accompanied by the decrease of the skin strength at annealing temperatures. Fine blisters show only a metallic luster that is different from the sheet matrix. The size of these defects varies from 1 to 2 mm in width and from 10 to over 1000 mm in length. The thickness from the surface of the metal skin across the crushed clusters to the surface of the sheet matrix is 4 to 6 μm for slivers and 6 to 8 μm for blisters, all depending on the reduction ratio and annealing conditions.

In Ti-stabilized stainless steels, the clusters and “crust” are two major sources of surface defects that deteriorate the surface of cold rolled sheet.

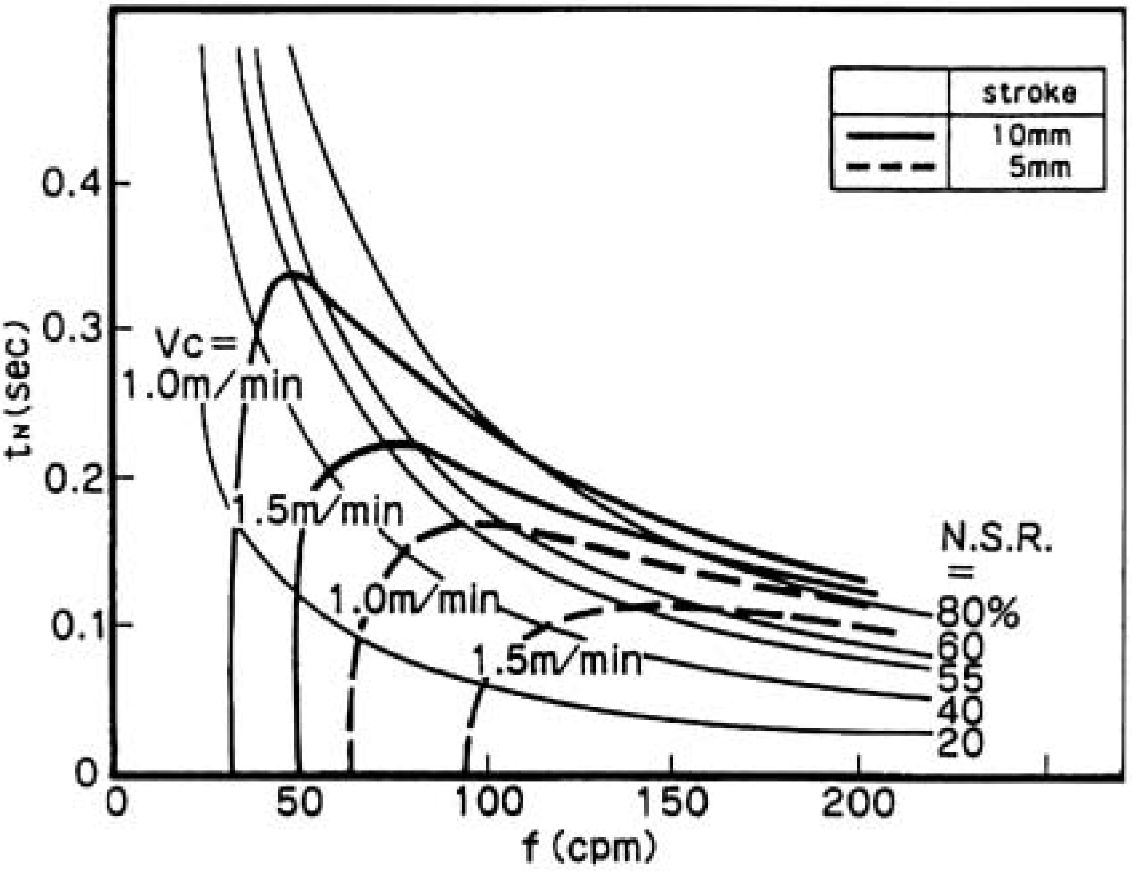

Fig. 21.43 Calculated negative strip time.

21.6.1 Characteristics

Inclusion clusters, detectable on the strand surface by inspection after scarfing, are at least larger than 200 μm, mostly several hundreds to a thousand micrometers. They consist mostly of fine Al_2O_3 particles in Al-killed steels, or sometimes carbide or nitride particles in steels containing Ti, Nb and/or V, all particles being a few micrometers in size and agglomerated together.

These clusters are often associated with fine holes that contain Ar and H_2 gas, described later in detail in the gas holes section. The Ar comes from finely dispersed bubbles of Ar injected into the SEN to reduce nozzle clogging by alumina accretion, and the H_2 arises from the diffusion of dissolved hydrogen into the Ar holes during and after solidification.

In Ti-stabilized austenitic stainless steels, the clusters consist of TiN and Al_2O_3 particles. In addition, a so-called “crust” tends to form. The crust consists mostly of a solidified steel crust containing TiN precipitates that are often associated with N_2 bubbles.

21.6.2 Influential Factors, Causes and Countermeasures

In steels cast with a well-refined Al-deoxidized melt, such huge clusters are mostly of exogenous origin, i.e., reoxidation of the Al-containing melt by air or an oxidizing slag during melt transfer from ladle to tundish and tundish to mold. The other major cause is the occasional break-off of the alumina accretion on the tundish nozzle and SEN. With the melt containing appreciable amounts of fine, suspended alumina particles, collision and agglomeration of the particles can form the clusters as well.

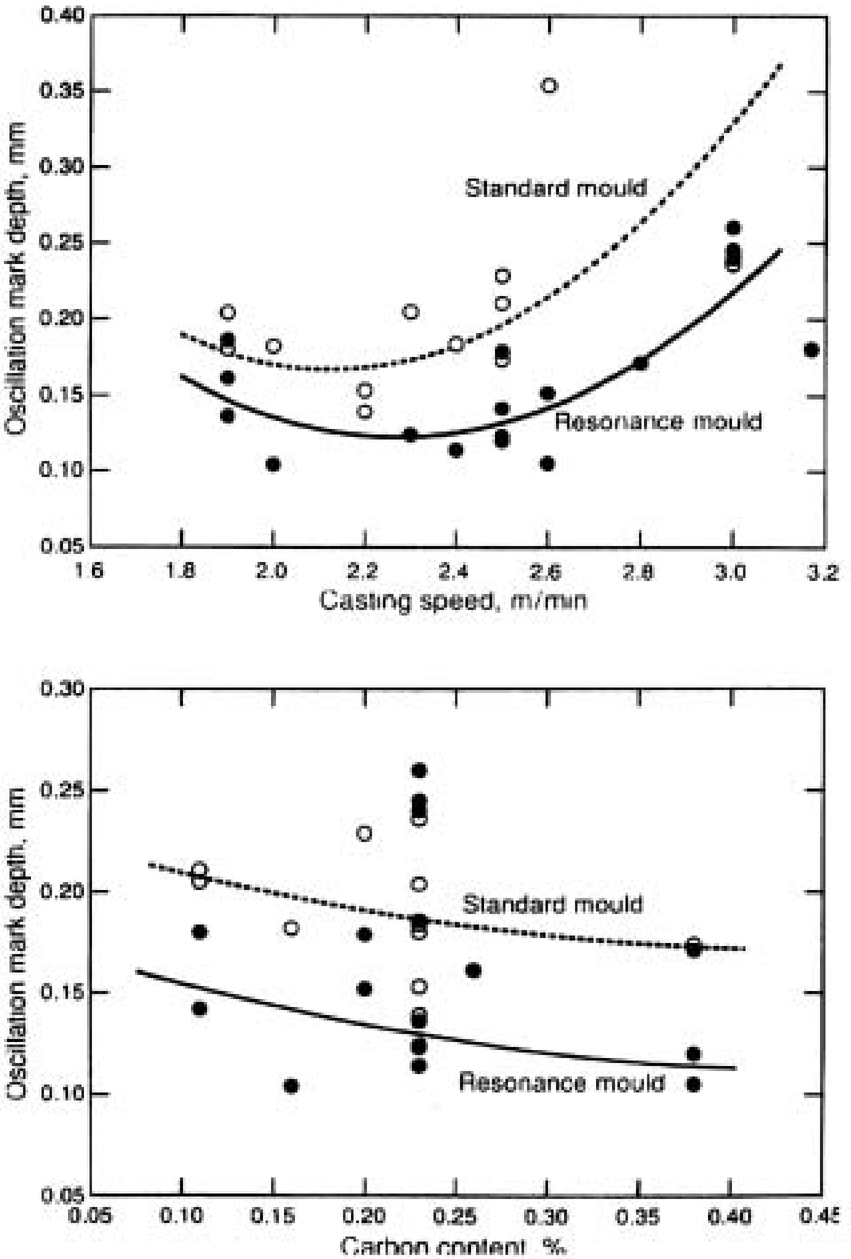

Fig. 21.44 Resonance mold. *From Ref. 53.*

These clusters are carried over with the melt flow into the mold, brought close to the perimeter of the meniscus during flotation or by the flow directed toward the meniscus, and entrapped in a thin initial solidification shell, mostly by the nail/hook mechanism. Another extreme case is that, when the amount of floating alumina clusters surpasses the assimilation capability of the mold flux melt, the clusters will accumulate beneath the flux melt and be captured by the top edge of the initial shell extending from the perimeter of the mold.

All measures to reduce reoxidation, nozzle clogging and extended nail/hook formation are effective in minimizing the occurrence of inclusion clusters. Also, a controlled flow to wash the clusters away from the nails/hooks has proved to be effective. In many reports on the effect of electromagnetic flow control devices, critical metal flow velocity at which the Ar bubbles and clusters are washed away from the nails/hooks is about 40–60 cm/sec. Preventive measures to avoid nozzle clogging are still sought as longer sequential casting of large tonnage heats is practiced. These measures are all in common with those for producing clean steels. In practice, these translate into:

- Minimize slag carryover from the BOF/EAF into the ladle, and deactivate the ladle slag with the addition of MgO and deoxidizers to increase viscosity and reduce FeO.
- Minimize carryover of ladle slag into the tundish by controlling the pouring practice with a slag detector and melt flow controller.
- Install a long nozzle between the ladle and tundish, and avoid air ingress by supplying Ar at the ladle/long nozzle joint.
- Make the tundish atmosphere inert with Ar (or N_2).
- Practice a filled start of the tundish with fine Ar-bubble injection from the outlet of the tundish.
- Increase the size of the tundish to accommodate bath depth fluctuation during transient operation (large tundish); optimize the melt flow in the tundish to avoid short circuiting, vortex formation and entrainment of tundish slag, and to secure a sufficient residence time for the flotation of exogenous large inclusion clusters (pour box, weir, dam).
- Keep superheat in the tundish to prevent it from cooling during transient periods (tundish heater).
- Choose an SEN made of alumina graphite with a minimum amount of porosity and binder silica to avoid oxygen transfer as SiO gas and CO gas through the wall. Surface roughness of the SEN inner wall should be minimal.
- Install an electromagnetic flow controller on the mold to dampen meniscus flow turbulence while heating the melt near the meniscus (FC-mold, EMBR) or to generate reasonable flow near the meniscus to wash the cluster away from the shell (EMLA, LMF).
- Choose a mold flux that has a reasonable melting rate to assure acceptable thickness of the flux melt layer; it should have sufficient capacity for alumina assimilation and provide the mold/shell gap with a flux film for mild cooling of the shell (basic and relatively high crystallization temperature).
- The large clusters in Ti-stabilized stainless steels are caused by the peel-off of the nozzle accretion. Smaller ones are due to the reaction between TiN and (SiO_2) in the mold flux to form $CaTiO_3$ with a high melting temperature. This inhibits further dissolution of TiN and Al_2O_3 in the flux melt.
- The crust formation in Ti-stabilized stainless steels is due to the following sequence:
  - First, TiN particles are formed, some of which enhance the nucleation of the steel crust.
  - The remainder of TiN particles also react with (FeO) in the mold flux to form N_2 gas.
  - The N_2 bubbles inhibit heat supply from the bulk of the melt to the crust, promoting crust growth.

21.7 Slag Patches/Entrapped Scums

An example of entrapped scum found on a CC slab is shown in Fig. 21.45.

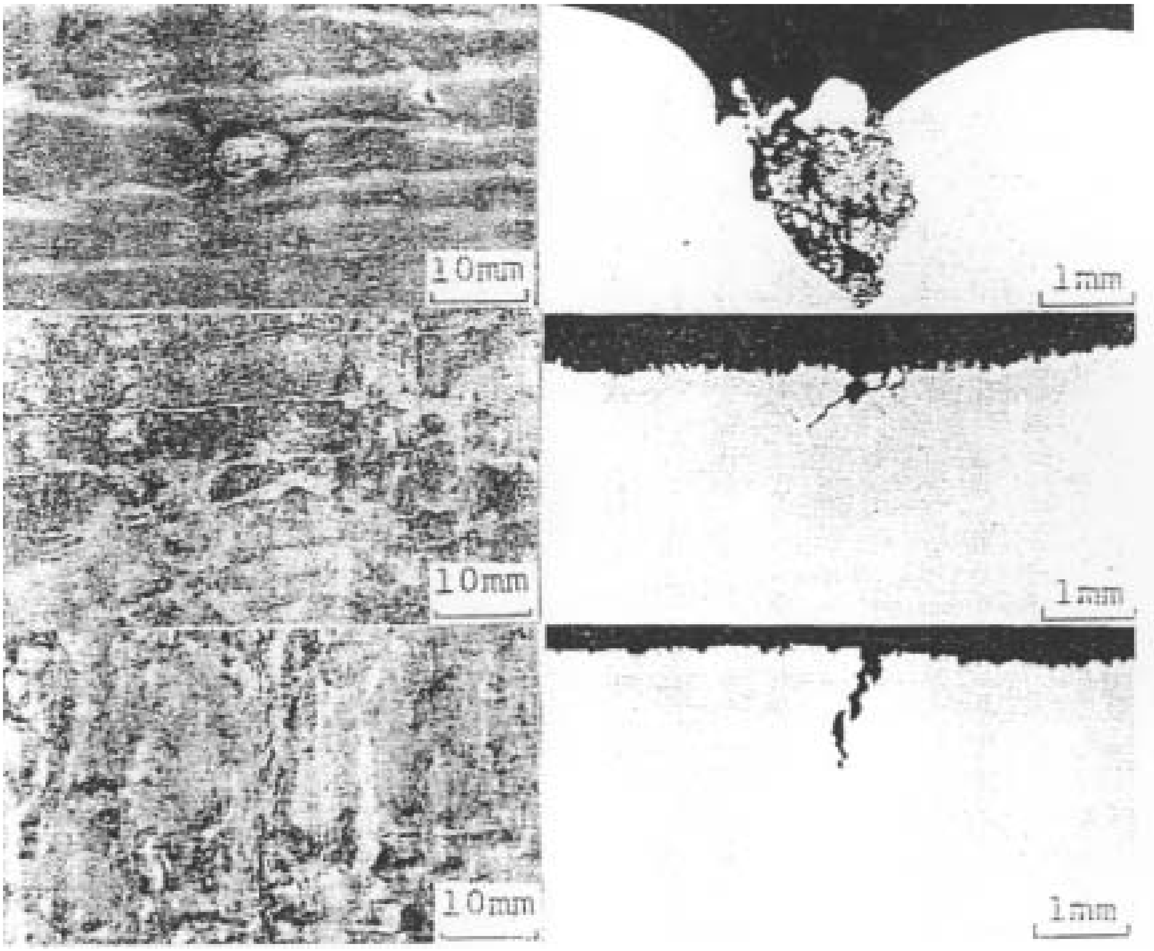

Fig. 21.45 Entrapped scum on the oscillation marks of an SUS304 CC slab.

21.7.1 Characteristics

These are the less frequently observed subsurface mass or surface patches of ladle slag, tundish slag or mold flux, mostly in sizes up to a few millimeters, but extreme cases are larger than 10 mm. Smaller ones are usually have compositions close to these slags or flux but occasionally are enriched to some extent by Al_2O_3 for Al-killed steels. Except for unusually poor transient operation, it is not common to have slag patches of large sizes of ladle- and tundish-slag origin. Larger ones are likely to be of mold flux origin, and hence their chemistry is close to the mold flux composition. The origin of slag patches can be identified by analyzing the composition of the slag patches for CaO/SiO_2, MgO, Al_2O_3, Na and F and comparing that with respective slag or flux composition.

Those patches and scums that are attached on the surface of strands are usually removed by downstream processing. In a limited number of cases, cracks might be found beneath the slag patches/scums. Those that are covered partly by the solidified shell can be scabs, double skin and the like, become slag streaks, chevron cracks, rusting on pickling, etc. upon subsequent rolling.

21.7.2 Influential Factors, Causes and Countermeasures

The origin of slag patches or entrapped scums is either ladle slag or tundish slag carried over into the mold, mostly in transient operation at ladle open, ladle empty, tundish open or tundish empty. They are usually removed by flotation in the tundish or mold, but some are entrapped at the perimeter of the meniscus by the initial solidification shell.

The first measures to avoid their occurrence include the following: minimizing BOF/EAF slag carryover to the ladle, ladle slag stiffening (e.g., MgO more than 8–10%), a ladle slag detector/stopper system, and every means to enhance slag flotation in the tundish.

Another major cause is the mold flux on top of the meniscus in the mold. Irregular changes in the meniscus level during transient operations make the steel melt come in contact with unmelted mold flux (the sintered or yet powdery part of the flux), resulting in the formation of an initial shell that has entrapped the flux. Also, excessive turbulence and vortexing of the submeniscus metal flow entrains the flux melt into a metal bath in the mold. The entrained flux melt is entrapped by the initial shell during flotation.

In casting stainless steels, Cr_2O_3 formed by the reoxidation of steel melt reacts with the mold flux, forming a semisolid crust floating on the meniscus. When it comes to the periphery of the mold, the shell will capture it as scum/slag patch.

Measures to prevent slag patches/entrapped scums in the mold are largely the same as those for inclusion clusters, i.e., reduce the turbulence of the submeniscus metal flow, minimize meniscus level fluctuation and decrease the extension of nails/hooks on the initial shell. In addition, increasing the melting rate and optimizing the viscosity of the mold flux within an acceptable operating window works to decrease, respectively, the entrapment of sintered and powdery flux and the flux melt.

21.8 Gas Holes

Gas holes in the surface layers of the strand arise in three kinds:

1. Insufficient deoxidation that results in blowholes.
2. Air ingress in Al-killed steel during metal transfer to the mold to form pinholes.
3. Injection of Ar to prevent nozzle clogging that also forms pinholes.

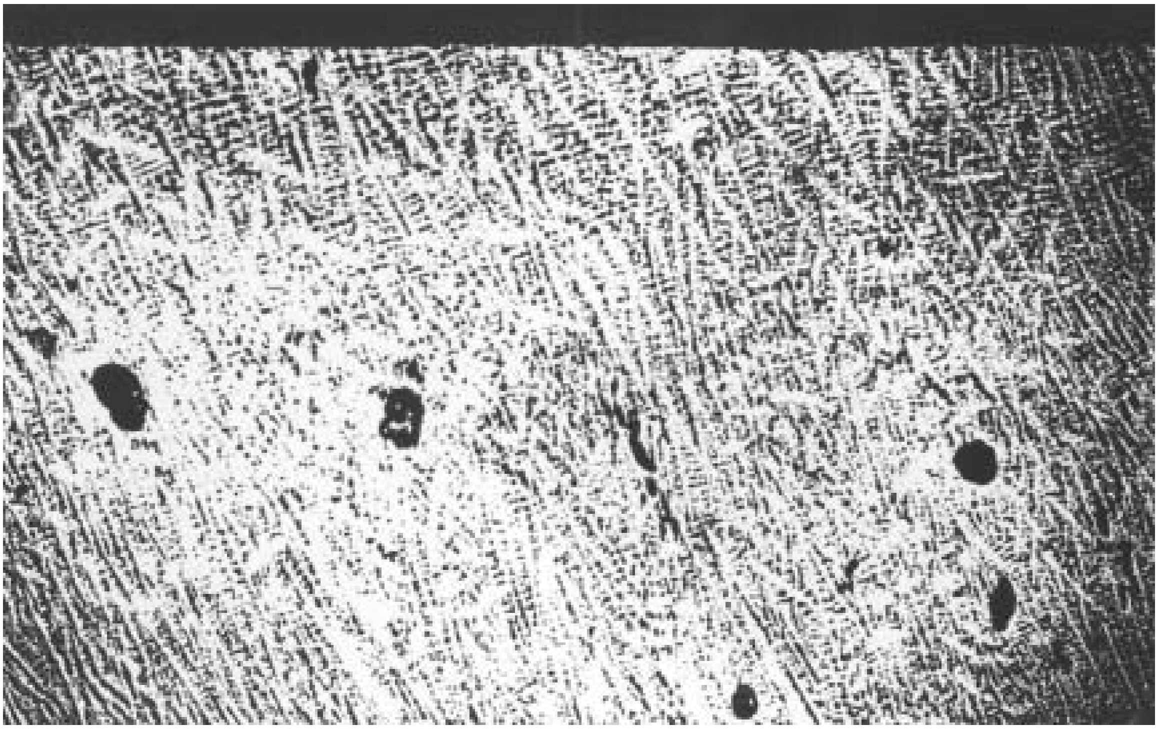

Fig. 21.46 Blowholes in a weakly deoxidized CC slab.

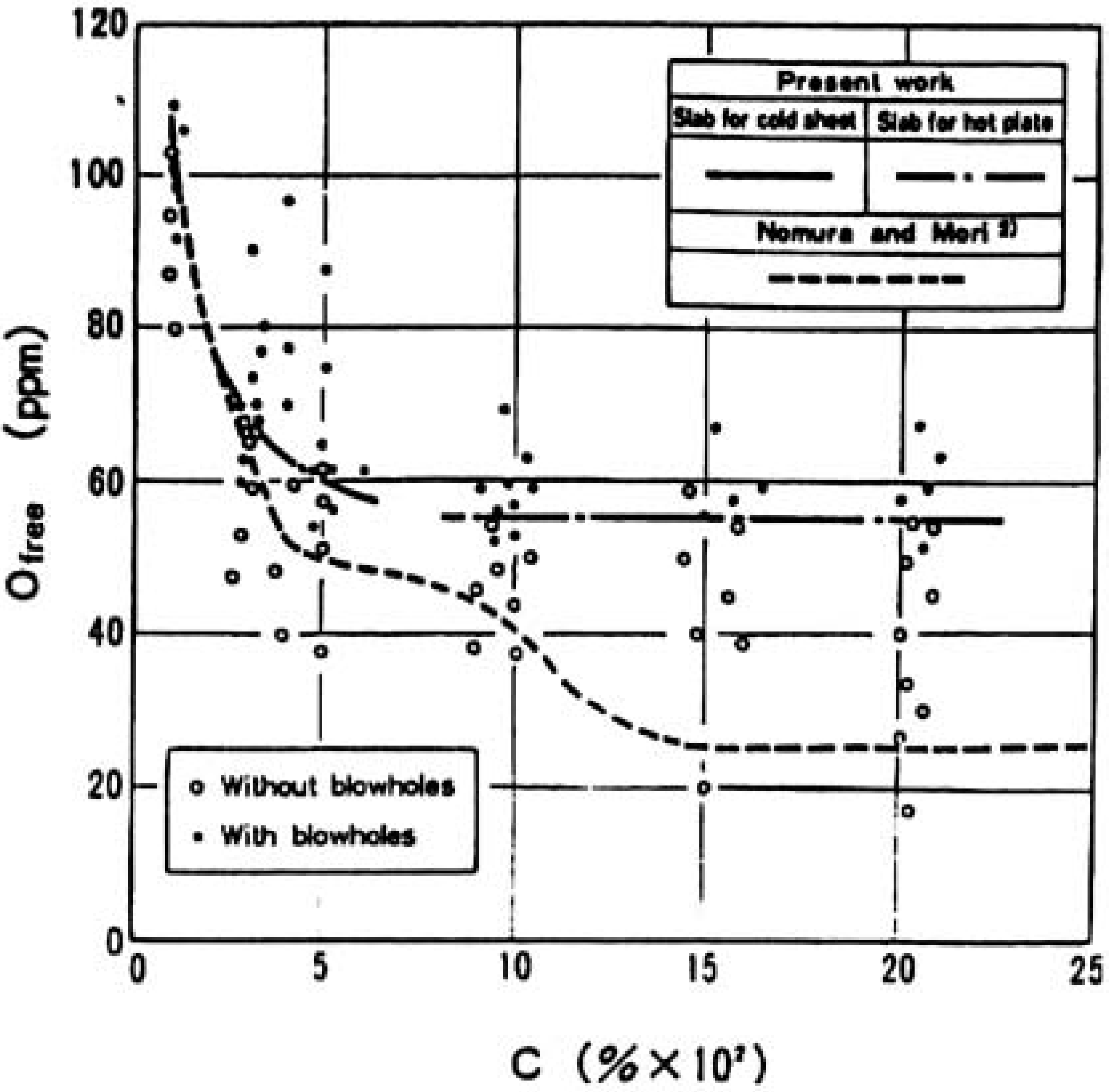

Fig. 21.47 Critical concentration of C and O for blowhole formation. *From Ref. 55.*

Characteristics, influential factors, causes and countermeasures for each will be discussed in the following sections.

21.8.1 Blowholes

21.8.1.1 Characteristics

These gas holes are tubular in shape and located in the subsurface, within a few tens of millimeters from the surface of the strand, with sizes up to 3 mm in diameter and 25 mm in length. They usually contain CO and some H_2 and are occasionally associated with inclusions. An example is shown in Fig. 21.46. If they open up during reheating and rolling, the surface of the holes is oxidized; hence, large ones often cause streaks or a double skin with a scale layer in between. Similar defects occur with closed gas holes when they are associated with Al_2O_3 inclusion clusters. Smaller blowholes without clusters may weld together during rolling, leaving no defects.

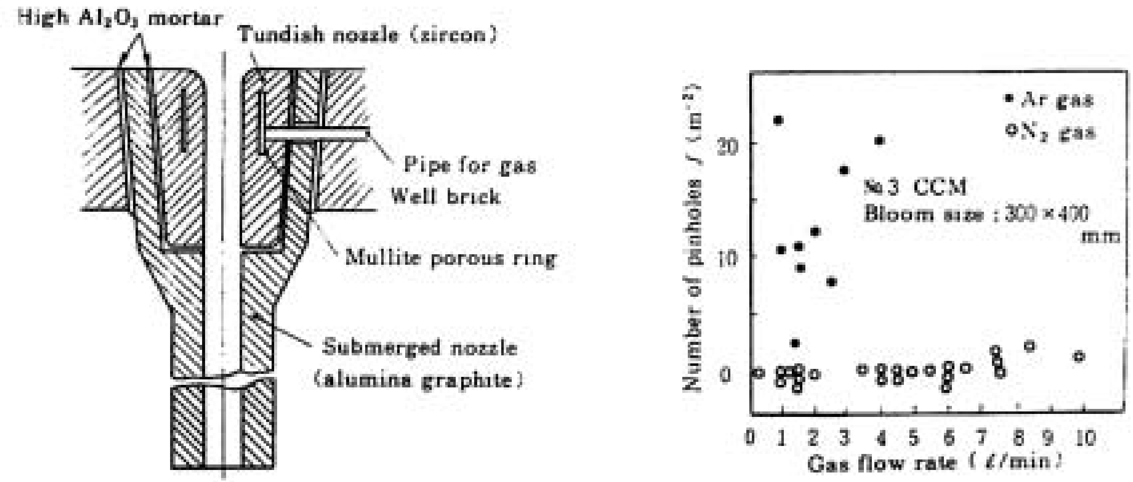

Fig. 21.48 Blowholes in a weakly deoxidized CC slab.

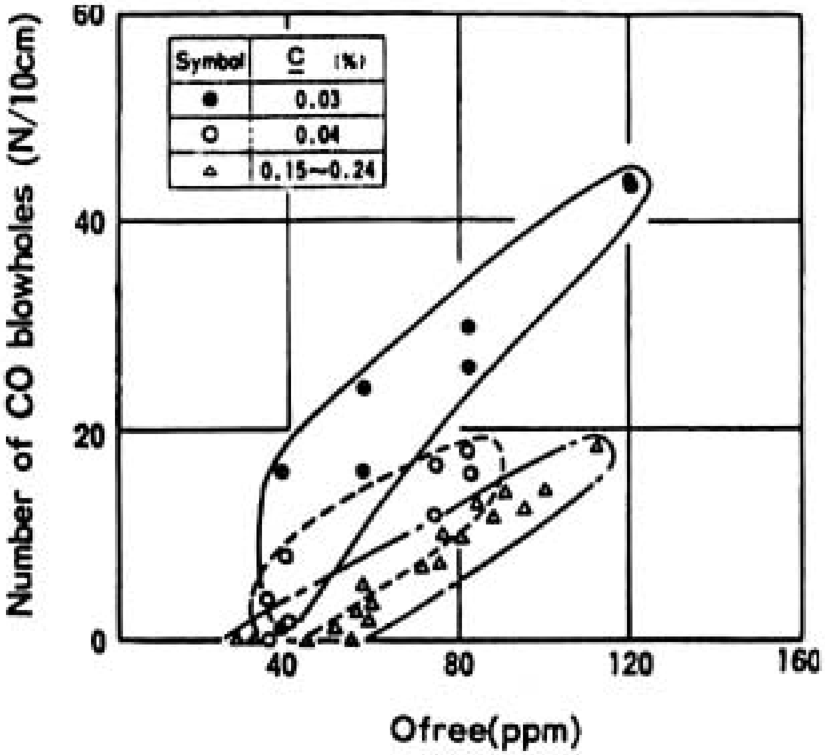

Fig. 21.49 Frequency of blowhole formation as a function of free oxygen.

21.8.1.2 Influential Factors, Causes and Countermeasures

According to detailed on-line experiments with curved CC machine casting of a 250 mm x 1150 mm slab at 0.3–0.8 m/min and 1540–1550°C, critical concentration of free oxygen, $[O]_{Crit.}$, for CO blowhole formation changes with [C], as shown in Fig. 21.47. It decreases with [C] from 100 ppm at 0.01% C to 60 ppm at 0.05% [C], leveling off beyond 0.05% [C] due to oxygen transfer control. The diameter and number concentration of the blowholes change with $[O]_{Crit.}$, as shown in Figs. 21.48, 21.49 and 21.50.[55] The CO blowhole formation is caused by solute enrichment at the solidification front, and hence can be suppressed by washing the solute accumulation away with electromagnetic stirring of the melt along the perimeter of the mold. At the melt flow velocity of 0.8

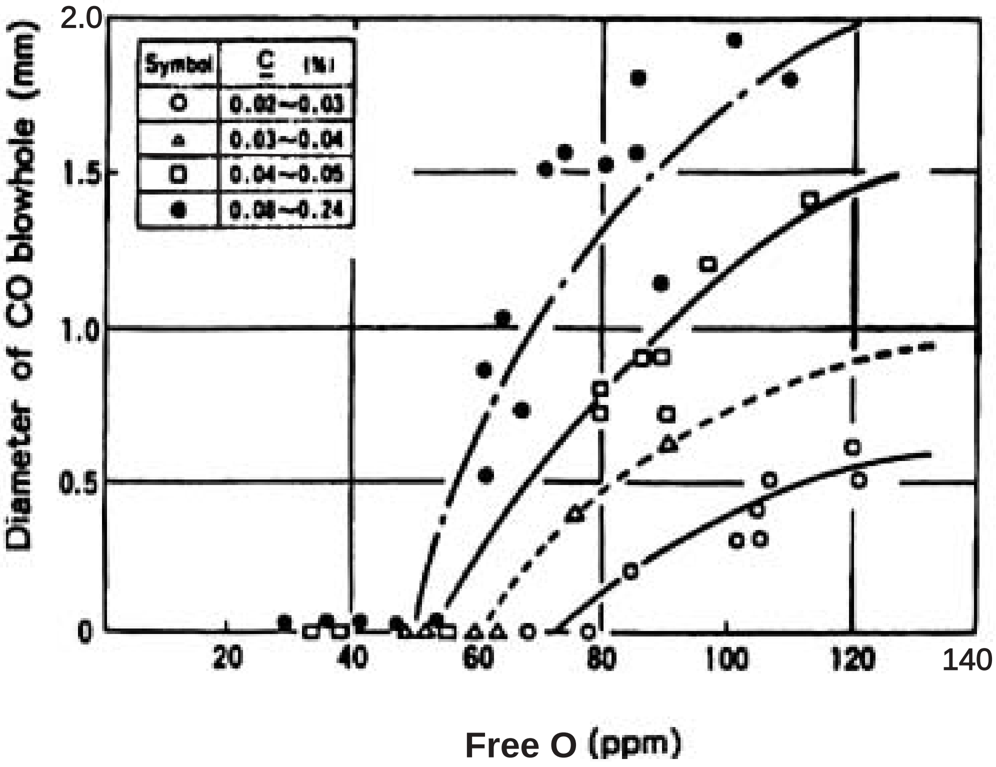

Fig. 21.50 Blowhole diameter as a function of free oxygen.

m/s, $[O]_{Crit.}$ could be increased from 60 to 85 ppm at 0.05% [C],[56] effectively suppressing the blowhole formation.

21.8.2 Pinholes

21.8.2.1 Characteristics

These are exclusively found in IF steels, more frequently in those containing Ti or P, as subsurface holes with smaller diameters (0.1–3 mm). The pinholes contain a mixture of Ar and H_2 of varying fractions. The number concentration of the pinholes steeply decreases with increasing depth from the strand surface. Alumina clusters are often found adhering to the inner surface of the pinholes, but the volume fraction of the clusters in the pinholes is usually small. The pinholes do not weld during hot rolling of slabs, as Ar has virtually no solubility in steel at reheating temperatures, and they cause blisters and slivers during and after cold rolling and annealing depending on their location (depth from the surface) and contents of the clusters.

The pinhole problems are common all over the world where IF steels are produced. More detailed characteristics of pinholes in slabs and resulting blisters and slivers in sheet product will be summarized in the following section.

21.8.2.2 Characteristics of Blisters/Slivers Formed in Ultralow-Carbon Steel from Pinholes

An extensive round-robin cross-examination[57] sponsored by ISIJ was carried out among representative steel producers in Japan. It has confirmed the following regarding the characteristics of blisters/slivers caused by Ar bubbles often associated with alumina clusters:

- Formation of blisters is almost exclusively found on ultralow-carbon steel sheet.
- The cause of the blister formation is identified to be the entrapped Ar gas bubbles often accompanied by Al_2O_3 clusters.
- Most blisters with Al_2O_3 clusters turn out to be slivers by annealing after cold rolling or sometimes even during cold rolling.
- The bubbles without acompanying Al_2O_3 clusters show up as light scabs.
- More slivers appear when the S content in the steel is relatively high, 30–100 ppm.
- The size of entrapped Ar gas bubbles in the shell (slab) that are critical for sliver formation was found to be in the range of 0.5–3.0 mm in diameter (1.5 mm and above in diameter is more harmful).
- Sheet product rejections and downgrades are likely when the number of the bubbles exceeds 5 per 100 cm^2 of sheet surface.
- Sliver formation increases as the location of the bubbles comes closer to the surface of the slabs.
- The bubbles are less frequently associated with mold flux than alumina clusters.
- Electron microprobe image analyses show that a sliver contains elementary Al_2O_3 particles sized about 4–6 mm at number concentrations of 300–600/mm^2.
- The area occupation ratio of Al_2O_3 particles in a sliver ranges from 0.006 to 0.012.
- The above range in occupation ratio is in good agreement with the calculated value of 0.004–0.009 that corresponds to the volume fraction of Al_2O_3 particles in an Ar bubble when the surface of the bubble is completely covered by a monolayer of elementary Al_2O_3 particles.
- The bubbles are located within 8 mm from the slab surface, decreasing sharply from the surface to 2–3 mm inside the shell. The location corresponds to the fact that bubble entrapment in the shell took place between 0 and 240 mm below the meniscus, decreasing with the depth from the meniscus.

21.8.2.3 Influential Factors, Causes and Countermeasures

These observations and associated investigations show the following:

1. For billets and blooms, pinholes of air ingress origin can be prevented by converting the SEN from an attachment type to an insert type, as the latter provides a better gas seal. When practicable, conversion of the injection gas from Ar to N_2 decreases pinholes substantially (see Fig. 21.47). Erratic formation of oscillation marks, often experienced while superheat is low, steeply increases pinholes located within 2–3 mm from the surface of the shell.

2. Ar gas bubbles introduced into the SEN/SG (to prevent nozzle clogging and assist the flotation of elementary Al_2O_3 particles) are carried over with the melt flow out of the SEN into the mold. A majority of the bubbles are entrapped by an overhanging hook of solidifying shell near the meniscus during flotation, while some part is trapped by dendrites extending from the shell further below the meniscus (e.g., 300 mm below).

3. For IF steels, solidus temperature is so high and close to liquidus temperature that the nails/hooks extend longer from the shell in an irregular way to entrap more bubbles that are flotating in front of the nails/hooks.

4. The entrapment is enhanced in steels with high residual [S], Ti-bearing steels and rephosphorized steels. This is believed to be due to the concentration gradient of [S], [Ti] and [P] developing in front of the liquid/solid interface that causes the interfacial force gradient to pull the bubbles toward the interface.[58]
5. The following measures have been found effective in preventing the bubbles from coming near the interface (where the concentration gradient is built up) and being entrapped:
    - Minimizing the amount of Ar gas injection into the SEN (e.g., less than 6–8 l/min),
    - Reducing the occurrence of alternating, deep-penetrating, asymmetric-biased metal flow from the SEN by improving the design of the SEN.
    - Electromagnetic braking of the melt flow so that it does not allow carryover of the bubbles with the flow deep into the melt pool, thereby preventing them from coming near the interface during flotation.
    - Washing the bubbles away from the proximity of the interface by electromagnetic stirring of the metal flow along the interface (e.g., 40–50 cm/sec).
    - Avoiding the extended formation of coarse nails/hooks at the meniscus by keeping a sufficient superheat at the meniscus (e.g., +5°C and up), heating the melt at the meniscus by electromagnetic braking (e.g., FC-Mold), and insulating the meniscus with a sufficient thickness of mold flux. During the start of casting, use of exothermic starting powder helps.

21.9 Conclusions

Representative defects occurring on the surface and subsurface of continuously cast strands have been reviewed. Emphasis is placed on the characteristics, influential factors, causes and countermeasures based largely on the authors' experiences and understanding. Statements are intended to be practical, but important fundamentals are addressed. Steel products are user-specific, depending on each user's processing technology and product quality requirements. The requirements to minimize surface defects continue to be more demanding, yet remain rewarding. Changes in demands trigger major alterations of processes and products, as clearly seen in the development of high-rate production/high-speed casting and IF steels for stringent applications. For surface defects, there are still some problems left unsolved. Even today, turbulence in the submeniscus flow, variation in the meniscus level and accretion on the SEN persist as major root causes of surface defects. Further research and development are needed in the search for the ultimate solution that addresses these problems in an economically feasible manner.

21.10 Acknowledgment

The authors are grateful to Dr. M. Suzuki (NKK), Dr. T. Watanabe, Dr. K. Isobe and Mr. A. Yamauchi for their generous efforts to provide us with valuable information and photographs of some of the surface defects.

References

1. T. Emi, "Developments in Continuous Casting at Macro Mills and Future Outlook," *Proc. Brimacombe Memorial Symposium,* edited by G.A. Irons and A.W. Cramb (Oct., 2000, Vancouver), (TMS, ISS, MetSoc. CIM, Oct., 2000), 23–38.

2. J.K. Brimacombe and K. Sorimachi, “Crack Formation in the Continuous Casting of Steel,” *Metall. Trans. B,* 8B (1977): 489–505.
3. “Metallurgy of Continuous Casting: Casting and Solidification of Steel,” and “Crack Susceptibility of Steels in Continuous Casting and Hot Forming,” edited by K. Schwerdtfeger, VDEh, Stahleisen Verlag, Dusseldorf, Germany (1992, 1994).
4. “History of Continuous Casting Technology in Japan,” *ISIJ,* Tokyo, Japan (1996).
5. N.A. McPherson and A. McLean, eds., *Continuous Casting,* Vol. 8 (Warrendale, Pa.: Iron and Steel Society, 1997), 1–46.
6. M.M. Wolf, ed., *Continuous Casting,* Vol. 9 (Warrendale, Pa.: Iron and Steel Society, 1997), 1–111.
7. T. Emi, “Mechanical Properties of Steel near Solidus Temperatures,” *Handbook of Iron and Steel,* 3rd edition, Vol.1, in *Fundamentals*, ISIJ (1979), 217–224.
8. G. Shin, T. Kajitani, T. Suzuki and T. Umeda, “Mechanical Properties of Carbon Steels During Solidification,” *Tetsu-to-Hagane,* 78 (1992): 587–593.
9. E. Schmidtmann and L. Pleugel, *Arch. Eisenhuttenw.*, 51 (1980): 49–61.
10. H. Mizukami, A. Yamanaka and T. Watanabe, “Tensile Strength of Chromium Steel During and after Solidification,” *Tetsu-to-Hagane,* 85 (1999): 592–598.
11. T. Umeda, “Fundamentals of Solidification in Slab Castings,” 153th/154th Nishiyama Memorial Lecture, ISIJ (1994), 45–87.
12. P. Ackermann, W. Kurz and W. Heinemann, *Mater. Sci. Eng.*, 75 (1985): 79.
13. K. Schwerdtfeger and Sha, *Metall. Trans. B,* 31B (2000): 813–826.
14. J.K. Brimacombe, F. Weinberg and E.B. Hawbolt, “Formation of Longitudinal, Mid-face Cracks in Continuously-Cast Slabs,” *Metall. Trans. B*, 10B (1979): 279–292.
15. T. Kohno, K. Shima, T. Kuwabara, S. Mizoguchi, T. Yamamoto, H. Misumi and A. Tsuneoka, “The Metallographical Characteristics and the Formation Mechanism of Longitudinal Surface Cracks in CC Slabs,” *Tetsu-to-Hagane,* 82 (1982): 1764–1772.
16. T. Saeki, S. Ohguchi, S. Mizoguchi, T. Yamamoto, H. Misumi and A. Tsuneoka, “Effect of Irregularity in Solidified Shell Thickness on Longitudinal Surface Cracks in CC Slabs,” *Tetsu-to-Hagane*, 68 (1982): 1773–1781.
17. T. Matsumiya, T. Saeki, J. Tanaka and T. Ariyoshi, “Mathematical Model Analysis on the Formation of Longitudinal Surface Cracks in Continuously Cast Slabs,” *Tetsu-to-Hagane,* 68 (1982): 1782–1971.
18. H. Nakato, M. Ozawa, K. Kinoshita, Y. Habu and T. Emi, “Factors Affecting the Formation of Shell and Longitudinal Cracks in Mold During High-Speed Continuous Casting of Slabs,” *Tetsu-to-Hagane,* 67 (1981): 1200–1209. See also *Trans. ISIJ,* 24 (1984): 957–965.
19. K. Schwerdtfeger, “Fundamentals for Refining and Solidification Processing,” *Proc. 6th Intl. Iron and Steel Congress,* Vol.1, ISIJ, Tokyo, in *Fundamentals* (1990), 580–590.
20. Y. Sugitani, M. Nakamura and T. Watanabe, *Tetsu-to-Hagane,* 67 (1981): 1508.
21. K. Nakai, T. Sakashita, M. Hashio, M. Kawasaki, K. Nakajima and Y. Sugitani, “Effect of Mild Cooling in Mold on Solidified Shell Formation of Continuously Cast Slab,” *Tetsu-to-Hagane,* 73 (1987): 498–504.
22. H. Kyoden, T. Doihara and O. Nomura, “Development of Mold Powders for High-Speed Continuous Casting of Steel,” *Mold Powders for Continuous Casting and Bottom Pour Teeming* (Warrendale, Pa.: Iron and Steel Society, 1987), 45–57.
23. S. Ohmiya, K.H. Tacke and K. Schwerdtfeger, *Ironmaking and Steelmaking,* 10 (1983): 24–30.
24. A. Yamauchi, K. Sorimachi, T. Sakuraya and T. Fujii, “Heat Transfer Between Mold and Strand Through Mold Flux Film in Continuous Casting of Steel,” *ISIJ Intl.,* 33, (1993): 140–147.
25. J.-W. Cho, H. Shibata, T. Emi and M. Suzuki, “Thermal Resistance at the Interface Between Mold Flux Film and Mold for Continuous Casting of Steels,” *ISIJ Intl.*, 38 (1998): 440–446.
26. K. Kinoshita, T. Emi and M. Kasai, “Thermal Elasto-Plastic Stress Analysis of Solidifying Shell in Continuous Casting Mold,” *Tetsu-to-Hagane,* 65 (1979): 2022–2031.
27. H.G. Suzuki, S. Nishimura and S. Yamaguchi, “Characteristics of Hot Ductility in Steels Subjected to the Melting and Solidification,” *Trans. ISIJ,* 22 (1982): 48–56.

28. A. Yamauchi, S. Itoyama, N. Bessho and K. Sorimachi, "Heat Transfer Characteristics and Surface Quality of Strand Cast with Mild Cooling Mold," Japan Soc. Promoting Sci., Steelmaking 19th Committee, 19-11628 (1996): 1–8.
29. T. Kohno, K. Shima, T. Kuwabara, T. Yamamoto, M. Wake and A. Tsuneoka, Improvement of Longitudinal Surface Cracks in CC Slabs by Air-Water Mist Cooling Method," *Tetsu-to-Hagane,* 68 (1982): 1792–1798.
30. K. Kinoshita, H. Kitaoka and T. Emi, "Influence of Casting Conditions on the Solidification of Steel Melt in Continuous Casting Mold," *Tetsu-to-Hagane,* 67 (1981): 93–102.
31. T. Murakami, T. Yamada, K. Okamura, M. Hashio, T. Kawakami and Y. Watanabe, "Improvement of Longitudinal Corner Cracks at High-Speed Casting," *CAMP-ISIJ,* 5 (1992): 1291.
32. T. Saito, M. Kodama and K. Komoda, *Iron and Steel Intl.,* 48 (Oct. 1975): 391.
33. K. Kim, H.N. Han, T. Yeo, Y. Lee, K.H. Oh and D.N. Lee, "Analysis of Surface and Internal Cracks in Continuously Cast Beam Blank," *Ironmaking and Steelmaking,* 24 (1997): 249–256.
34. S. Harada, S. Tanaka, H. Misumi, S. Mizoguchi and H. Horiguchi, "A Formation Mechanism of Transverse Cracks on CC Slab Surface," *ISIJ Intl.,* 30 (1990): 310–316.
35. Kusano, H. Misumi and S. Harada, "Estimation of the Formed Position of the Surface Cracks on the Slabs in the Continuous Caster," *Tetsu-to-Hagane,* 82 (1990): 35–40.
36. H.G. Suzuki, S. Nishimura and Y. Nakamura, *Trans. ISIJ,* 24 (1984): 54, 169.
37. B.G. Thomas, J.K. Brimacomb and I.V. Samarasekera, "The Formation of Panel Cracks in Steel Ingots: A State-of-the-Art Review," *ISS Trans.,* 7 (1986): 7–20.
38. Y. Miyashita, M. Suzuki, K. Taguchi, S. Uchida, H. Sato and M. Yamamura, *Nippon Kokan Technical Report Overseas,* 36 (1982): 55–64.
39. B. Mintz, "The Influence of Composition on the Hot Ductility of Steels and to the Problem of Transverse Cracking," *ISIJ Intl.,* 39 (1999): 833–855.
40. T. Kato, N. Kasai, M. Kawamoto, A. Yamanaka and T. Watanabe, "Formation Mechanism of Slab Surface Transverse Cracking in Continuously Cast Ni-bearing Steel," *Tetsu-to-Hagane,* 84 (1998): 856–860.
41. M. Suzuki, H. Hayashi, H. Shibata, T. Emi and In-Jae Lee, "Simulation of Transverse Crack Formation on Continuously Cast Peritectic Medium-Carbon Steel Slabs," *Steel Research,* 70 (1999): 412–419.
42. T. Emi, H. Nakato, Y. Iida, K. Emoto, R. Tachibana, T. Imai and H. Bada, "Influence of Physical and Chemical Properties of Mold Powders on the Solidification and Occurrence of Surface Defect of Strand Cast Slabs," *Steelmaking Proc.,* formerly *Proc. NOH-BOSC,* 61 (1978): 357.
43. H. Tomono, W. Kurz and W. Heineman, *Metall. Trans. B,* 12B (1981): 409–411.
44. Y. Maehara, K. Nakai, K. Yasumoto and T. Mishima, "Hot Cracking of Low-Alloy Steels in Simulated Continuous Casting Direct Rolling Process," *Tetsu-to-Hagane,* 73 (1987): 876–883.
45. H. Fredriksson, K. Hansson and A. Olsson, "On the Mechanism of Liquid Copper Penetration into Iron Grain Boundaries, *Scand. J. Metallurgy,* 29 (2000): 41–50.
46. T.J.H. Billany, A.S. Normanton, K.C. Mills and P. Grieveson, "Surface Cracking in Continuously Cast Products" *Ironmaking and Steelmaking,* 18 (1991): 403–410.
47. T. Kajitani, M. Wakoh, N. Tokumitsu, S. Ogibayashi and S. Mizoguchi, "Influence of Temperature and Strain on Surface Crack due to Residual Copper in Carbon Steel," *15th PTD Conf. Proc.* (Warrendale, Pa.: Iron and Steel Society, 1996), 87–92.
48. M.I.U.T. van Wijingaarden and G.P. Visagie, "The Effect of Residuals on the Presence of Intergranular Surface Cracks on Continuously Cast Billets," *15th PTD Conf. Proc.,* (Warrendale, Pa.: Iron and Steel Society, 1996), 93–97.
49. I.V. Samarasekera, J.K. Brimacombe, S. Kumar and A. McLean, "The Tundish Pouring Stream and Cast Billet Quality," *Near Net Shape Casting in the Minimills, CMS & TMS,* 135–160.
50. B.G. Thomas and H. Zhu, "Thermal Distortion of Solidifying Shell Near Meniscus in Continuous Casting Steel," JIM/TMS Solidification Science and Processing Conf., Honolulu, Hawaii (Dec. 13–15, 1995).

51. H. Takeuchi, S. Matsumura and Y. Ikehara, “Actual State and Formation Mechanism of Surface Segregation on Oscillation Marks of Continuously Cast Austenitic Stainless Steel Slabs,” *Tetsu-to-Hagane,* 69 (1983): 1995–2001.
52. M. Hojo, S. Fukumoto, I. Mizuchi, S. Tanaka and H. Takeuchi, “Formation Mechanism of Surface Segregation Zone of SUS304 Stainless Steel Slab,” *CAMP ISIJ,* 5 (1992): 1256.
53. H.-J. Ehrenberg, H.P. Kaiser, J. Kluge and K. Wunnenberg, “Casting of Round Strands in a Resonance Mold,” *MPT Int.l,* 23:2 (2000): 50–54.
54. M. Hasegawa, S. Maruhashi, H. Muranaka and N. Hoshi, “Mechanism of Formation of Surface Defects in Continuously Cast Stainless Steel Slabs Containing Titanium,” *Tetsu-to-Hagane,* 73 (1987): 505–512.
55. E. Takeuchi, H. Fujii, N. Miyasaka, T. Ohashi, T. Hiraoka and M. Yamahiro, “CO Blowhole Formation and Suppression in Continuously Cast Slab,” *Tetsu-to-Hagane,* 69 (1983): 1607–1622.
56. E. Takeuchi, H. Fujii, T. Ohashi, H. Tanno, S. Takao, I. Furugaki and H. Kitamura, “Continuous Casting of Pseudo-Rimmed Steel with Electromagnetic Stirring in the Mold,” *Tetsu-to-Hagane,* 69 (1983): 1615–1622.
57. “Recent Advance in the Research on Nonmetallic Inclusions in Steel,” Japan Society for Promoting Science, Steelmaking No. 19 Committee, 19-11514 (Sept. 1994).
58. H. Yasuanaka, R. Yamanaka, T. Inoue and T. Saito, “Pinhole and Inclusion Defects Formed at the Subsurface in Ultralow-Carbon Steel,” *Tetsu-to-Hagane,* 81 (1995): 529–534.
59. Y. Ueshima et al., *ISIJ Intl.,* 83 (1997).